

Theoretical Challenges in Galaxy Formation

THORSTEN NAAB¹ & JEREMIAH P. OSTRIKER^{2,3}

¹ *Max-Planck-Institute for Astrophysics, Karl-Schwarzschild-Str. 1, 85748 Garching, Germany; email: naab@mpa-garching.mpg.de*

² *Department of Astronomy, Columbia University, 550 W, 120th Street, New York, NY10027, USA; email:jpo@astro.columbia.edu*

³ *Department of Astrophysical Sciences, Princeton University, Princeton, NJ 08544, USA*

Key Words

theoretical models, cosmology, galaxy formation, galaxy evolution

Abstract

Numerical simulations have become a major tool for understanding galaxy formation and evolution. Over the decades the field has made significant progress. It is now possible to simulate the formation of individual galaxies and galaxy populations from well defined initial conditions with realistic abundances and global properties. An essential component of the calculation is to correctly estimate the inflow to and outflow from forming galaxies since observations indicating low formation efficiency and strong circum-galactic presence of gas are persuasive. Energetic 'feedback' from massive stars and accreting super-massive black holes - generally unresolved in cosmological simulations - plays a major role for driving galactic outflows, which have been shown to regulate many aspects of galaxy evolution. A surprisingly large variety of plausible sub-resolution models succeeds in this exercise. They capture the essential characteristics of the problem, i.e. outflows regulating galactic gas flows, but their predictive power is limited. In this review we focus on one major challenge for galaxy formation theory: to understand the underlying physical processes that regulate the structure of the interstellar medium, star formation and the driving of galactic outflows. This requires accurate physical models and numerical simulations, which can precisely describe the multi-phase structure of the interstellar medium on the currently unresolved few hundred parsecs scales of large scale cosmological simulations. Such models ultimately require the full accounting for the dominant cooling and heating processes, the radiation and winds from massive stars and accreting black holes, an accurate treatment of supernova explosions as well as the non-thermal components of the interstellar medium like magnetic fields and cosmic rays.

1 Introduction

1.1 What do we want to learn?

Do we understand galaxy formation? Galaxies have been called the building blocks of the Universe and they are clearly the fundamental units within which stars are organized. They do show characteristic sizes ($R_{\text{gal}} \sim kpc$) and masses ($M_{\text{gal}} \sim 10^{10} M_{\odot}$). Their abundance ($\sim 10^{-2} Mpc^{-3}$) is set by their characteristic mass and the fact that they constitute a moderate fraction ($f_{\text{gal}} \sim 10\%$) of the cosmic baryon budget. Can we derive these numbers ($R_{\text{gal}}, M_{\text{gal}}, f_{\text{gal}}$) from first principles? Can we, from straightforward numerical simulations, chart the history of when, where and how the formation and evolution of galaxies occurred? And, finally, do we understand it all well enough to characterize the internal properties of these systems, their ages, kinematics and mass distributions and their organization into families having properties describable using relatively few parameters?

As a problem in physics, there are four clearly definable aspects: (1) specification of the initial conditions; (2) knowledge of the physical processes primarily responsible for understanding each phase of galactic evolution; (3) computational tools that permit us to start with (1), utilize (2) to construct models predicting the detailed properties of representative samples of galaxies to be (4) tested by direct comparison with the rich treasury of information provided by nature revealed by modern observational technology.

We will argue that the current, standard cosmological models are sufficiently accurate to provide initial conditions as required to any specified accuracy. With regard to physical processes, the problem is divided into two parts: (A) what would the evolution be if we only had to consider dark matter; and (B) how is the picture altered if we include the primordial radiation fields, the baryonic gas as well as the energy, processed interstellar matter and momentum input from the stars and massive black holes? The current state of the art shows a good grasp of problem (A) - different investigators using different codes recover quite similar descriptions of the universe; but with regard to the more complex problem (B) - allowing for 'feedback' from stars and black holes, we have only preliminary gropings toward physical understanding. One simple example suffices. The non-thermal and relativistic components of the interstellar medium - magnetic fields and cosmic rays - are not thought to be primordial but in our Galaxy have energy densities comparable with kinetic energy densities, significantly higher than thermal energy densities (e.g. Boulares & Cox 1990, Ferrière 2001). Are these components essential to understanding galaxy formation or are they mere byproducts? They are not included in most treatments, and the omission may (or may not) be crucial. However, the situation is improving.

As a result of our success with regard to problem (A) - the 'stage setting' so to speak - we have a moderately good grasp of the physics that determines the approximate values of the three scales, the numbers for size, mass and abundance, noted as the fundamental characteristics of galaxies, but we have a poor knowledge of the details that are important in determining the internal structure and evolution of these systems. Finally, our computational tools are marginally adequate for the simpler part (A) of the task, but perhaps not up to the challenge of the multi-dimensional, multi-component, time-dependent computation involving the necessary range of temporal and spatial scales.

So far we have been describing this as an *ab initio* problem of physics, like the motion of a playground swing - though more complex - but of course this is not the way that the history unfolded. Observational discoveries have guided us every step of the way, often pointing out to us how much too simple our models have been. These observations have been of two kinds, those that describe the Universe as it is (e.g. galaxy rotation curves or the details of

the multi-phase interstellar medium) and those that tell us of the time development, either through using the archaeological method of examining the stellar populations of nearby galaxies and determining when/how the various components were assembled, or by using the Universe as a time machine and looking at the progenitor populations at earlier cosmic epochs. In any case, direct observations are the facts that all models have to be tested against and in most cases they are the drivers for progress in theoretical galaxy formation, both on the small scales of individual galaxies as well as on the large scale distribution and redshift evolution of galaxy populations.

Galaxy formation has become such a large field in astrophysics that a full overview of all theoretical challenges is beyond the scope of a single review. Here we focus on a subset of problems in computational astrophysics. Numerical implementations of 'feedback' processes have traditionally been tested with idealised galaxy models and merger simulations. These models have resulted in important insights on star formation, morphological and kinematic transformations, merger driven gas flows, triggering of star formation, the impact of accreting black holes on the termination of star formation, and size evolution. We give an overview of these feedback models and their use in modern cosmological simulations of galaxy formation. We briefly highlight major steps forward like the successful simulation of spiral galaxies and the cosmological evolution of galaxy populations. Some other major theoretical challenges that can be addressed with cosmological galaxy formation simulations are not discussed here in detail. One of these is how galaxies accrete their gas. Gas accretion is a necessary and fundamental process for galaxy formation but surprisingly it has not yet been conclusively observed. From numerical studies it is still unclear whether the gas is accreted onto the galaxies cold filaments (Dekel et al. 2009, Kereš et al. 2005) or whether the filaments dissolve in the halos and accretion is more smooth (Nelson et al. 2013). A related question is how galactic outflows actually transport metal enriched material into the circumgalactic medium (see e.g. Oppenheimer & Davé 2006, Schaye et al. 2015). This is also a numerically challenging question, as the spatial resolution in the halos of galaxies is typically much lower than in the dense regions and mixing processes are highly complex (e.g. Scannapieco & Brügger 2015). We also do not address issues that test galaxy formation on small scales in the context of the underlying cold dark matter cosmological model like the 'Too big to fail' problem (Boylan-Kolchin, Bullock & Kaplinghat 2011) or the question whether small dark matter halos have cusps or cores (e.g. Kravtsov et al. 1998, Pontzen & Governato 2012). We accept the standard cold dark matter paradigm because of its numerous proven successes on large scales, while fully aware of the challenges it faces on small scales. Instead we focus on the physics of the interstellar medium (ISM). The ISM strongly influences galaxy formation. Many processes determining star formation and galactic outflows as well as major observable features act in the ISM and a better understanding and more accurate modelling of these processes are, in our view, the major theoretical challenge for galaxy formation in the future.

1.2 Some relevant observations

Our summary of observations that put important constraints on theoretical galaxy formation models will necessarily be brief and does not attempt to provide a full list of references. The first and most obvious is the observational information accumulated in the last century specifying the four principle components of all massive galaxies; stars, gas, dark matter and super-massive black holes:

1.2.1 STARS From Hubble’s time onwards we realized that the bulk of the mass in the visible parts of galaxies resides in one of two components, a spheroidal part having a scale length typically of only a few kpc to a few tens of kpc with a roughly de Vaucouleurs surface density profile (de Vaucouleurs 1948) and a flattened, rotationally supported disk/spiral component, which is typically somewhat larger (apart from the highest mass systems) and has a roughly exponential profile (e.g. Blanton & Moustakas 2009, Shen et al. 2003, van der Kruit & Freeman 2011). These two components appear to be distinct, and environmental considerations must be important in understanding their formation, since isolated systems tend to be disk dominated and those in regions of high galactic density tend to be dominated by the spheroidal component (e.g. Blanton & Moustakas 2009, Cappellari 2011, Dressler 1980, Kormendy et al. 2010). Recent integral field studies have significantly improved our understanding of the complex kinematics of galaxies (Bundy et al. 2015, Cappellari et al. 2011, de Zeeuw et al. 2002, Fogarty et al. 2014, Sánchez et al. 2012). Stellar dating indicates extended and relatively flat star formation histories for the disks with typical ages of a few billion years and peaked star formation histories with typical stellar ages of ~ 10 billion years for massive early type galaxies (e.g. Heavens et al. 2004, Kauffmann et al. 2003, Kormendy et al. 2009, Renzini 2006, Thomas et al. 2005). Large surveys made it possible to observe relatively accurate stellar mass functions not only in the local Universe (e.g. Bernardi et al. 2013, Li & White 2009, Pérez-González et al. 2008) but also towards higher redshifts (e.g. Bouwens et al. 2012, Duncan et al. 2014, Moustakas et al. 2013, Muzzin et al. 2013, Song et al. 2016).

1.2.2 GAS Typical Milky Way like spiral galaxies roughly have $\sim 10\%$ of their mass in cold interstellar medium gas ($\lesssim 10^4 K$). An even larger fraction (some of it hotter and ionised) gas might be stored in the so called ‘circum galactic medium’, the region extending from the star-forming interstellar medium into the galaxies halos (e.g. Somerville & Davé 2015, Werk et al. 2014). More massive early-type galaxies typically have significantly lower cold gas fractions, although they are not devoid of cold gas, contrary to the traditional picture (Catinella et al. 2010, Saintonge et al. 2011, Serra et al. 2012, Young et al. 2011). Massive early-type systems are usually embedded in hot ($> 10^5 K$) X-ray emitting gas comprising a significant fraction of the total baryonic mass (e.g. Anderson et al. 2015, Dai et al. 2010, Giodini et al. 2009, Kravtsov & Borgani 2012, Mulchaey 2000, Renzini & Andreon 2014, Sun et al. 2009, Vikhlinin et al. 2006).

1.2.3 DARK MATTER Following Zwicky’s and Babcock’s work in the 1930s and then the work of many authors on the rotation curves of normal galaxies in the 1970s and 1980s (e.g. Sofue & Rubin 2001), it became apparent that the stars in most normal galaxies are embedded in massive halos comprised of some unknown type of dark matter with a total mass and size roughly 10 times that of the stellar component. The generally flat observed rotation curves of spiral galaxies are an important test for cosmological formation models (see Courteau et al. 2014). Recent result from strong lensing have contributed to our knowledge of the dark matter content of massive galaxies, which have typical contributions of 5% to 20% within their stellar half-light radii (e.g. Koopmans et al. 2009, Treu 2010, see also lensing measurements of the stellar-to-halo mass ratio, Mandelbaum et al. 2006). Dwarf galaxies like Sculptor or Fornax or the recently discovered category of large utradiffuse galaxies (c.f. van Dokkum et al. 2015) are dominated by dark matter throughout (see also Kormendy & Freeman 2016).

1.2.4 SUPER-MASSIVE BLACK HOLES A number of studies have indicated that super massive black holes typically reside in the centers of normal galaxies (having stellar masses $\gtrsim 10^{10.3} M_{\odot}$), with their masses tightly correlated with the masses (and stellar velocity dispersions) of the spheroidal components of the galaxies, the ratio being roughly 5:1000 (see e.g. Genzel et al. 1997, Kormendy & Ho 2013 for a review). Given the evident association with AGN, it is widely believed that the energy emitted by these monsters during their formation is roughly 10 % of their rest mass (Shakura & Sunyaev 1973, Soltan 1982), that makes them competitive with high mass stars with regard to energy input (in various forms) into the surrounding galaxies (e.g. Silk & Rees 1998).

1.2.5 THE MILKY WAY The archaeological method was used very successfully in the last half of the 20th century to reconstruct a plausible history of our own galaxy, the Milky Way. The Sun is a typical star in the disk component that gradually formed from relatively metal rich gas. It appears that this disk component grew slowly, in size and mass, as rotationally supported gas was steadily turned into stars over cosmic time, and the typical stars in our cosmic neighborhood were formed only 3-6 billion years ago, relatively late in the evolution of the Universe. The fact that much less than 10 % of the disk stellar mass has a metallicity that is less than 10 % of the latest formed stars tells one immediately that the disk is temporally a 'secondary' structure heavily contaminated by the metal rich ejecta from earlier stellar generations (Ostriker & Thuan 1975). The age distribution tells us that it formed 'inside-out' with the stars in the low metallicity, gas rich outer parts of the disk formed most recently (see e.g. Rix & Bovy 2013). The somewhat tri-axial, bar-like, inner structure is old and may have formed via the instability of a cold rotating disk (e.g. Ostriker & Peebles 1973), but the outer spheroidal halo, is likely the debris from in-falling, captured, smaller systems that has accumulated over time. The stars in this extended spheroidal (or elliptical) component are typically ~ 10 billion years old, are lower in heavy element abundances and tend to have an isotropic or even somewhat radially biased distribution of orbits.

Most of the stars (the fraction might be as high as $\gtrsim 95\%$) in our Galaxy were made from gas that was added to the Galaxy, forming into stars within the system and only a very small fraction of the stellar mass comes from stars made in other galaxies that were added to our system via galactic mergers (Kennicutt & Evans 2012). Thus 'major mergers' might not have been at all important in the late formation history of our Galaxy, or of others with very similar structures.

Work by Eggen, Lynden-Bell & Sandage (1962) in the early 1960s provided solid evidence that our galaxy began in a phase of dramatic collapse. Other, spheroidal, systems observed in detail, while more massive and more metal rich, seemed to be composed of stars of similar age and orbital properties, so it was plausible that they formed by a similar process. In this simple picture the disk is a later addition as higher angular momentum, already contaminated material drifted into the galaxy, accumulated in a rotating disk and was gradually turned into the bulk of the stars. This provides a natural explanation for the two components of the Hubble classification and also a reason for the absence of the disk components in dense environments within which tidal or ram-pressure effects prevent the late formation of disks. While the details of this story have evolved, the overall picture has withstood the test of time remarkably well. The archaeological approach to galaxy formation and evolution continues, with much useful work being done in teasing out the details of how the extended spheroidal component was put into place. If this picture is

correct, then in the much more massive elliptical galaxies like M87 the secondary, stellar component added by the cannibalization of numerous smaller systems, may comprise 20 % up to 50 % of the total, in contrast to the much smaller fraction of accreted stars in the common, lower mass, disk-like spiral systems.

The Milky Way also holds most information about the detailed structure of the multi-phase interstellar medium (ISM). Most of the gas is found in three phases, the cold neutral medium, the warm neutral medium and the hot ionized medium. The hot phase fills about 30% of the volume (Ferrière 2001) in the disk but dominates further than a few kpc from the disk midplane (see Kalberla & Kerp 2009, and Sec. 3).

1.3 Learning from galaxy evolution with redshift

Observations of galaxies extending towards higher redshift (and thus earlier times) have given additional insight in galaxy properties of fundamental importance.

1.3.1 UBIQUITOUS WINDS Galactic winds, with velocities up to 500 km s^{-1} and most likely of bi-conical nature, carrying large amounts of material out of star forming galaxies (the rate being comparable to and higher than the star formation rate) are ubiquitous, not only in the nearby Universe (e.g. Heckman, Armus & Miley 1990; Heckman et al. 2000; Martin 1999; Rubin et al. 2014; Veilleux, Cecil & Bland-Hawthorn 2005) but also at higher redshift at the cosmic peak of conversion of gas into stars (Martin et al. 2013, Pettini et al. 2001, Shapley 2011, Steidel et al. 2010). At low as well as high redshift these winds most likely enrich the circum-galactic medium with gas, metals and possibly magnetic fields (Bernet, Miniati & Lilly 2013; Steidel et al. 2010; Werk et al. 2014), providing the material which, if falling back in at later times with added angular momentum (Peebles 1969), can be the source of the secondary disk systems. These winds transport gas out of the galaxies at rates similar to which gas is converted into stars and therefore have to be of importance for regulating the formation efficiency of stars in galaxies. Even at high redshift the launching sites of star formation driven (Newman et al. 2012b) and AGN driven (Genzel et al. 2014) winds can now be resolved with modern instruments.

1.3.2 SIZE EVOLUTION OF EARLY-TYPE GALAXIES Today's massive ($\sim 10^{11} M_{\odot}$) early-type galaxies can form early and become 'red and dead' by $z \sim 2$ as much smaller systems than those seen today ($\sim 1 \text{ kpc}$), with the growth in size (while not forming stars) to be understood as a likely sign of subsequent addition of stars in minor mergers at larger radii (e.g. Daddi et al. 2005, Danjanov et al. 2011, Trujillo et al. 2007, van Dokkum et al. 2010). Observations of significant structural evolution of massive early-type galaxies disfavor any singular monolithic collapse or binary merger formation scenario (van Dokkum et al. 2008). Also the observed strong increase in size and the weak decrease in velocity dispersion (Cenarro & Trujillo 2009) of the early-type galaxy population as a whole, which also includes additions to the red sequence at lower redshifts (see e.g. Fagioli et al. 2016, Patel et al. 2013b, van der Wel et al. 2014), poses tight constraints on any formation model. From the observed age distribution of stars in normal massive early-type galaxies we know that the substantial observed evolution was not caused primarily by the addition of newly formed stars but rather the addition and rearrangement of old stars in these systems.

1.3.3 EVOLUTION OF SPIRAL GALAXIES The high-redshift progenitors of Milky Way like disk systems are also smaller than local examples of similar systems and have formed

half of their mass below $z \sim 1$. Most of the mass is assembling at larger radii by in-situ star formation providing direct evidence for 'inside-out' growth accompanied by mass growth in the central regions which can be dominated by bars and bulges (Patel et al. 2013a). The central mass growth might originate from secular instabilities or merger events, but most stars currently in spiral systems were made from gas added to them rather than from accreted stars or stellar systems. In general the size evolution of spiral systems is, however, significantly less rapid than for early-type galaxies (van der Wel et al. 2014).

1.3.4 EVOLUTION OF STAR FORMATION RATES AND GAS FRACTIONS A significant fraction (if not most) of stars in the Universe are formed in galaxies with star formation rates that are almost linearly related to their stellar mass (the star formation main sequence) since $z \sim 2.5$ (see e.g. Daddi et al. 2007, Noeske et al. 2007, Renzini & Peng 2015, Whitaker et al. 2012). The tightness of the overall relation and the mostly disk-like morphology (Förster Schreiber et al. 2009, Genzel et al. 2006) of the highly star forming systems indicates that major merger driven starbursts are of minor importance for the universal star formation budget. The increase in star formation rate (the normalization of the main-sequence) towards high redshift is accompanied by increasing gas fractions reaching up to $\sim 50\%$ at redshift $z \sim 2$ (e.g. Daddi et al. 2010, Tacconi et al. 2010, 2013). This buttresses the simple picture that most star-formation comes from the gradual transformation of accumulated gas into stars.

1.4 Methods of solution

Let us return now to the physics problem to be solved given this observational background. First we look at what we have described as part (A) the evolution of radiation fields, dark matter and gas in the standard cosmological paradigm. This has been well summarized in several recent textbooks (e.g. Mo, van den Bosch & White 2010), so only some of the highlights need to be mentioned. A spectrum of adiabatic perturbations is imprinted onto the three components at high redshift producing cosmic microwave background radiation (CBR) fluctuations emitted at roughly redshift 1000, the analysis of which (cf. WMAP, Planck) uniquely specifies the cosmological model (Planck Collaboration et al. 2014, Spergel et al. 2007). If we take that to be the simplest one compatible with the data (the ' Λ CDM' cosmologically flat model), the model can be defined by five to six independent parameters that are typically known now (primarily, but not entirely from analysis of the CBR) to high accuracy. The composition of the dark matter remains unknown but the standard 'cold dark matter' model has been so successful that the principle remaining alternatives, Warm Dark Matter or Fuzzy Dark Matter behave essentially like Λ CDM on all large scales with (interesting) deviations becoming apparent below $\sim 1kpc$.

1.4.1 DIRECT SIMULATIONS OF DARK MATTER Accepting this model we can specify in a cosmologically representative volume the statistical distribution of gas, dark matter and radiation in a fashion sufficiently detailed to provide initial conditions for computation of the evolution of the various components. In the simplest treatments of this evolution, where dark matter is followed via Newton's laws and the transformation of gas into stars and black holes is ignored. Many different groups have worked on the problem producing extraordinarily successful (and convergent) results (see Frenk & White 2012). The Millennium simulation (Springel et al. 2005) was perhaps the most publicly successful such dark matter calculation, but other simulations (Klypin, Trujillo-Gomez & Primack 2011) also of

larger volumes (Angulo et al. 2012) or constrained to a certain halo mass scale (Diemand, Kuhlen & Madau 2007; Gao et al. 2012; Springel et al. 2008; Stadel et al. 2009) have made very important contributions. This is problem (A) and it is essentially a solved problem. But it leaves us a long way from understanding the evolution of real galaxies composed primarily of stars.

1.4.2 SEMI-ANALYTICAL MODELS FOR BARYONS There exist different approaches to the more difficult part (B), the allowance for star and black hole formation and the input from these sources of mass, energy, momentum and processed matter back into the gaseous component. The first approach to this hard problem was to set up comprehensible 'model problems' the solutions of which would be illuminating. One large class of such efforts has been broadly labeled the 'semi-analytic' method, where one takes the dark matter simulations as a given, and then tries, by one means or another, to estimate how the other components will react. Examples of progress made in the late 90's via the setting and solving of very informative 'model problems' consider the formation of disks from gas accumulating within dark matter halos (Dalcanton, Spergel & Summers 1997; Mo, Mao & White 1998). Modern attempts to input what are thought to be the most important physical processes in a simple fashion (e.g. Bower et al. 2006; Croton et al. 2006; Guo et al. 2011; Henriques et al. 2015; Kauffmann, White & Guiderdoni 1993; Somerville & Primack 1999) aim at finding that set which best produces realistic mock observations (see review by Somerville & Davé 2015). Another class of more analytical models makes the simplifying assumption that star forming galaxies evolve in a quasi-equilibrium fashion regulated by gas inflow and outflow, star formation and the change of mass in the galactic gas reservoir. The above approaches are extensively reviewed in Somerville & Davé (2015).

1.4.3 DIRECT SIMULATIONS INCLUDING BARYONS While these methods have been most helpful in furthering our understanding, the technical and algorithmic progress has enabled the direct and ambitious effort to include as much of the detailed physics as possible and simply compute forwards from the well established initial conditions to the current time using gravity, hydrodynamics, radiation transfer and all of the elaborate apparatus developed by physics to address continuum mechanics. The computational tools to follow the evolution of dark matter and stars (gravity) as well as gas (hydrodynamics) have been developed since the early 1980s.

The first three-dimensional coupled hydrodynamical simulations including self-gravity used the smoothed particle hydrodynamics (SPH) technique (Efstathiou & Eastwood 1981, Evrard 1988, Hernquist & Katz 1989). The Lagrangian particle based SPH method (Gingold & Monaghan (1977), Lucy (1977), see also Springel (2010b) and Somerville & Davé (2015) for recent reviews) is relatively simple to implement and due to its adaptive spatial resolution and good conservation properties has been very popular for galaxy formation simulations until today. However, the basic implementation has to be modified for typical astrophysical conditions including shocks, shear and large temperature gradients and it has become clear that some standard implementations have serious difficulties to properly model fluid mixing and sub-sonic turbulence (Agertz et al. 2007, Springel 2010b). Most of the recent SPH work on cosmological galaxy formation is based on derivatives of either the *GASOLINE* (Wadsley, Stadel & Quinn 2004) code or the *GADGET* (Springel 2005) code and include updated implementations to treat the mixing problem better (see e.g. Hopkins et al. 2014; Hu et al. 2014; Read & Hayfield 2012; Schaller et al. 2015; Schaye et al. 2015; Wadsley, Veeravalli & Couchman 2008 and references therein). As an alternative to the SPH method particle based

meshless-finite-mass and meshless-finite-volume methods have been proposed (Gaburov & Nitadori 2011). The recent *GIZMO* implementation is based on the *GADGET* framework and shows some significant improvements on idealised test problems, in particular for low Mach number gas (Hopkins 2015).

Eulerian hydrodynamic codes have also been widely used for cosmological simulations, some with adaptive mesh refinement capabilities. These codes typically perform better than SPH in terms of mixing and shock problems but might suffer from artifacts due to grid structure and numerical diffusion, which, for some solvers, can become significant. The first rough Eulerian treatment was by Cen & Ostriker (1992a) and the recently most used, greatly improved, Eulerian adaptive mesh refinement codes are *ENZO* (Bryan et al. 2014), *RAMSES* (Teyssier 2002), and ART (Kravtsov, Klypin & Khokhlov 1997) and also *FLASH* (Fryxell et al. 2000) as well as *ATHENA* (Stone et al. 2008) for ISM simulations on smaller scales. The newly developed moving mesh code *AREPO* (Springel 2010a) similarly suffers from numerical diffusion but combines advantages of the Lagrangian and Eulerian approaches and performs much better than traditional SPH codes like *GADGET* on mixing problems with a high convergence rate (Sijacki et al. 2012, Springel 2010b).

There are ongoing efforts to better understand the strengths and weaknesses of different numerical schemes (e.g. Hayward et al. 2014; Heitsch, Naab & Walch 2011; Hubber, Falle & Goodwin 2013; Kim et al. 2014; Price & Federrath 2010) and to constantly improve on accuracy and performance of all major codes. It has been realized early on that different numerical schemes applied to cosmological simulations can result in systems with different physical properties (Frenk et al. 1999), even if only gravity and hydrodynamics are considered. In addition, there is a wealth of published sub-resolution models (see Section 2.2.1) which are used to model galaxy formation. These models are often designed for particular numerical schemes and introduce even stronger variations in physical properties for a given set of initial conditions (Scannapieco et al. 2012). One of the major challenges in computational galaxy formation is to further improve on the numerical schemes and reduce the contribution of sub-resolution modeling to numerically resolved physical scenarios.

These numerical methods, which we could label 'ab initio' computations aiming to solve part (B), will be discussed in the second part of this review. But first we will address two other extremely useful idealized and empirical approaches which preceded and accompanied them.

1.5 Disks, Ellipticals and Mergers - a very useful set of idealized simulations

In the early 70s a definite cosmological model had not emerged and the computational resources as well as the numerical algorithms were still limited. This was the start of idealized merger simulations as it had been realized that galaxies actually interact and merge for bridges, tidal tails and other merger phenomena are observed (Joseph & Wright 1985, Sanders et al. 1988, Toomre & Toomre 1972). Early self-consistent N-body simulations (e.g. White 1978) were limited to the stellar component of galaxies with a few hundred gravitating particles (stars), a situation that has significantly improved until now when millions of star particles, dark matter particles and complicated gas dynamical processes can be studied (e.g. Hopkins et al. 2013). With methods for creating equilibrium models for multi-component galaxies (i.e. Hernquist 1993a) it became possible to simulate the evolution of the stellar and gaseous components of disk galaxies in more detail. For more than 20 years such setups are playing a major role for developing star formation and feedback

models in direct comparison with observations of star forming spiral galaxies (e.g. Agertz et al. 2013; Dalla Vecchia & Schaye 2008; Hopkins, Quataert & Murray 2011; Li, Mac Low & Klessen 2005; Mihos & Hernquist 1994b; Springel & Hernquist 2003). In most cases it is tested under which conditions a given model reproduces the observed relation between gas surface density and star formation rate surface density (Kennicutt 1998). Only successful models are then considered for more complex simulations of galaxy mergers or the cosmological formation of galaxies.

A number of important physical processes have been investigated with merger simulations and the insight into galaxy formation physics has been significant. We know that equal-mass mergers are rare and relatively unimportant for the cosmic star formation budget (see Sec. 1.3.4 and Bluck et al. 2009; Man et al. 2012; Williams, Quadri & Franx 2011). For intermediate mass galaxies (e.g. Milky Way) and low mass systems stars are primarily formed from streams of gas that accumulate centrally or in disks (e.g. Qu et al. 2017, Rodriguez-Gomez et al. 2016). For high mass systems (i.e. massive early-type galaxies) mergers become important. Stars added in major and minor mergers can make up as much as 50 % of the largely outer envelopes (in case of minor mergers) of these systems (Naab, Johansson & Ostriker 2009; Qu et al. 2017; Rodriguez-Gomez et al. 2016). But the initial proposal that normal ellipticals are made by morphological transformations of disk galaxies in binary major mergers of spirals, though not generally applicable (Ostriker 1980), is influential and instructive. In particular, it was shown that observed nearby disk galaxy mergers most likely evolve into systems with structural similarities to young early-type galaxies (e.g. Rothberg & Joseph 2004).

1.5.1 COLLISIONLESS MERGERS Merger simulations might be separated into two groups. Collisionless simulations of stars and dark matter mutually interacting by gravity alone were evolved by the collisionless Boltzmann equation (see e.g. Binney & Tremaine 2008). Such idealized systems can be considered energy conserving (no radiative losses). In reality almost no galactic system meets these conditions. Even massive galaxies have some amount of hot and cold gas (e.g. Serra et al. 2012, Sun et al. 2009, Young et al. 2011). But if the gas components can be considered dynamically unimportant it is justified to consider a system collisionless (the term 'dry' has been used in the literature). When spheroidal one-component systems merge, their structural evolution can -to good accuracy- be estimated using the virial theorem with only a few assumptions (Bezanson et al. 2009; Cole et al. 2000; Naab, Johansson & Ostriker 2009). Following Naab, Johansson & Ostriker (2009) one can assume that a compact initial stellar system has formed (e.g. involving gas dissipation) with a total energy E_i , a mass M_i , a gravitational radius $r_{g,i}$, and the mean square speed of the stars is $\langle v_i^2 \rangle$. According to the virial theorem (Binney & Tremaine 2008) the total energy of the system is

$$\begin{aligned} E_i &= K_i + W_i = -K_i = \frac{1}{2}W_i \\ &= -\frac{1}{2}M_i\langle v_i^2 \rangle = -\frac{1}{2}\frac{GM_i^2}{r_{g,i}}. \end{aligned} \quad (1)$$

This system then merges (on zero energy orbits) with other systems of a total energy E_a , total mass M_a , gravitational radii r_a and mean square speeds averaging $\langle v_a^2 \rangle$. The fractional mass increase from all the merged galaxies is $\eta = M_a/M_i$ and the total kinetic energy of the material is $K_a = (1/2)M_a\langle v_a^2 \rangle$, further defining $\epsilon = \langle v_a^2 \rangle / \langle v_i^2 \rangle$. Here $\epsilon = 1$ represents

an equal mass merger and $\epsilon \sim 0$ for very minor mergers. Under the assumption of energy conservation (e.g. Khochfar & Burkert (2006) indicate that most dark matter halos merge on parabolic orbits) the ratio of initial to final mean square speeds, gravitational radii and densities can be expressed as

$$\frac{\langle v_f^2 \rangle}{\langle v_i^2 \rangle} = \frac{(1 + \eta\epsilon)}{1 + \eta}, \quad \frac{r_{g,f}}{r_{g,i}} = \frac{(1 + \eta)^2}{(1 + \eta\epsilon)}, \quad \frac{\rho_f}{\rho_i} = \frac{(1 + \eta\epsilon)^3}{(1 + \eta)^5}.$$

For binary mergers of identical systems, $\eta = 1$, the mean square speed remains unchanged, the size increases by a factor of two and the densities decrease by a factor of four. In the limit that the mass is accreted in the form of a weakly bound stellar systems with $\langle v_a^2 \rangle \ll \langle v_i^2 \rangle$ or $\epsilon \ll 1$, the mean square speed is reduced by a factor two, the size increases by a factor four and the density drops by a factor of 32. These estimates are, however, idealized assuming one-component systems, no violent relaxation and zero-energy orbits with fixed angular momentum. In the presence of a dark matter halo the structural changes become more complicated and e.g. the fraction of dark matter at the center (inside the half-mass radius of the stars) may increase due to violent relaxation (Boylan-Kolchin, Ma & Quataert 2005; Hilz et al. 2012). In general a fraction of the orbital angular momentum of the galaxies will be transferred to rotation in the central galaxy, so that the merger remnants in most cases rotate significantly (Bois et al. 2010; Bois 2011; Di Matteo et al. 2009a; Naab, Khochfar & Burkert 2006; White 1979a). Major mergers of spheroidal galaxies are also expected to flatten existing abundance gradients (Di Matteo et al. 2009b, White 1979b).

If a spheroidal system experiences collisionless minor mergers (with satellite galaxies of much lower mass than the central) violent relaxation effects in the central galaxy are negligible and the satellite stars are stripped at larger radii (Villumsen 1983), a mechanism that offers a plausible explanation for the observed structural evolution of massive galaxies (Hilz et al. 2012; Nipoti, Londrillo & Ciotti 2003) and the formation of extended stellar envelopes in early-type galaxies leading to the very high observed Sersic indices and outer metallicity gradients (Hilz, Naab & Ostriker 2013; Villumsen 1983). Whether minor mergers alone can explain the observed strong size evolution of massive early-type galaxies will depend on the actual merger rates as well as the structure of the satellite galaxies (Bédorf & Portegies Zwart 2013; Cimatti, Nipoti & Cassata 2012; Newman et al. 2012a; Nipoti et al. 2009; Oogi & Habe 2013). Per added unit of stellar mass this process can also increase the fraction of dark matter within a half-mass radius more efficiently than major mergers (Boylan-Kolchin, Ma & Quataert 2005; Hilz, Naab & Ostriker 2013).

Another important process investigated is the morphological transformation of kinematically cold disk galaxies to kinematically hot spheroidal galaxies (Barnes 1992, Barnes & Hernquist 1992, Farouki & Shapiro 1982, Hernquist 1992, Negroponte & White 1983). Violent relaxation heats the disk stars and some fraction of the orbital angular momentum and of the spin of the initial disk systems can be absorbed by the dark matter halos (Barnes 1988). This results in stellar remnants that can have early-type galaxy morphology and kinematics if the progenitor galaxies had a bulge component of sufficiently high phase space density (Hernquist 1993b). Therefore merging is important for the formatin of hot stellar systems. Depending on the mass-ratio of the merging disks - and the amount of 'damage' that is done to the primary disk, the remnants rotate fast or slow, have disky, round or boxy isophotal shapes and are more or less flattened (Barnes 1998; Bekki 1998; Bendo & Barnes 2000; Bournaud, Combes & Jog 2004; Bournaud, Jog & Combes 2005; Cretton et al. 2001; González-García & Balcells 2005; Heyl, Hernquist & Spergel 1994; Jesseit et al. 2009; Naab & Burkert 2003; Naab, Burkert & Hernquist 1999). For very low mass infalling systems

the disk might be only moderately heated and retains its flat and rotationally supported morphology for single events (Quinn, Hernquist & Fullagar 1993; Velazquez & White 1999). Repeated minor mergers will make the initial disk system more spherical and reduce its spin (Bournaud, Jog & Combes 2007; Qu et al. 2010).

1.5.2 MERGERS WITH GAS A major step in understanding galaxy mergers was established once the simulations included a dissipative gas component. The gravitational torques exerted on the gas during the merger were able to drive the gas from large radii to the nuclear regions of the merger remnant once it lost its rotational support in tidally induced shocks (Barnes & Hernquist 1996). This has important implications for galaxy formation. Using sub-resolution models for the conversion of gas into stars (see Section 2.1), it was shown by many studies that the gas inflow can trigger a nuclear starburst similar to what is observed in ultra-luminous infrared galaxies (ULIRGS) and explain observations of 'extra light' in the centers of low mass early-type galaxies (Hayward et al. 2014; Hopkins et al. 2009a, 2013, 2009c; Kormendy 1999; Kormendy et al. 2009; Mihos & Hernquist 1994a,c, 1996; Springel 2000; Teyssier, Chapon & Bournaud 2010). Gas accumulating at the center of merger remnants also makes the potential more spherical, favoring the population of stars on tube orbits (Barnes & Hernquist 1996; Jesseit, Naab & Burkert 2007). As a result, rotating remnants of gas rich mergers can form disk-like subsystems (Barnes 2002; Bekki & Shioya 1997; Bendo & Barnes 2000; Jesseit et al. 2009; Jesseit, Naab & Burkert 2007) and show observed line-of-sight velocity distributions with steep leading wings, which is not the case if gas is neglected (Hoffman et al. 2009, 2010; Naab, Jesseit & Burkert 2006).

The effect of dissipation in binary galaxy mergers has also been used to explain the detailed shape of scaling relations and the fundamental plane and its potential evolution with redshift (Cox et al. 2006a,b, Dekel & Cox 2006, Hopkins et al. 2009b, Robertson et al. 2006b). One branch of binary merger simulations focused on the potential feeding of supermassive black holes, which are observed in most nearby early-type galaxies. Here the merger-triggered inflow provides the low angular momentum gas to be accreted onto the black hole (Hernquist 1989). The energy released from the accreting black hole, on the other hand, has been suggested to drive gas out of the merger remnant, significantly reducing its star formation rate (Springel, Di Matteo & Hernquist 2005a). The idea of 'black hole feedback' to 'quench massive galaxies' was born. Assuming a Bondi-like accretion and a relatively simple scaling for energy feedback in a sub-resolution model, it was also possible to provide an explanation for the observed stellar mass black hole mass relation (Di Matteo, Springel & Hernquist 2005). This finding has led to a number of studies, based on idealized binary merger simulations investigating the evolution of the $M_{\text{bulge}} - M_{\text{BH}}$ and $\sigma_{\text{bulge}} - M_{\text{BH}}$ relation (e.g. Barai et al. 2014; Choi et al. 2014; Debuhr, Quataert & Ma 2011; Debuhr et al. 2010; Johansson, Naab & Burkert 2009; Robertson et al. 2006c) and the evolution of the quasar luminosity function based on the assumption that most of the AGN activity is driven by galaxy mergers (e.g. Hopkins et al. 2005, 2006).

Despite the explanatory successes of these studies, the drawback of idealized sub-resolution models used is that the actual physical processes (e.g. the feedback from central supermassive black holes) cannot be resolved and the cosmological context is omitted. This is true for most merger simulations even though the typical spatial and mass resolution is much higher than in larger scale cosmological simulations (Section 2). The assumptions are mostly simple and physical effects are condensed or hidden in parameters or scale factors, which are often scaled to a specific set of observations (see Section 1.1). Therefore the validity of the astrophysical implications always remains somewhat uncertain. For exam-

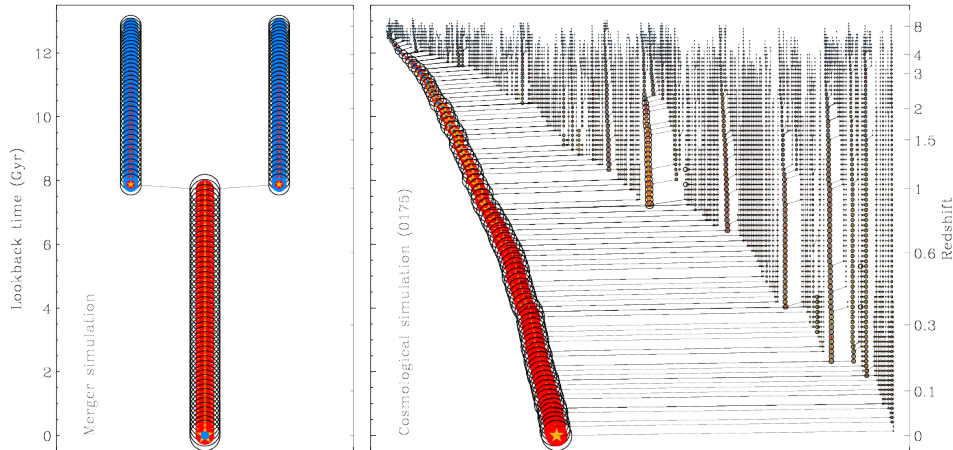


Figure 1:

Binary disk merger simulations are useful in understanding merging disk galaxies observed in the sky. In general, they lack the realism and complexity of the cosmological assembly of old massive early-type galaxies. In the left panel we show a schematic and very simplified binary disk 'merger-tree'. Two gas-rich (blue) stellar (yellow) disks with little hot gas (red) merge at $z \approx 1$ and form an elliptical galaxy. In a cosmological zoom simulation (right panel) of the formation of a dark matter halo (black circles) and its massive galaxy (cold gas: blue) is significantly more complex. It is evident that continuous infall of matter in small and large units is an important characteristic of the assembly of massive galaxies. The galaxy shown (0175 from Oser et al. 2010) is another extreme case as it has no major merger since $z \approx 3$. Others galaxies of similar mass can have up to three major mergers. Major mergers definitely happen and they have a strong impact on galaxy evolution. Cosmological assembly and mass growth, however, is always accompanied by numerous minor mergers and gas accretion (figure from Naab et al. 2014).

Many models adopted in binary merger simulations use a simple accretion scheme to determine the mass flow rates onto the black holes. The accretion rate depends on the sound-speed of the surrounding medium, which can vary significantly depending on the assumed star formation and feedback model (see Section 2.3). Alternative models link the accretion rates to gravitational instabilities and torques (Hopkins et al. 2012, Hopkins & Quataert 2011). Some models used for binary merger simulations assume feedback in the form of thermal energy to the gas surrounding the black hole (Springel, Di Matteo & Hernquist 2005a), others take into account the observed momentum output which significantly reduces the amount of hot coronal gas and the observable X-ray luminosities (Choi et al. 2014; Debuhr, Quataert & Ma 2011). Binary merger experiments have been used as test beds for sub-resolution models used in larger scale cosmological simulations.

1.5.3 CAVEATS OF THE MERGER HYPOTHESIS The importance of major mergers for the formation and evolution of massive galaxies is still under debate. Idealized merger simulations ignore the cosmological context where gas accretion, repeated minor mergers as well as environmental effects are important. As the expected major merger rates are low some massive galaxies might experience no major merger at all (see Fig. 1). It is clear that galaxy mergers, in particular of equal mass, can have a significant impact on

galaxy kinematics and mass growth if they happen at late times. The importance of stars formed in merger-triggered starbursts may have been overestimated as well, in particular due to the fact that most merger simulations ignored halo gas accretion. If halo accretion is included the disks have more realistic constant star formation rates and the contribution from merger triggered star formation is significantly lower and sometimes negligible (Moster et al. 2011). This is supported by observations indicating that most star formation in the Universe happens in relatively normal morphologically settled disk-like galaxies (e.g. Daddi et al. 2007). Merging systems with enhanced star formation rates seem to be of minor importance but might help in the transition to quenched early-type galaxies (Wuyts et al. 2011). Observations at low and high redshift also provide evidence that significant black hole accretion is not solely connected to merging but also gas rich disk like galaxies can host AGN of significant luminosity (Cisternas et al. 2011, Georgakakis et al. 2009, Kocevski et al. 2012, Schawinski et al. 2011). Also, cooling flow instabilities within the hot gas of elliptical galaxies lead to a secular branch of AGN fueling. Apparently major mergers can host luminous AGN but by no means are all AGN induced by mergers. Also it seems unlikely that the population of present day early type galaxies can have directly formed via mergers among the population of present day disk galaxies and their progenitors, as the early-type population is too old, too massive and too metal rich (Naab & Ostriker 2009). At earlier times the discrepancy in mass and size between observed Milky Way progenitors and massive early-type galaxies is even more pronounced (Patel et al. 2013a).

1.6 Ranking and Matching

A fundamental question in galaxy formation, embedded in the modern hierarchical cold dark matter framework, is how much of the available baryonic matter is converted into stars in the central galaxies in dark matter halos. This quantity might be termed galaxy formation efficiency or galaxy fraction f_{gal} . There have been a number of attempts to estimate this number for the Milky Way. Whereas the stellar mass of the Milky Way is relatively well determined (Rix & Bovy 2013), the major uncertainty is in the mass of the Milky Way's dark matter halo. Typically mass estimates are in the range of $1 - 2 \times 10^{12} M_{\odot}$ (Bland-Hawthorn & Gerhard 2016; Bovy et al. 2012; Li & White 2008; Watkins, Evans & An 2010; Xue et al. 2008). The masses result in galaxy fractions of $f_{\text{gal}} \sim 20 - 40\%$. With much better observed stellar mass functions at low and high redshifts and converged dark matter simulations for a given cosmological model, it has become possible to estimate the galaxy formation efficiency (or the relation of galaxy mass to halo mass) for a large range of halo masses locally and at higher redshifts. The methods used include halo occupation distribution modeling (Berlind & Weinberg 2002; Bullock, Wechsler & Somerville 2002; Kravtsov et al. 2004), conditional luminosity function modeling (Yang, Mo & van den Bosch 2003) or a rank ordered matching of observed galaxy mass functions to simulated halo mass functions (Behroozi, Conroy & Wechsler 2010; Behroozi, Wechsler & Conroy 2013; Conroy, Wechsler & Kravtsov 2006; Hearin & Watson 2013; Lu et al. 2015; Moster, Naab & White 2013; Moster et al. 2010; Shankar et al. 2006; Vale & Ostriker 2004, 2006).

Most of these studies indicate that around 10 - 20 % of the available baryons are converted into stars in dark matter halos of $\sim 10^{12} M_{\odot}$. This fraction is lower in dark matter halos of higher and lower mass with considerable uncertainties at both ends (see e.g. Gonzalez et al. 2013; Guo & White 2014; Kravtsov, Vikhlinin & Meshcheryakov 2014). The mismatch of most early cosmological simulations with these empirical estimates was highlighted in Guo et al. (2010) and galaxy fractions became a standard test presented in almost every publi-

cation about cosmological simulations. Also at higher redshift the tension with simulations was formerly much more severe (see e.g. Moster, Naab & White 2013) due to the overly efficient early conversion of baryons into stars.

The matching models also provide an independent estimate of the amount of stars formed in the galaxies (in-situ star formation as measured by the star formation rates) and the amount of stars accreted in galaxy mergers. The general conclusion is that all galaxies are dominated by in-situ star formation at high redshift ($z \gtrsim 1.5$). A trend that continues to low redshift for moderate mass (Milky Way type) galaxies which are predicted to have accreted between 5 % (Moster, Naab & White 2013) and 30 % (Behroozi, Wechsler & Conroy 2013) of their stellar mass. High mass galaxies assemble more and more of their stellar mass by mergers towards lower redshifts. However, the estimated fractions of accreted stars by $z=0$ of galaxies in massive halos ($M_{\text{halo}} \sim 10^{13}$) vary significantly between 20% and 60 % (Behroozi, Wechsler & Conroy 2013; Moster, Naab & White 2013; Yang et al. 2013). The general trend is similar to simulations (e.g. Gabor & Davé 2012, Lackner et al. 2012, Oser et al. 2010, Qu et al. 2017, Rodriguez-Gomez et al. 2016). It has also been highlighted that galaxies in massive halos ($M_{\text{halo}} \gtrsim 10^{13} M_{\odot}$) form their stars before the halo assembles. Low mass galaxies form their stellar components after their halos assemble (Conroy & Wechsler 2009).

2 Ab initio simulations of galaxy formation

2.1 Star formation and gas cooling

Most modern cosmological galaxy formation simulations allow for metal enrichment and metal dependent radiation equilibrium cooling (for specific implementations see e.g. Ceverino & Klypin 2009; Kravtsov 2003; Oppenheimer & Davé 2006; Scannapieco et al. 2005; Tornatore et al. 2007; Vogelsberger et al. 2013; Wiersma, Schaye & Smith 2009) of gas in the presence of the UV/X-ray background radiation from quasars and galaxies (e.g. Faucher-Giguère et al. 2009, Haardt & Madau 2012). If the gas is cooling rapidly, or in the presence of a rapidly changing radiation field, non-equilibrium cooling will be more accurate (see e.g. Gnat & Sternberg 2007, Oppenheimer & Schaye 2013a) and first steps in this direction have been made in galaxy scale simulations (Forbes et al. 2016; Hu et al. 2016; Oppenheimer et al. 2016; Oppenheimer & Schaye 2013b; Richings & Schaye 2016; Richings, Schaye & Oppenheimer 2014). Out of the cool gas reservoir the formation of the stellar populations is modeled in a simplified way as the relevant spatial and temporal scales as well as the complex ISM physics cannot be resolved in a cosmological context.

Cosmological simulations typically treat star formation in a Schmidt-type manner (Schmidt 1959) relating the local star formation rate density to the gas density divided by a time-scale. This time-scale depends on local gas properties like the dynamical and/or gas cooling time as introduced by Katz (1992) and Cen & Ostriker (1992b). Some implementations couple the star formation rate to molecular gas properties inspired by observed connections (Bigiel et al. 2008, Kennicutt & Evans 2012, Kennicutt et al. 2007, Leroy et al. 2008, Wong & Blitz 2002) and use a constant time-scale in combination with the variable local H_2 fraction (e.g. Christensen et al. 2012; Feldmann, Gnedin & Kravtsov 2012; Gnedin, Tassis & Kravtsov 2009; Kuhlen et al. 2012; Monaco et al. 2012; Pelupessy, Papadopoulos & van der Werf 2006; Robertson & Kravtsov 2008) which is, however, itself connected to the H_2 formation time-scale. It should be noted that H_2 based star formation models in galaxy simulations add another level of complexity and uncertainty. The small-scale structure of the ISM,

the detailed radiation field, ionization degrees, magnetic field strengths, all relevant for H_2 formation (e.g. Glover & Mac Low 2007, Hennebelle & Iffrig 2014, Walch et al. 2015), are unresolved in most galaxy scale and all cosmological simulations (see, however, Hopkins, Quataert & Murray 2012b) and it is unclear whether H_2 formation is the primary driver for star formation (see e.g. Glover & Clark 2012, Krumholz 2013).

The star formation models typically require a normalization, the star formation efficiency, as well as a parameter determining the scaling with gas density. The parameters are adjusted to match the zero point and the slope of the observed Kennicutt-Schmidt relation between star formation rate surface density and gas surface density (Kennicutt 1998). The basic implementations have been extended by sub-resolution models to capture some characteristics of the multi-phase structure of the gas (e.g. Springel & Hernquist 2003). An alternative implementation for star formation is based on gas pressure (see e.g. Schaye et al. 2015, Schaye & Dalla Vecchia 2008) assuming that galactic disks are in approximate vertical pressure equilibrium. Such a model has been shown to be in good agreement with the observed Kennicutt-Schmidt relation with no need for additional calibration (Schaye & Dalla Vecchia 2008). If used in combination with a fixed equation of state for the star forming gas the behaviour is similar to a density dependent criterion as the relation of gas pressure and density is fixed. In general, only gas below a certain temperature and above a certain density, which can be metal dependent, is eligible for star formation (see Hopkins, Narayanan & Murray (2013) for a discussion of star formation criteria). Also in large scale cosmological simulations these parameters must be calibrated as the ISM is in general unresolved and gas cooling is effectively not followed below a few thousand Kelvin (Khandai et al. 2015, Schaye et al. 2015, Vogelsberger et al. 2014).

2.2 The formation of disk dominated systems

Even though the formation of Milky Way systems has turned out to be the more difficult problem, it was historically the first one tackled. Can we make the Milky Way from reasonable cosmological initial conditions applying the relevant physical processes? Simulators typically have used the 'zoom technique' (Navarro & White 1994) wherein a representative region of the Universe is simulated first with a dark matter only code, and then a relevant high density piece is re-simulated with a hydro-dynamical code with allowance for the gravitational forces and gas inflow due to the surrounding matter.

In hierarchical cosmological models for the formation of galaxies, small structures form first, grow, and merge into larger objects. In this framework, galaxies form through the cooling of gas at the centers of dark matter halos, where it condenses into stars (White & Rees 1978). To match the observed properties of galaxies and galaxy clusters, purely gravitational processes on their own cannot account for cosmological structure formation, but gas cooling/dissipation processes must be considered (Binney 1977, Rees & Ostriker 1977, Silk 1977). These three very early papers already presented the physical arguments for the observed scales of galaxies noted in our first paragraph. It had been realized early-on from analytical estimates that the conservation of angular momentum of the cooling gas within dark matter halos could lead to the formation of galactic disks with flat rotation curves (Fall & Efstathiou 1980). In early work (White & Rees 1978) it was already noted that at high-redshift gas has to be prevented from excessive cooling into overly dense regions - possibly by feedback from massive stars to avoid the overproduction of condensed baryonic matter (Dekel & Silk 1986, Larson 1974, Navarro & Benz 1991). Also, to produce dynamically cold and thin stellar, extended disks, the accretion of high angular momentum gas

from outer regions of the halos is needed in the more recent past (Fall 1979). This would require feedback processes to eject gas and avoid early over-efficient star formation at high redshift as well as the formation of gas reservoirs to allow the gas to return at low redshifts with higher angular momentum.

Early cosmological simulations including the dissipative gas component (but neglecting star formation) confirmed the problem (Katz & Gunn 1991, Navarro & Benz 1991, Navarro & White 1994). Too many baryons settled into disks which were much more compact than observed spiral galaxies with too high rotation velocities due to substantial angular momentum loss during the assembly process caused by mergers. Not only was the angular momentum for the forming gaseous disks too low, but also too many baryons would be locked up in galaxies (Navarro, Frenk & White 1995; Navarro & Steinmetz 1997).

The over-cooling problem was confirmed by many studies that followed (see e.g. Balogh et al. 2001). Once a stellar component was included in the simulation it was possible to approximately treat the feedback from young stellar populations. In addition to radiative cooling the role of energy injection by supernovae could be tested. Investigators quickly discovered that, while the detailed implementation can change the results significantly (e.g. Navarro & White 1993; Okamoto et al. 2005; Robertson et al. 2004; Sommer-Larsen, Gelato & Vedel 1999; Thacker & Couchman 2000) almost all cosmological simulations resulted in the overproduction of stars, in low angular momentum bulges (e.g. Balogh et al. 2001; Katz, Weinberg & Hernquist 1996; Kereš et al. 2005). It was again suggested that the origin of the problem lies at higher redshift (D’Onghia & Burkert 2004, van den Bosch et al. 2002). Galaxies would be less concentrated and have higher specific angular momentum if gas cooling were suppressed before the host halo has assembled (Weil, Eke & Efstathiou 1998). Still, simulations experimenting with thermal and kinetic energy injection (e.g. Abadi et al. 2003a and many that followed) resulted in similar problems, with the conclusion that the assumed feedback models were insufficient to prevent the early collapse of low angular momentum baryons and their conversion into stars, a problem that remained unsolved for a long time.

Thus, the early attempts at ab initio cosmological computations failed or only partially succeeded to make disk systems that were as low mass and extended in space and time of formation as those in the real Universe (Abadi et al. 2003a,b; Agertz, Teyssier & Moore 2011; Governato et al. 2004; Piontek & Steinmetz 2011; Robertson et al. 2006a, 2004; Scannapieco et al. 2009). It is important to recall that observations had shown (see Section 1.1) that real, forming galaxies were embedded in strong gaseous outflows that were missing from the simulations.

Recently, a number of groups have made significant progress on reducing the galaxy fraction, f_{gal} , in halos of $\sim 10^{12}M_{\odot}$ and at the same time forming spiral galaxies with more realistic properties. In Fig. 2 we show examples from six groups who recently succeeded in producing disks with spiral like morphologies but very different simulation codes. These studies utilize a variety of qualitatively different sub-resolution approaches to the response of the high-density star forming gas on newly formed and dying stellar populations. All these ‘successful’ approaches have in common that gas in dense star forming regions can efficiently be pushed out in a galactic outflow and, possibly, escape from the galaxies and their dark matter halos. With outflow launching, Milky Way like halos develop disk-like galaxies. Detailed investigations of gas flows in the forming galaxies - which are most easily followed in Lagrangian SPH simulations (see also Genel et al. 2013, Nelson et al. 2016, 2015)- have revealed most characteristics and consequences of galactic outflows. With strong stellar feedback, a significant fraction of the low angular momentum gas cooling to the centers of

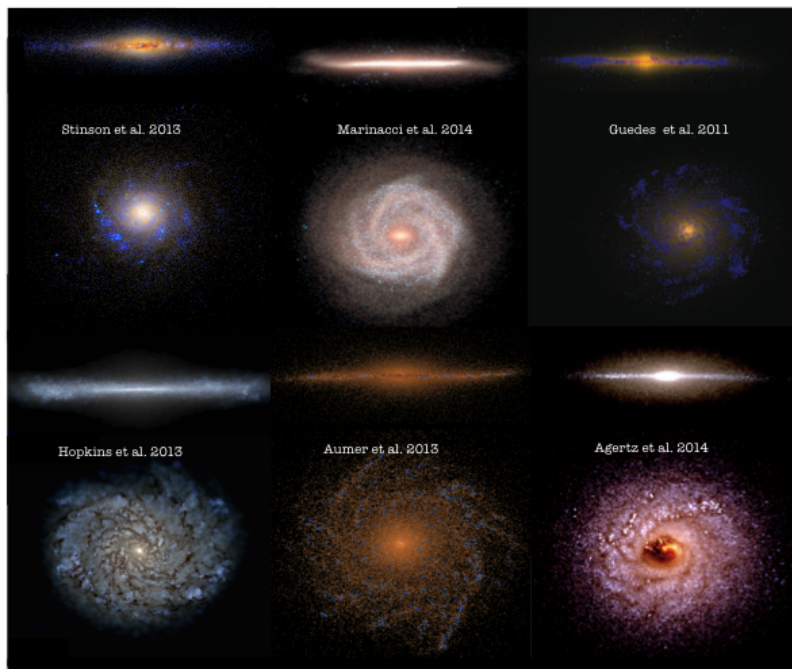


Figure 2:

Recent cosmological zoom simulations with strong stellar feedback of galaxies with spiral like morphologies. The pictures show mock images of the stellar light. *Top left:* SPH (*GASOLINE*) simulation of Stinson et al. (2013) including dust attenuation. *Top middle:* Moving-mesh (*AREPO*) simulation of Marinacci, Pakmor & Springel (2014). *Top right:* SPH (*GASOLINE*) simulation of Guedes et al. (2011). *Bottom left:* SPH (*GASOLINE*) simulation of Hopkins et al. (2014). Only the face-on view includes dust attenuation. *Bottom middle:* SPH (*GADGET*) simulation of Aumer et al. (2013). *Bottom right:* AMR (*RAMSES*) simulation of Agertz & Kravtsov (2015). Only the face-on view includes dust attenuation.

dark matter halos at high redshift is prevented from being converted into stars and can be blown out of the galaxies. When the proto-galaxies are still small and have shallow potential wells, this gas will leave the galaxies and never return or can return at much later times with angular momentum enhanced by non-linear gravitational torques or mixing (e.g. Marinacci et al. 2011) with the rotating halo gas (Brook et al. 2011, Übler et al. 2014). The outflow suppresses the formation of stellar bulges from the low angular momentum gas at high redshift and enriches the circum-galactic medium with metals (Brook et al. 2012, Christensen et al. 2016, Governato et al. 2010, Marinacci et al. 2014). It also reduces the previously reported dramatic effects of mergers. The gas still loses angular momentum but a significant fraction can be ejected before stars are formed. This is particularly efficient if the mergers happen early in smaller proto-galaxies (Übler et al. 2014).

Contrary to what has been believed for a long time, even galaxies with early major mergers can evolve into present day disk-like galaxies with low bulge fractions (Aumer, White & Naab 2014; Robertson et al. 2006a; Springel & Hernquist 2005). For more massive

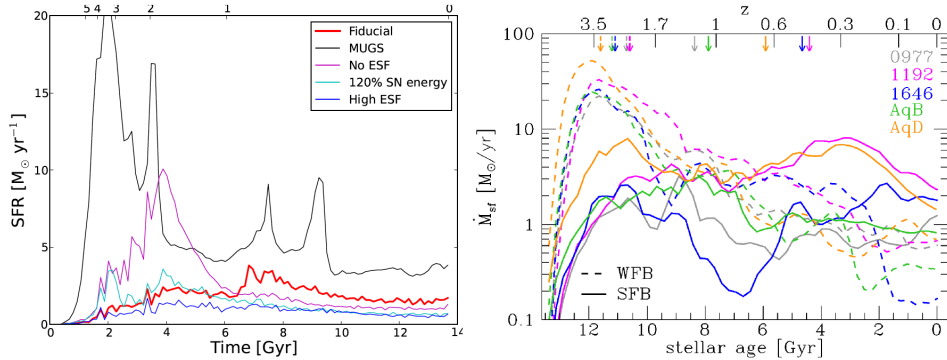


Figure 3:

The effect of stellar feedback on the star formation histories of simulated disk galaxies. Stronger feedback results in the suppression of early star formation, relatively flat star formation histories and, in the cases shown here, disk like morphologies. The flatter star formation rate histories but not the disk-like morphologies are generic for all simulations with strong feedback. Flat star formation histories are in better agreement with observations of Milky Way-sized spiral galaxies. *Left panel:* The simulations presented in Stinson et al. (2013) show peaked star formation histories for simulations with weak feedback (MUGS Stinson et al. 2010, No ESF). Star formation at high redshift is suppressed for models with strong feedback (Fiducial, 120% SN energy, High ESF). *Right panel:* The same trend is seen in a comparison of five galaxies simulated with weak (dashed lines, Oser et al. 2010) and strong feedback (solid lines, Aumer et al. 2013). The stellar half-mass formation times (arrows) are shifted from $z \sim 2$ to $z \lesssim 1$ (Übler et al. 2014).

systems the enriched gas is kept within the halo (in a galactic fountain) and is accreted back onto the galaxy later on with metallicity enhanced, sometimes repeatedly (Brook et al. 2014, Genel et al. 2015, Oppenheimer & Davé 2008, Oppenheimer et al. 2010, Pilkington et al. 2012). This process reduces star formation and delays the onset of galaxy formation in halos of all masses, in much better agreement with high redshift abundance matching constraints (e.g. Hirschmann et al. 2013, Hopkins et al. 2014, Stinson et al. 2013). The late accretion of gas with high angular momentum from outside the halo is increased as fewer baryons were converted into stars in accreted structures. This is pretty much as it was predicted 38 years ago (Fall 1979).

In addition, at low redshift a moderately constant gas accretion rate onto spiral galaxies can be sustained by enriched gas that has been cycling within the halo of the galaxy (Christensen et al. 2016, Oppenheimer et al. 2010, Übler et al. 2014). Therefore gas accretion onto the galaxy is decoupled from the halo assembly, resulting in flatter star formation histories more consistent with observations (Hirschmann et al. 2013, Hopkins et al. 2014, Stinson et al. 2013, Woods et al. 2014). In Fig. 3 we show two recent examples of the generic effect of strong feedback on galactic star formation rate histories. Additionally, Milky Way progenitor galaxies are larger (with strong feedback models) already at high redshift and the overall cosmological evolution in size is significantly reduced (Aumer, White & Naab 2014; Hirschmann et al. 2013) in much better agreement with observations. The above results rely on 'recipes' to treat physical processes that are relevant below the resolution scale of the simulations and sometimes even impact the simulation in well resolved regions. The variety of these models is remarkable and a good understanding of the strengths and weaknesses of these models is relevant to assess whether scientific progress has been made

or whether the good agreement with observations is the result of an empirical matching exercise. In the following we review the general pathways followed by different groups.

2.2.1 CURRENT SUB-RESOLUTION MODELS FOR FEEDBACK FROM STELLAR POPULATIONS

Feedback from massive stars has long been suggested to resolve the over-cooling problem in galaxy formation and various different sub-resolution feedback models have been presented to approximate the complex physical processes. Here we call a sub-resolution model an empirical, physically motivated numerical recipe representing the large scale impact of energy, mass and momentum during the life and death of massive stars in state of the art cosmological simulations of large volumes. These models are necessary as the finest resolution elements (in large scale cosmological simulations) are typically a few hundred parsecs which makes it impossible for these simulations to capture the small-scale multi-phase structure of the galactic ISM. In Section 3.1 we will demonstrate why these models can only be a crude representation of reality, limiting the predictive power of present day galaxy formation simulations.

One class of models might be termed 'delayed cooling' models (Gerritsen 1997, Thacker & Couchman 2000). In one incarnation of this approach (Stinson et al. 2006) the energy from supernova explosions is injected into neighboring gas but the cooling is 'turned off' for gas inside the expected Sedov blast wave radius (McKee & Ostriker 1977). This way gas can efficiently be heated and accelerated. Although often being criticized as being unphysical due to the suppression of gas cooling, the model attempts to allow for formation of super-bubbles (e.g. Mac Low & McCray 1988, see Keller, Wadsley & Couchman (2015) for a modern implementation of superbubble formation in cosmological simulations and Section 3.1). The 'delayed cooling model significantly reduces the galaxy stellar masses and promotes the formation of disk dominated systems (Governato et al. 2007; Guedes et al. 2011; Keller, Wadsley & Couchman 2016). The models have been extended, in a simplified way, by taking into account the additional energy release from massive stars before they explode as supernova (Kannan et al. 2014, Stinson et al. 2013, Wang et al. 2015). It has been pointed out by Rosdahl et al. (2016) that the delayed cooling approach results in a significant amount of thermally unstable circumgalactic gas, which can be problematic when estimating the gas emission and absorption in galactic halos.

A related approach is 'stochastic thermal' feedback (Dalla Vecchia & Schaye 2012), which does not suffer from some of the problems of the 'delayed cooling' approach (see e.g. Rosdahl et al. 2016). Here the mean thermal energy injection per unit formed stellar mass is fixed and neighboring star particles are, stochastically, only heated if their temperature can be moved above a certain temperature threshold (e.g. $\gtrsim 10^{7.5} K$). This guarantees long cooling times, the onset of a Sedov phase and efficient momentum generation similar to the 'delayed cooling' models. The total energy injection is an adjustable parameter and can slightly exceed the available supernova energy (Crain et al. 2015, Schaye et al. 2015) compensating for the artificial overcooling. However, the model has been demonstrated to drive strong winds (Dalla Vecchia & Schaye 2012). It has been used for one of the most successful cosmological galaxy formation simulation suite (the Eagle simulations, Schaye et al. 2015) in terms of matching observed galaxy population properties and their evolution with redshift (Bahé et al. 2016, Furlong et al. 2015, Rahmati et al. 2015, Schaye et al. 2015).

The gas cooling is also delayed in 'non-thermal' heating models (Teyssier et al. 2013). Here the energy is injected into a non-thermal energy component, representing turbulence, magnetic fields or cosmic rays, with a dissipation time-scale of $\sim 10 Myr$. The energy injection procedure follows the 'stochastic thermal' heating (e.g. Roškar et al. 2014).

A 'two phase' approach is followed in Scannapieco et al. (2006) where the hot and the cold gas phase are evolved separately using SPH (Marri & White 2003). The supernova energy added to a cold gas particle is stored (i.e. decoupled from the hydrodynamics) and only released when it can become a constituent of the hot phase. Accounting for the momentum input by supernovae and (potential) radiation pressure in a simplified way this model also produces spiral galaxies with realistic properties (see Fig. 2, Aumer et al. 2013).

Another popular approach might be termed 'wind feedback'. Some fraction of the energy released by massive stars is injected into the surrounding gas in the form of energy or momentum by which it is driven away from the region of star formation. The wind is parameterized by a mass loading factor η , i.e. the ratio of wind mass-loss to the star formation rate and by a wind velocity v_{wind} . The original implementation assumed a constant mass loading and a fixed wind velocity coupled to a stiff effective equation of state for the gas resulting from thermal energy input from supernovae (Springel & Hernquist 2003). Here the gas in the wind is decoupled from the hydrodynamical calculations when leaving the star forming regions with its given velocity and is later (the conditions depend on the respective implementations) incorporated in the calculations again (see also Vogelsberger et al. 2014). Observations and theoretical considerations, however, indicate decreasing mass-loading and increasing wind velocities in higher-mass galaxies with higher star formation rates (Martin 2005; Murray, Quataert & Thompson 2005). This motivated Oppenheimer & Davé (2006, 2008) to introduce a momentum driven wind model. The wind velocity scales with the velocity dispersion of stars in the galaxies (or the dark matter, Vogelsberger et al. 2013) $v_{\text{wind}} \propto \sigma$, the momentum input scales with the star formation rate, $\dot{m}_{\text{wind}} \times v_{\text{wind}} \propto \dot{m}_*$, and the mass loading is inversely proportional to the velocity dispersion $\eta \propto dm_{\text{wind}}/dm_* \propto 1/v_{\text{wind}} \propto 1/\sigma_*$. Again, to ensure that the gas leaves the star-forming regions it is then decoupled and later re-incorporated in regions with lower gas density.

Although this model has become popular, some authors (Schaye et al. 2010) turned off the 'wind decoupling' the consequences of which are discussed in Dalla Vecchia & Schaye (2008). Although empirical in nature, the galactic wind models results in realistic (compared to observations) enrichment histories of galaxies and the circum-galactic medium (Davé, Finlator & Oppenheimer 2011; Finlator & Davé 2008), lower conversion efficiencies in particular in the regime of disk galaxies (Puchwein & Springel 2013, Sales et al. 2010), reasonable abundances and flatter star formation histories for low mass galaxies and higher gas fraction for star forming galaxies at high redshift (Davé, Finlator & Oppenheimer 2011; Hirschmann et al. 2013; Oppenheimer & Davé 2008) and a more realistic cosmic star formation history (Schaye et al. 2010). Although originally developed for SPH simulations, decoupled 'momentum driven' winds have also been used in recent moving mesh simulations with wind velocities scaled to the local dark matter velocity dispersions (e.g. the Illustris simulation, Vogelsberger et al. 2014). With cosmological zoom simulations it has been demonstrated that realistic present day spiral galaxies (Grand et al. 2016; Marinacci, Pakmor & Springel 2014) as well as gas rich massive high-redshift disks (Anglés-Alcázar et al. 2014, Genel et al. 2012) can be formed with a momentum driven wind model in which 'decoupling' has been applied.

Alternatively, an energy driven wind model has been proposed (Okamoto et al. 2010) to explain the low abundance of satellite galaxies in the Milky Way. Here the wind velocity also is assumed to scale with the velocity dispersion $v_{\text{wind}} \propto \sigma$, the energy input scales with the star formation rate, $\dot{m}_{\text{wind}} \times v_{\text{wind}}^2 \propto \dot{m}_*$, and the mass loading is taken to be inversely proportional to the square of the stellar velocity dispersion $\eta \propto dm_{\text{wind}}/dm_* \propto$

$1/v_{\text{wind}}^2 \propto 1/\sigma^2$. This model results in the same wind speeds but higher mass-loading for lower mass galaxies and better agreement for the Milky Way satellites luminosity function (Okamoto et al. 2010). In a hybrid model Davé et al. (2013) combine a momentum driven wind scaling with the energy driven wind scaling for galaxies below $\sigma = 75 \text{ km s}^{-1}$ to obtain a better match to the galaxy mass function at low masses (see also Barai et al. (2013) for a 'radially varying wind model'). This transition was motivated by the idea that low mass galaxies are more affected by supernova explosions whereas the effect of radiation pressure takes over at higher masses (Murray, Quataert & Thompson 2005, 2010). In an updated incarnation of the 'decoupled' wind model Davé, Thompson & Hopkins (2016) have used scaling from high-resolution cosmological zoom simulations (Muratov et al. 2015) to set the mass-loading and wind velocities. Efforts are underway to replace these heuristic methods with others based more closely on high-resolution multi-phase physical modeling.

2.3 The formation of bulge dominated systems

Spheroidal early-type galaxies have been 'easier' to simulate from straightforward cosmological initial conditions (any cosmological simulation with weak feedback will result in the overproduction of spheroidal galaxies). The escape velocities are larger for these more massive systems and so the energy input from feedback matters somewhat less, and, while still important, stellar feedback appears to be less critical to the formation process. Empirically they are known to form in dense regions starting at early times and the observed structures of proto-ellipticals are quite small as seen at redshift $z = 2-3$ (see Section 1.3). Thus, the difficulties encountered in making disk-like systems - too early star formation in too concentrated systems - are alleviated for the construction of physically plausible spheroidal systems. As a consequence, cosmological simulations with weak stellar feedback and without AGN feedback have effectively been used as reasonable initial models for the formation of massive, early type galaxies. In these simulations the final galaxies follow observed early-type galaxy scaling relations of size and velocity dispersion with stellar mass (Feldmann, Carollo & Mayer 2011; Feldmann et al. 2010; Johansson, Naab & Ostriker 2012; Naab et al. 2007; Oser et al. 2010). They also have plausible stellar populations with metallicity distributions that are modulated by their merger history (Kobayashi 2004, 2005). However, compared to observations based on abundance matching constraints, their stellar masses are about a factor of 2 - 4 too high at a given halo mass (Oser et al. 2010). This has been presumably due to the lack of sufficient energy input (see e.g. Croton et al. 2006, Meza et al. 2003), and it was alleviated as AGN feedback simulations have been improved.

For high halo masses, the evolution of the galaxies shows a clear two-phase characteristic (Feldmann et al. 2010; Johansson, Naab & Ostriker 2012; Naab et al. 2007; Navarro-González et al. 2013; Oser et al. 2010; Qu et al. 2017; Rodriguez-Gomez et al. 2016). At early times ($z \gtrsim 1.5$) the galaxies grow by in-situ star formation in the deep potential wells of massive halos. As the low angular momentum gas is efficiently converted into stars, some of the systems can be remarkably small (also supported by mergers, Bournaud et al. 2011a, Wuyts et al. 2010), very similar to the population of observed high-redshift compact galaxies (Oser et al. 2012, 2010, Sommer-Larsen & Toft 2010, Wellons et al. 2016). Towards lower redshifts in-situ star formation becomes less important as cold gas can no longer easily penetrate the shocked hot gaseous halos (e.g. Birnboim & Dekel 2003) and the mass assembly becomes dominated by the accretion of stars that have formed in other galaxies. Cosmological simulations clearly indicate that stellar accretion is more important at higher galaxy masses (Gabor & Davé 2012, Lackner et al. 2012, Oser et al. 2010, Qu et al. 2017,

Rodríguez-Gomez et al. 2016). This robust trend is also found in abundance matching estimates (Section 1.6) and semi-analytical galaxy formation models (Guo & White 2008, Khochfar & Silk 2006) and it is strongest for central galaxies in galaxy clusters (De Lucia & Blaizot 2007, Ostriker & Hausman 1977). The late, collisionless assembly has important consequences for the structural evolution of the system. As a significant fraction of mass can be accreted in mergers with smaller and less bound systems (Gabor & Davé 2012, Lackner et al. 2012), this stellar mass is added to the systems at large radii (Navarro-González et al. 2013, Oser et al. 2010, Qu et al. 2017, Rodríguez-Gomez et al. 2016). The resulting strong increase in galaxy size is driven by accreted stars. Simple arguments based on the virial theorem (Bezanson et al. 2009; Naab, Johansson & Ostriker 2009) show that the same mass added in many minor mergers will produce a much more extended galaxy than if that mass had been added in fewer, more major mergers (Eq. 1, Section 1.5). Together with the weak decrease in velocity dispersion the evolution of the individual model galaxies is consistent with observational estimates.

The low present day star formation rates and spheroidal shapes of galaxies simulated with weak stellar feedback are primarily caused by the efficient early gas depletion and early conversion of gas into stars in combination with efficient shock heating of the halo gas and gravitational heating caused by the accretion of smaller systems (Johansson, Naab & Ostriker 2009; Khochfar & Ostriker 2008). Still, the weak feedback models provide an attractive start for the physical solution of the observed structural evolution of massive galaxies (see also Feldmann, Carollo & Mayer 2011; Feldmann & Mayer 2014). In its extreme limit the assembly of brightest cluster galaxies and the size evolution of cluster galaxies can be well explained in a substantially collisionless cosmological assembly model assuming that all stars in cluster progenitor galaxies have formed before $z \sim 2$ (Laporte et al. 2013).

With simulations neglecting AGN feedback it has been shown that the formation history of massive galaxies leaves its imprint on the gas and stellar kinematic properties of present day early-type galaxies (Naab et al. 2014, Serra et al. 2014, Wu et al. 2014). Epochs dominated by gas dissipation will result in the formation of flattened stellar distributions (disks), supported by rotation. Major mergers are rare, and during minor merger dominated phases the stellar systems experience stripping and violent relaxation, existing cold gas may be driven to the central regions causing starbursts, trigger the formation and growth of super-massive black holes or be expelled from the systems in galactic winds. This, in turn, will impact the distribution of cold gas and the kinematics of stars forming thereof. With improved cosmological simulations we move towards a better understanding of the angular momentum evolution of galaxies (see Genel et al. 2015, Zavala et al. 2016). In a first step, using cosmological zoom simulations (Naab et al. 2014) have been able to demonstrate that gas dissipation and merging result in observable features (at present day) in the two-dimensional kinematic properties of galaxies, which are clear signatures of distinct formation processes.

Many of these features are in agreement with all the valuable predictions from isolated merger simulations (see Section 1.5). Dissipation favors the formation of fast rotating systems and line-of-sight velocity distributions with steep leading wings, a property that can be directly traced back to the orbital composition of the systems (Röttgers, Naab & Oser 2014, see also Bryan et al. (2012) for the orbital distribution of dark matter). Merging and accretion can result in fast or slowly rotating systems with counter-rotating cores, cold nuclear or extended (sometimes counter-rotating) disks showing dumbbell-like features all observed in real galaxies and in part well understood from binary merger experiments.

We have seen that models with stronger feedback and metal cooling, applied to cosmological simulations, delay the onset of star formation in more massive halos and the systems become more gas rich at high redshift, a trend that continues towards low redshift. This makes galaxies too massive with too high star formation rates in particular at the central regions (e.g. Kravtsov & Borgani 2012). This had also been found prior to cosmological simulations (e.g. Ciotti et al. 1991, Ciotti & Ostriker 1997), due simply to the inevitable cooling flows occurring in massive systems. One dimensional and two dimensional high resolution simulations of the effect of AGN feedback (Binney & Tabor 1995; Ciotti & Ostriker 2001; Novak, Ostriker & Ciotti 2011; Sazonov et al. 2005) indicated that AGN feedback alleviates this problem. With ab initio cosmological simulations a number of groups have now demonstrated that ‘feedback’ from an accreting supermassive black hole can suppress the residual star formation in the central regions of massive galaxies, confirming the proposal put forward by Silk & Rees (1998). In the following we review some sub-resolution approaches for implementing feedback from supermassive black holes.

2.3.1 CURRENT MODELS FOR FEEDBACK FROM SUPER-MASSIVE BLACK HOLES Several different models have been proposed to approximate the effect of AGN feedback and to follow it in cosmological simulations. In most galaxy scale sub-resolution models (starting from Springel, Di Matteo & Hernquist 2005b) the accretion rate onto the black hole \dot{M}_{BH} is computed based on the Bondi-Hoyle-Lyttleton formula (actually invented for spherical accretion of interstellar gas onto the Sun, Bondi 1952, Bondi & Hoyle 1944, Hoyle & Lyttleton 1939)

$$\frac{dM_{BH}}{dt} = \alpha_{\text{boost}} \frac{4\pi G^2 M_{BH}^2 \rho}{(c_s^2 + v_{\text{rel}}^2)^{3/2}}. \quad (2)$$

Here c_s is the sound speed of the surrounding gas and v_{rel} is the relative velocity of the black hole and the gas (see Rosas-Guevara et al. (2015) for modifications of the Bondi rate due to an assumed viscous accretion disk, see also Hopkins et al. (2016) for the possible failure of Bondi accretion in high-resolution simulations). Also included in many models is an adjustable accretion ‘boost factor’ α_{boost} which can have values up to 100 in some implementations. The general motivation for using a boost factor is the low resolution of the simulations which are unable to follow the accurate multi-phase gas structure near the black holes and therefore the accretion rates (see discussion in Booth & Schaye 2009). In fact many implementations use Bondi accretion in combination with a stiff equation of state for the high density gas resulting in gas with increasing temperature at higher densities - contrary to the expected structure in the dense ISM (Hirschmann et al. 2014, Khandai et al. 2015, McCarthy et al. 2010, Puchwein & Springel 2013, Schaye et al. 2015, Vogelsberger et al. 2013, 2014). As a result the sound speed becomes artificially high and a high α_{boost} compensates for this. From a practical, not physical, point of view the boost factor ensures that enough gas is accreted to grow super-massive black holes of reasonable masses. As in Springel, Di Matteo & Hernquist (2005b), the accretion in most models is limited by the Eddington rate. In some recent implementations (see, however, Pelupessy, Di Matteo & Ciardi 2007) the relative velocity between the black hole and the ambient medium is not considered (the Lyttleton part) as the black holes are continuously centered to the potential minimum of the host halo (e.g. Puchwein & Springel 2013, Vogelsberger et al. 2014). Choi et al. (2012) take an alternate approach that does not have a boost factor; they stochastically treat the overlap of the smoothing sphere and the Bondi sphere, thereby

statistically allowing for the resolution limits. Also Schaye et al. (2015) have eliminated the boost factor and regulate the Bondi rate with the ratio of the Bondi to viscous time-scale (Rosas-Guevara et al. 2015). Still, the same limitations apply for the temperature and density structure of the nuclear gas.

It has been proposed by Shlosman, Frank & Begelman (1989) that black holes might be primarily fed by gas driven to the center by gravitational torques from non-axisymmetric perturbations (see also e.g. Bournaud et al. 2011b, Gabor & Bournaud 2013, Hopkins & Quataert 2011). Hopkins & Quataert (2011) argue that 'torque limited' accretion behaves qualitatively different to other accretion models and produces reasonable scaling relations with a smaller scatter. The parametrized version of this accretion model is a bit more complicated and less straight forward to be included in larger scale cosmological simulations, but the first attempts are promising (Anglés-Alcázar et al. 2016; Anglés-Alcázar, Özel & Davé 2013). Clearly the choice between the two approaches should be driven by the ratio of the amount of angular momentum in the gas to be accreted with the 'torque limited' model when the ratio of the centrifugal radius to the Bondi radius becomes larger than unity.

Approaches following the traditional feedback models assume that some fraction ($\epsilon_{\text{therm}} \sim 0.05$) of the bolometric luminosity $L_{\text{bol}} = \epsilon_r dM_{\text{BH}}/dt c^2$ (Shakura & Sunyaev 1973, Soltan 1982), with c being the speed of light and a radiative efficiency of $\epsilon_r = 0.1$ (Shakura & Sunyaev 1973), is converted into and deposited as thermal energy in the surrounding ISM such that the energy injection rate is $dE_{\text{therm}}/dt = \epsilon_{\text{therm}} \epsilon_r \dot{M}_{\text{BH}} c^2$. Sijacki et al. (2007) proposed a 'jet bubble' modification to this simple model depending on the gas accretion rate onto the black hole. For accretion rates above 1% of the Eddington rate the usual fraction of $\epsilon_{\text{therm}} \epsilon_r$ of the accreted rest mass energy is deposited as thermal energy to the surrounding medium. For lower accretion rates the feedback efficiency is increased from 0.5% to 2% of the rest mass energy and is injected into heated off-center bubbles that can then buoyantly rise (see Fabjan et al. (2010), Hirschmann et al. (2014), and Vogelsberger et al. (2014) for slightly modified versions). Such models are designed to mimic the observed jet induced bubble formation (Fabian 2012, Fabian et al. 2006) and, due to the enhanced coupling efficiency at low accretion rates, i.e. low black hole growth rates (see e.g. Churazov et al. 2005, Merloni & Heinz 2008), it helps to prevent the formation of cooling flows and nuclear star formation in massive halos (Sijacki et al. 2007). Dubois et al. (2012), in a RAMSES implementation, also identify a 'radio mode' at low accretion rates and inject kinetic energy into a jet-like bipolar outflow with a velocity of $10,000 \text{ km s}^{-1}$ (see also Omma et al. (2004) and Brighenti & Mathews (2006) for the impact of jet feedback in isolated models).

Originally developed for SPH, the Sijacki et al. (2007) AGN feedback model has also been used in recent large scale simulations with the moving mesh code AREPO extended by the influence of the radiation field of the accreting black holes on the cooling rate of the gas (Sijacki et al. 2015, Vogelsberger et al. 2014). Here the effect of AGN feedback on reducing the galactic stellar masses was confirmed, however, at the cost of depleting the massive halos of gas due to the 'jet bubble' feedback, inconsistent with observations (Genel et al. 2014). In general, these relatively straight forward models not only give reasonable galaxy and black hole masses at the high mass end, they also result in plausible evolutions of the black hole populations and AGN luminosity functions across cosmic time (Hirschmann et al. 2014, Khandai et al. 2015, Puchwein & Springel 2013, Sijacki et al. 2015).

Instead of using a constant boost factor, Booth & Schaye (2009) scale α_{boost} with the local density for high ambient gas densities and set it to unity for low densities - in combination

with a stiff equation of state for dense gas (Schaye & Dalla Vecchia 2008, see (Booth & Schaye 2009) for a detailed discussion). The thermal feedback is regulated such that the black hole stores the energy until the surrounding particles can be heated to a certain high temperature (in this case $\gtrsim 10^8$ K), disfavoring rapid cooling of the gas and making the immediate feedback efficient by construction. The approach is similar to the stellar 'stochastic thermal' feedback discussed in Section 2.2.1. It is clear that the density scaling of α_{boost} makes the accretion more sensitive to the feedback, which in turn strongly affects the density. In general, however, the introduction of a temperature limit for the black hole feedback results in a stronger effect than for the Springel, Di Matteo & Hernquist (2005b) model with no need for changing the energy conversion efficiency and the feedback methodology. This model also results in reasonable baryon fractions and stellar masses for massive galaxies and black hole masses (Schaye et al. 2015). In particular it reproduces reasonable gas fractions and X-ray luminosities for galaxy groups (Choi et al. 2014, Le Brun et al. 2014, McCarthy et al. 2010) which are over-predicted by models with a constant boost factor and thermal feedback.

An Eddington limited thermal black hole feedback scheme similar to Booth & Schaye (2009) with a density dependent α_{boost} and the same underlying equation of state for the gas, has also been implemented in the adaptive mesh refinement code RAMSES (Dubois et al. 2012, Teyssier et al. 2011). The black holes are not seeded in halos above a certain mass but the accreting sink particles are generated when certain conditions on the stellar component and gas density are met (Teyssier et al. 2011, see e.g. Di Matteo et al. 2012, Dubois et al. 2012, Hirschmann et al. 2014, Puchwein & Springel 2013 for different implementations of black hole seeding).

Zoom simulations of group and cluster sized halos in particular have highlighted the impact of AGN feedback on reducing the stellar mass in the central galaxies by preventing cooling flows and subsequent star formation (McCarthy et al. 2010; Sijacki et al. 2007; Teyssier, Chapon & Bournaud 2010). AGN feedback also has important consequences for the hot gas in these halos. By removing low entropy gas at higher redshifts (at the peak of the black hole growth) AGN bring the simulated present day hot gas properties in much better agreement with observations of thermal X-ray emission (Le Brun et al. 2014, McCarthy et al. 2011, 2010).

The above simulations also indicate a potentially interesting effect of AGN feedback on the stellar kinematics. As the amount of gas cooling and subsequent star formation in the central galaxies is efficiently suppressed (Martizzi, Teyssier & Moore 2012; Martizzi et al. 2012), the ratio of in-situ formed to accreted stars is significantly reduced, increasing the size of the system but also reducing the amount of rotational support (Dubois et al. 2013a, Martizzi et al. 2014). AGN feedback transforms BCGs from fast rotators to slow rotators, possibly in better agreement with observations (Dubois et al. 2013b, Martizzi et al. 2014). This highlights the potentially important role of AGN feedback for regulating the ratio of in-situ star formation to accretion (Dubois et al. 2013b, Hirschmann et al. 2012) determining the stellar kinematics of the systems and regulating the stellar density distributions.

The strength of these kinematic signatures will not only be influenced by feedback from AGN and stars, but also by the mass of the galaxies and their environment. Low mass, star forming disk galaxies favored in low-density environments, predominantly grow by accretion of gas and subsequent in-situ star formation, and are affected by stellar feedback, and less so by AGN. Higher mass, early-type galaxies form in high-density environments - primarily affected by feedback from accreting super-massive black holes - and their late assembly involves merging with other galaxies, which might also be of an early type (e.g.

Qu et al. 2017, Rodriguez-Gomez et al. 2016). So far it has not been possible to perform a statistically meaningful comparison of kinematic properties of galaxy populations to observed population properties, like the observed increasing fraction of slow versus fast rotators for early-type galaxies as a function of environmental density (Cappellari 2011). With the newly performed Eagle (Schaye et al. 2015) and Illustris (Vogelsberger et al. 2014) simulations this might now be possible for the first time, due to the large simulated volume and the relatively high spatial resolution attained ($\lesssim 1kpc$). Not only can the simulated two-dimensional kinematic properties be compared to observations, it will also be possible to make (statistical) connections to characteristic formation histories, properties of progenitor galaxy populations and to investigate trends with environment. This will not only be limited to stellar kinematics but will also include gas kinematics and metallicity and two-dimensional stellar abundance patterns. In addition, we will be able to assess the impact of the major feedback mechanisms (from massive stars and AGN) on the kinematic properties of high and low mass galaxies in all environments, a study that will be supported by higher resolution, cosmological zoom simulations for characteristic cases. Also several recent papers (e.g. Bogdán et al. 2013; Choi et al. 2014; Crain et al. 2010; Le Brun, McCarthy & Melin 2015; Le Brun et al. 2014,?) have shown that a proper prediction of the thermal X-ray halos of massive galaxies provides a stringent test of the correctness of any implemented feedback scheme. We discuss mechanical and radiative AGN feedback models in Sec. 3.5.

3 The need for accurate modelling of the galactic interstellar medium and 'feedback'

The large differences of sub-resolution models presented in the previous section are noteworthy but also a bit worrying as the models should be representations of the same underlying physical processes. Many groups have been able to design and calibrate feedback procedures that allow them to more or less successfully match the present day galaxy mass function, or more accurately, the ratio of dark matter to galaxy masses, the cosmological evolution of galaxy abundances, and the evolution in galaxy sizes and stellar populations (the Eagle project seems to have done this most successfully). In Fig. 4 you can assess to which level the different groups have succeeded in this calibration to present day galaxy mass functions similar to the one presented in Li & White (2009). With the large conceptual differences in the respective feedback models the good (or not so good) agreement with the observed mass function can be attributed to a more or less successful tuning of the normalizations and scalings in the sub-resolution models. The theoretical predictions are stellar mass functions from large scale cosmological simulations in recent publications: from Davé et al. (2013) using traditional SPH, 'energy and momentum driven' decoupled winds and a heuristic model for gas heating in massive halos (no AGN feedback); from Davé, Thompson & Hopkins (2016) using a meshless finite mass method with star formation feedback scaling motivated by higher resolution simulations and an improved empirical gas heating model to Davé et al. (2013) for massive halos; from Puchwein & Springel (2013) using traditional SPH with momentum driven winds and thermal and 'bubble' AGN heating; from Dubois et al. (2014) (Horizon-AGN) with AMR, mechanical supernova feedback, thermal AGN feedback with variable boost factor and jet-feedback for low accretion rates, from Vogelsberger et al. (2014) (the Illustris simulations) with a moving mesh code, decoupled 'momentum driven' winds, thermal and 'bubble' AGN heating and radiation input from the AGN; Schaye et al. (2015) (the Eagle simulations) with improved SPH, 'stochastic thermal' heating from stars and AGN; from Hirschmann et al. (2014) (the Magnetium

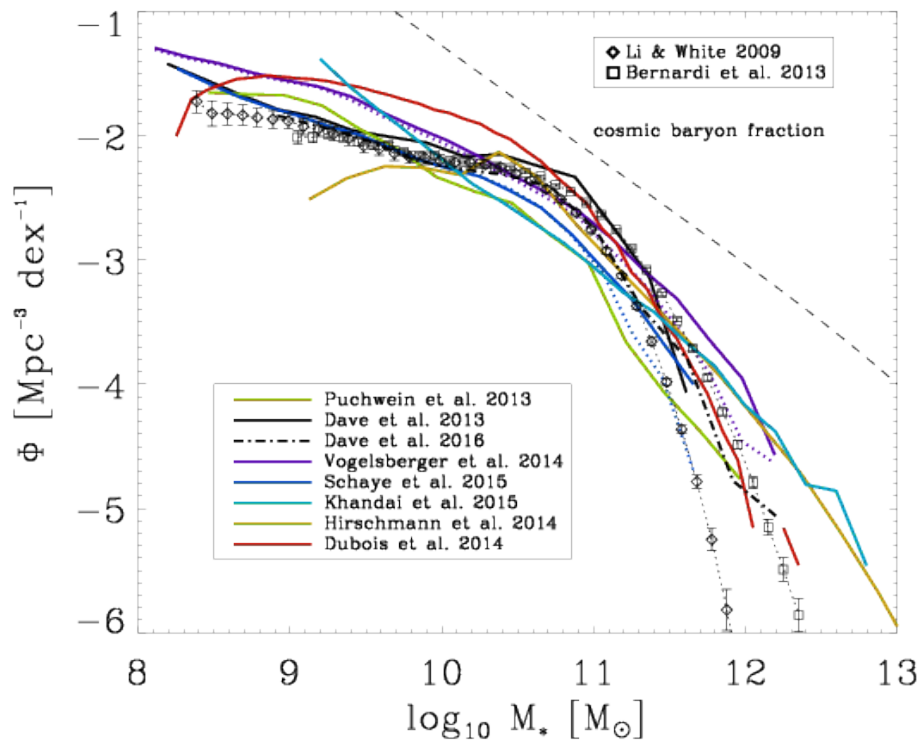


Figure 4:

Comparison of galaxy stellar mass functions from recent large scale cosmological simulations of representative volumes of the Universe (see text). The simulations include stellar and AGN feedback with the exception of (Davé et al. 2013) who use an empirical heating model in massive halos. The different groups typically adjust the key parameters in the varying sub-resolution models to match observations of galaxy mass functions like the one of Li & White (2009). For reference we show an alternative mass function with different mass estimates for massive galaxies (Bernardi et al. 2013). At a given mass the abundance can vary by up to an order of magnitude, still considering the range in spatial resolution (from 0.5 kpc to 3 kpc) and the significant difference in sub-resolution models the agreement between the simulations is remarkable for some models. The dashed line for Vogelsberger et al. (2014) and Schaye et al. (2015) indicate different mass estimates. The dashed line shows the hypothetical galaxy mass function assuming the cosmic baryon fraction.

simulations) with traditional SPH, constant winds, thermal AGN heating and a modified 'bubble' heating; from Khandai et al. (2015) (the MassiveBlack II simulations) with traditional SPH, 'decoupled wind' and thermal AGN feedback. The simulations have more or less succeeded in this exercise. For comparison we show a (typical) observed galaxy mass function in the local Universe (Li & White 2009). Again, we point out that such a mass function is used for most simulations and alternative mass functions take extended stellar

mass distributions in massive galaxies into account (Bernardi et al. 2013). Even with the significant differences in the sub-grid model assumptions it seems that many simulations capture the basic characteristics. Still to be achieved are cosmological simulations yielding good matches to galaxy population properties on the basis of numerically resolved ab initio physical modeling of feedback processes.

Returning to the outline of the physical problems encountered in studying galaxy formation and evolution we had already noted earlier that for Part (B) of the problem - feedback - there were a number of physical processes that we know are important but remain unsolved. Primary among them is the questions of which physical processes regulate the multi-phase structure of the ISM and what is the main driver for galactic outflows.

3.1 Supernova explosions

Core-collapse supernova explosions have for long been the primary suspect to play a crucial role in galaxy formation (Dekel & Silk 1986, Larson 1974, Navarro & White 1993). During these singular and final events in a massive star's live typically 2 - 5 M_{\odot} of gas are ejected into the ambient interstellar medium (ISM) at supersonic velocities of $v_{eject} \sim 6000 - 7000 km s^{-1}$ (Janka 2012) driving a shock into the ambient ISM. Apart from the injection of metals, supernovae can - in the energy conserving phase of the blast wave - heat about three orders more ambient mass than their ejecta to high temperatures. This makes them the prime sources of hot ($T \sim 10^6 K$) gas in the star forming ISM. By creating the hot, X-ray emitting, phase they impact the large-scale multi-phase structure of the ISM (Li et al. 2015, McKee & Ostriker 1977, Walch et al. 2015) and might be important for driving galactic outflows, fountain flows, and galactic winds through hot, low density, chimneys (Chevalier & Clegg 1985; Girichidis et al. 2016b; Heckman 2003; Heckman, Armus & Miley 1990; Hennebelle & Iffrig 2014; Hill et al. 2012; Joung & Mac Low 2006; Norman & Ikeuchi 1989; Strickland & Stevens 2000). The momentum injected by supernovae contributes to the kinetic energy content of the ISM. With pure momentum injection simulations it has been argued that supernovae can create realistic turbulence (see reviews on ISM turbulence by Elmegreen & Scalo 2004, Scalo & Elmegreen 2004) in the warm and cold ISM and regulate the scale heights of galactic disks (by large scale turbulent pressure) as well as their star formation rates (see Kim & Ostriker 2015b, Ostriker & Shetty 2011).

The importance of supernova explosions for setting the ISM structure motivates a more detailed review of the different phases of supernova blast waves (see also Blondin et al. 1998; Chevalier 1982; Cioffi, McKee & Bertschinger 1988; Draine 2011; Haid et al. 2016; Kim & Ostriker 2015a; Ostriker & McKee 1988). The direct momentum of supernova ejecta is insufficient to accelerate a significant amount of gas to high velocities in the early *free expansion phase*. Once the supernova ejecta have swept up cold interstellar material of comparable mass the remnant enters the energy conserving *Sedov-Taylor phase* (Sedov 1959, Taylor 1950, Truelove & McKee 1999). In this phase about 1000 times the ejecta mass is heated and about 10 times the initial (ejecta) radial momentum can be generated as long as the temperature changes are dominated by adiabatic expansion (this can amount to 100 times the ejecta momentum in the absence of cooling). As soon as radiative losses become dominant a cooling shell forms and the amount of hot gas decreases rapidly. Analytical estimates for the time t_{sf} , radius r_{sf} , velocity v_{sf} , temperature T_{sf} , mass M_{sf} , and radial momentum p_{sf} at shell formation as a function of explosion energy E_{51} in units of $10^{51} ergs$, and the number density of a homogenous ambient medium in cm^{-3} result in the following relations (taken from Kim & Ostriker (2015a), but see also Draine 2011):

$$t_{\text{sf}} = 4.4 \times 10^4 \text{yr} E_{51}^{0.22} n_0^{-0.55} \quad (3)$$

$$r_{\text{sf}} = 22.6 \text{pc} E_{51}^{0.29} n_0^{-0.42} \quad (4)$$

$$v_{\text{sf}} = 202 \text{km s}^{-1} E_{51}^{0.07} n_0^{0.13} \quad (5)$$

$$T_{\text{sf}} = 5.67 \times 10^5 \text{K} E_{51}^{0.13} n_0^{0.26} \quad (6)$$

$$M_{\text{sf}} = 1680 M_{\odot} E_{51}^{0.13} n_0^{-0.26} \quad (7)$$

$$p_{\text{sf}} = 2.17 \times 10^5 M_{\odot} \text{km s}^{-1} E_{51}^{0.93} n_0^{-0.13} \quad (8)$$

Kim & Ostriker (2015a) have shown in detail that these analytic estimates agree well with direct, high-resolution, three-dimensional numerical simulations (see also Iffrig & Hennebelle (2015); Martizzi, Faucher-Giguère & Quataert (2015); Walch & Naab (2015)).

After shell formation the supernova enters a short *transition phase* and the following *pressure driven snowplow phase* is powered by the homogenous pressure inside the shell. Once all excess thermal energy is radiated away, no radial momentum can be generated any more and the remnant enters the *momentum conserving snowplow phase*. Travelling into the interstellar medium the shock wave transforms into a sound wave (when the expansion velocity reaches the sound speed of the interstellar medium) and fades away. It can be shown that for solar neighborhood conditions an initially uniform medium will be completely changed within 2Myrs by overlapping remnants in their fade-away stage (Draine 2011). This simple argument indicates that supernovae alone might determine the thermal and dynamical state of the ISM (McKee & Ostriker 1977). Subsequent to this phase supernova remnants will propagate in the multi-phase medium with greater efficiency and reduced losses. These properties have yet to be fully assimilated into cosmological simulations of galaxy formation.

Radiative cooling, i.e. the actual ambient density and metallicity at the time of the supernova explosions, determines the duration of the momentum generating phases of which the *Sedov-Taylor phase* is the most important. For single supernovae exploding in ambient densities of $\sim 100 - 0.1 \text{cm}^{-3}$ cooling becomes dominant after about $\sim 10^4 - 10^{5.5}$ years limiting the momentum generation to factors of $\sim 10 - 30$ (Haid et al. 2016). For reliable simulations of the galactic ISM it is important that the momentum generating phases of supernovae remnants can be captured accurately. While analytic estimates are useful for homogeneous ambient media they cannot simply be applied to the more complex multi-phase structure of a realistic ISM. Here, numerical simulations have made a significant progress in recent years. We discuss this effort a bit more in detail as we think it is a good example of how resolved numerical simulations with different simulation codes can be used to understand a specific relevant physical process in more complex environments.

In Fig. 5 we show an overview of mostly three-dimensional numerical simulations measuring the momentum injection into the interstellar medium for the various conditions of the ambient ISM. Martizzi, Faucher-Giguère & Quataert (2015) have used the adaptive mesh refinement code *RAMSES* for homogeneous ambient medium and one with a lognormal density distribution representing a Mach 30 turbulent ISM. The simulations of Kim & Ostriker (2015b) have been performed with the *ATHENA* code for a homogenous and a structured two-phase medium (cold and warm phase). Additional simulations for a three-phase medium have been performed by Li et al. (2015) with the AMR code *ENZO*. We have to note that even at low resolution the total momentum input of a supernova can be correctly computed. However, the swept up mass and the velocity of the shell can still be incorrect (Hu et al. 2016)

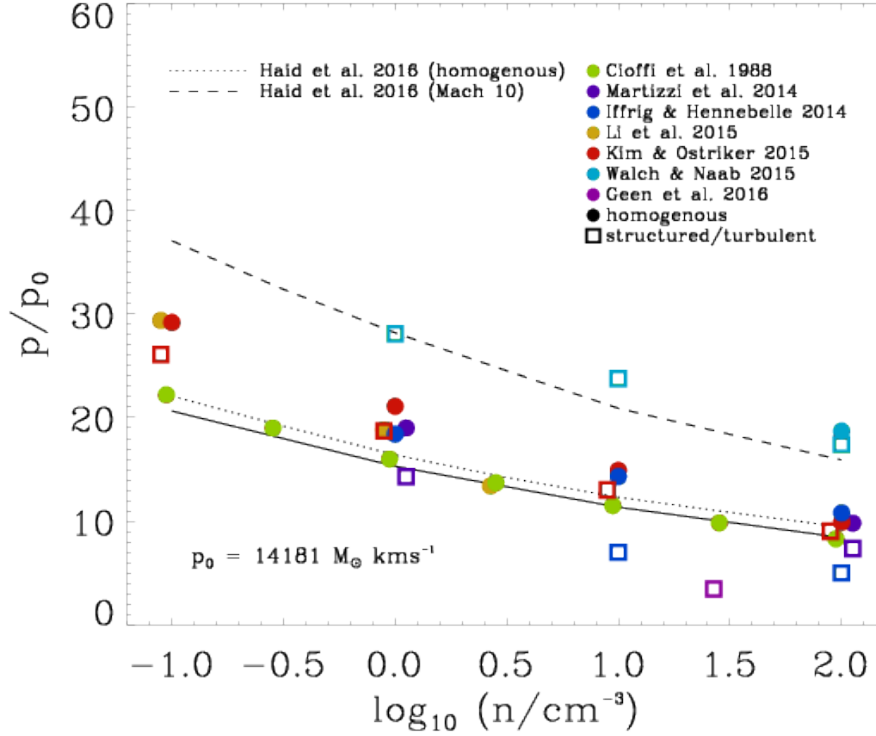


Figure 5:

Momentum generated in radiative supernova remnants for various ambient densities normalized by a fiducial initial momentum of $p_0 = 14181 M_{\odot} \text{ kms}^{-1}$ for an explosion energy of 10^{51} erg and two solar masses ejecta. The analytically derived momentum at shell formation (Eqn. 8, solid line) terminates the energy conserving Sedov-Taylor phase (Kim & Ostriker 2015a) and the momentum can increase a bit more until the beginning of the momentum conserving snowplow phase (dotted line). The dashed line indicates the momentum injection for an analytical model of a log-normal (Mach 10) density distribution (Haid et al. 2016). Colored symbols show results from three dimensional numerical simulations (with the exception of the one-dimensional simulations by Cloffi, McKee & Bertschinger 1988) with homogenous, structured or turbulent ambient media carried out with three different grid codes and a particle based SPH code.

A supernova does not only inject momentum into the ISM. It also generates hot gas in the early phases of the remnant's evolution. The maximum amount of hot gas is reached at the time of shell formation, marking the end of the Sedov-Taylor phase. If no other supernova explodes within the remnant's radius until the time of shell formation T_{sf} the remnant will cool rapidly and no stable hot phase can be generated. For a homogenous ISM of density n_0 and a given supernova rate density S we can estimate the expectation value N_{hot} for a supernova to explode in a hot phase within the shell formation radius r_{sf} :

$$N_{\text{hot}} = S \frac{4\pi}{3} r_{sf}^3 t_{sf}. \quad (9)$$

With Eqns. 4 and 7 this results in

$$N_{\text{hot}} = S 2.13 \times 10^{-6} kpc^3 Myr E_{51}^{1.09} n_0^{-1.81}. \quad (10)$$

For a typical gas surface density similar to the solar neighborhood of $10 M_{\odot} pc^{-2}$ the Kennicutt relation (Kennicutt 1998) gives an observed star formation rate surface density of $7 \times 10^{-2} M_{\odot} yr^{-1} kpc^{-2}$. With a Salpeter like initial mass function and an assumed disk thickness of $250 pc$ the resulting supernova rate density is $S \sim 280 kpc^{-3} Myr^{-1}$. For an average gas number density of $n_0 = 1 cm^{-3}$ the expectation value would be only $N_{\text{hot}} \sim 6 \times 10^{-4}$. Due to the strong power-law dependence on the density in Eqn. 10 a lower density of $n = 0.015 cm^{-3}$ results in $N_{\text{hot}} \gtrsim 1$ and a stable volume filling hot phase can form. Once such a condition is reached and the system cannot vent the hot gas it will undergo a *thermal runaway*. Subsequent supernovae explode in even hotter and lower density regions with even less thermal losses and larger shell formation radii. Once the volume is dominated by over-pressured hot gas no shell will form, cooling losses are minimal and most of the mass is in small cold clumps. This process has recently been described by Gatto et al. (2015) and Li et al. (2015) with hydrodynamical simulations in periodic boxes. If the ISM can vent the hot gas, an outflow is driven.

The strong dependence of the hot gas volume filling fraction in Eqn. 10 on the environmental density of the supernova explosions has significant consequences for the evolution of the galactic ISM. In Fig. 6 we illustrate this with three numerical experiments (part of the SIMulating the Life Cycle of molecular Clouds [SILCC] simulation project, Walch et al. 2015). The setup is a stratified galactic disk with a surface density of $\Sigma_{\text{gas}} = 10 M_{\odot} pc^{-2}$ embedded in a stellar disk potential. The initially homogenous ISM is driven by supernova explosions at a constant rate based on observational estimates. If all supernovae explode at the current density peaks (typical densities of $n = 100 cm^{-3}$, see Girichidis et al. 2016b) the explosions suffer from radiative losses, no hot phase develops and the impact is limited to momentum injection. Rapidly a turbulent, pressure supported two phase (warm and cold gas) medium develops and the scale height is set by the turbulent pressure. Draine (2011) presents a simple estimate for this process to take only $2 Myrs$. This behavior is reported from pure momentum injection models (Kim, Kim & Ostriker 2011; Kim & Ostriker 2015b; Kim, Ostriker & Kim 2013; Ostriker & Shetty 2011). The major shortcomings of these models are that no hot phase can develop and the cold phase cannot become dense enough for molecular gas formation (see e.g. Walch et al. 2015). If some half of the supernovae do not explode in density peaks but rather at random locations in the disk, as would be expected from the number of early-type 'runaway' stars discussed below, the ambient density distribution for supernovae becomes bimodal. Random supernovae in low density regions $n \sim 0.1 cm^{-3}$ compress the cold gas to higher densities $n \gtrsim 100 cm^{-3}$, where the peak supernovae explode. The system can form a hot phase (see middle panels of Fig. 6). Once all supernovae explode at random positions (most ambient densities $n \lesssim 0.1 cm^{-3}$) the ISM becomes highly structured and rapidly develops a stable hot phase, which is expanding into the halo and drives a galactic outflow (see Girichidis et al. (2016b) for the models shown in Fig. 6). This behavior has already been reported by pioneering three-dimensional hydrodynamical simulations of stratified disks by Korpi et al. (1999), de Avillez (2000), de

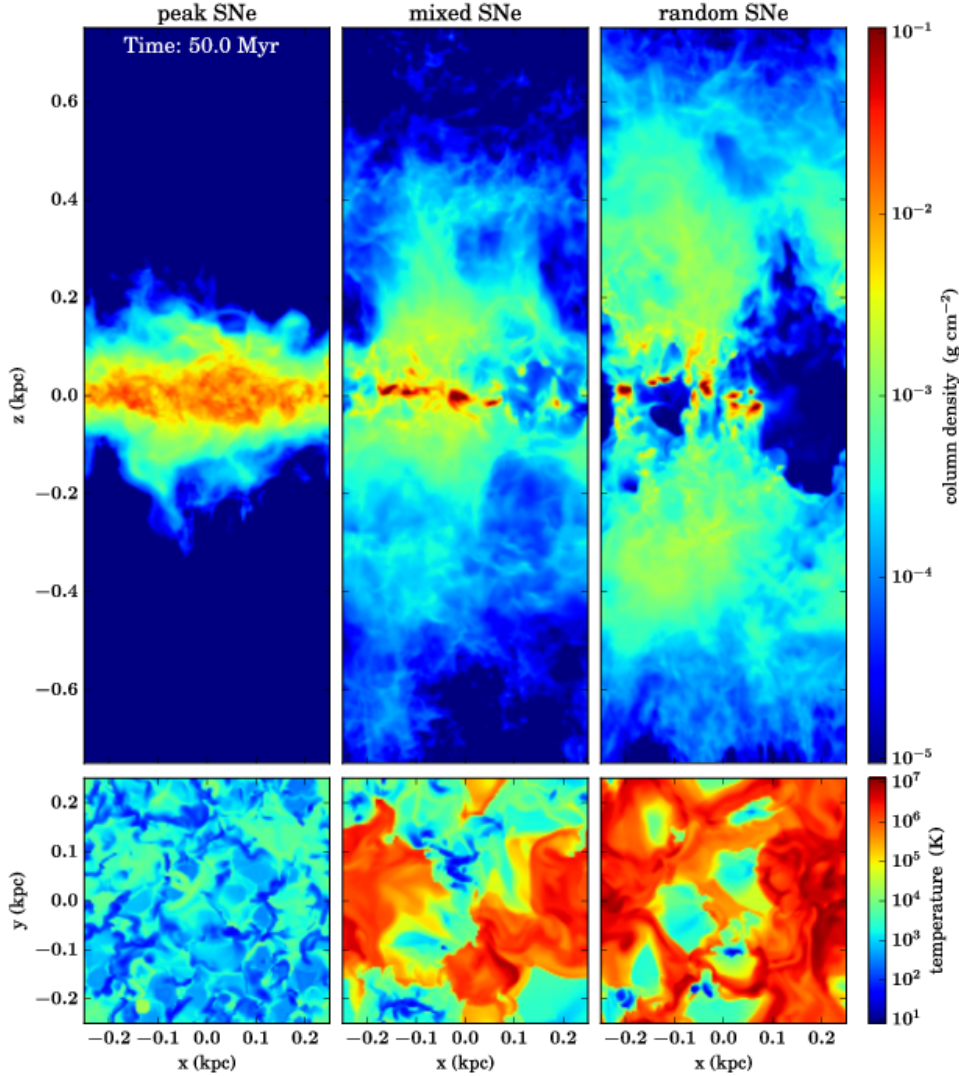


Figure 6:

Snapshots of the vertical gas column density distribution (top panels) and mid-plane temperatures (bottom panels) for three simulations of stratified galactic disk ($\Sigma_{\text{gas}} = 10M_{\odot}pc^{-2}$ shaped by supernovae (SNe) exploding at a constant rate (taken from the SILCC simulations, Girichidis et al. 2016b, Walch et al. 2015). In peakSNe (left panels) each supernova explodes at the current density peak. Rapid thermal losses limit the SN impact to momentum ejection driving an (unrealistic) turbulent two-phase medium with no outflows and no hot gas. With 50 per cent of the supernovae exploding at random positions at lower densities a hot phase appears (mixed SNe, middle panel). If all SNe explode at random positions the hot phase becomes volume filling and drives a vertical outflow (random SNe, right panels, see Girichidis et al. 2016b). This figure clearly illustrates the strong impact of the actual location of SN explosions on the multi-phase structure of the ISM and the driving of outflows (see Eqn. 10). We note that non of these variations can be captured in current large scale cosmological simulations which have single resolution elements of the size of the above simulation boxes ($\sim 500pc$) and rely on sub-resolution models.

Avillez & Breitschwerdt (2004), and Joung & Mac Low (2006). The major shortcomings of these type of models are that they neglect the galactic environment (radial gas flows and inflows) and, due to the idealized geometry, gas flows into and out of galactic halos cannot be modelled accurately (see e.g. Martizzi et al. 2016).

OH maser measurements indicated that only about 15 per cent of core collapse supernovae interact with dense molecular gas (Hewitt, Yusef-Zadeh & Wardle 2009). Therefore the typical ambient density for explosions is lower than the dense birth places of massive stars. Now the question is which astrophysical processes determine the ambient densities of supernova explosions? There are two phenomena which can result in this: the massive stars move away from their dense birth places into gas with lower volume densities and larger volume filling fractions and/or the stars change their environmental densities by stellar winds, ionising radiation and clustered supernova explosions.

Most, if not all, stars form in star clusters and are expected to be temporally and spatially correlated, eventually driving super-bubbles with more efficient energy coupling and momentum generation (e.g. Joung & Mac Low 2006, Mac Low & McCray 1988, Sharma et al. 2014). The typical velocity dispersion in newly born star clusters is $\sim 1 \text{ km s}^{-1}$ or 1 pc Myr^{-1} . Assuming the cluster becomes unbound massive stars can travel up to 40 pc before they explode (assuming typical supernova delay times for single stellar populations). These 'walkaway' stars can therefore easily leave their dense birthplaces and explode in lower density regions. As most of the volume of the ISM is not in the cold phase most supernovae might explode in the warm or hot phase, significantly changing the coupling efficiency (Ceverino & Klypin 2009, Slyz et al. 2005). There is also the 'runaway' star population (Gies & Bolton 1986) (about 45 % of O-stars and 15 % of B-stars are 'runaways') with typical velocities of $\sim 30 - 40 \text{ km s}^{-1}$ and maximum velocities as high as a few hundred km s^{-1} (e.g. Silva & Napiwotzki 2011). These high-velocity stars originate from close binary systems becoming unbound by a supernova explosion (Blaauw 1961, Zwicky 1957) and/or from dynamical interactions in dense regions of star clusters (Poveda, Ruiz & Allen 1967). They can travel up to several hundreds of parsecs away from their birthplaces far into inter-arm regions or the lower galactic halo. Their explosion locations in galactic disks can therefore be considered as almost random, similar to the explosions of SNe Ia which contribute about 20 -25 % to the supernova rate in the solar neighborhood (Tammann, Loeffler & Schroeder 1994). They explode independently of the gas mass distribution within the ISM, a process approximately taken into account in high-resolution simulations of stratified disks which are most useful to study the launching of outflows and, at the same time, create a realistically structured ISM (e.g. de Avillez & Breitschwerdt 2005; Hill et al. 2012; Joung & Mac Low 2006; Li, Bryan & Ostriker 2016). Such detailed small scale simulations with a realistic ISM structure will help to bridge the gap in scale and physical understanding to galaxy scale simulations.

3.2 Stellar winds

Massive stars themselves also impact their ambient medium. Radiation driven stellar winds from O- and B-stars (Castor, Abbott & Klein 1975; Kudritzki & Puls 2000; Puls et al. 1996) create bubbles of low density gas around the stars. Typical B-stars with masses $\sim 9 M_{\odot}$, mass-loss rates of $\dot{M}_{\text{wind}} \sim 10^{-9} M_{\odot} \text{ y}^{-1}$, and wind velocities of $v_{\text{wind}} \sim 2000 \text{ km s}^{-1}$ have an integrated wind luminosity of only a few times $\sim 10^{47} \text{ erg}$. However, very massive stars can reach as much as $E_{\text{wind}} \sim 10^{51} \text{ erg}$. Although energetically much less important than supernova explosions, stellar wind blown bubbles can significantly reduce the gas densities

around massive stars and thereby increase the impact of the supernovae. Furthermore, since momentum injection goes as \dot{E}/v , winds from massive stars can contribute more direct momentum than the supernovae themselves. Interestingly, stellar winds can also significantly reduce the star formation process in forming star clusters (Dale & Bonnell 2008, although Dale et al. (2013, 2014) argue that the combined effect of stellar winds and ionising radiation only has modest impact on star formation) and might be a stronger regulator for galactic star formation than supernovae (Gatto et al. 2016).

3.3 Radiation

Stellar evolution models indicate that the total energy released by newly formed stellar populations is, by a large margin of two orders of magnitude, dominated by stellar radiation, which itself is dominated by massive stars (e.g. Leitherer et al. 1999). By the time the first supernova, with a canonical energy of 10^{51} erg , has exploded, the stars would have already emitted $\sim 10^{53} \text{ erg}$ as radiation, and $\gtrsim 10^{50} \text{ erg}$ in stellar winds. It has been realized lately that, in galaxy scale simulations, accounting for the stellar luminosity (and winds) might significantly enhance the coupling of the stellar energy and momentum output to the ISM (e.g. Agertz et al. 2013; Hopkins, Quataert & Murray 2011, 2012a; Roškar et al. 2014). The generation of momentum is of particular interest as it cannot easily be radiated away like thermal energy. The efficient cooling results in only a moderate, 10%, contribution of the thermal energy density in the ISM (Boulares & Cox 1990). Due to the generally severe radiation losses in dense interstellar environments it is, however, unclear, how much of the injected energy can be converted into momentum. If this process is efficient, then stellar radiation might significantly contribute to the driving of turbulence and the launching of galactic winds (e.g. Agertz & Kravtsov 2015; Geen et al. 2015; Murray, Ménard & Thompson 2011; Murray, Quataert & Thompson 2005, 2010).

Ionizing UV photons create HII regions around young massive stars by heating the parental cloud from $\lesssim 100 \text{ K}$ to $\sim 10^4 \text{ K}$. At this stage the dynamics of the ISM is dominated by the thermal pressure of the ionized gas with sound speeds $\lesssim 10 \text{ km s}^{-1}$. The momentum input by direct absorption of UV photons (single scattering) seems sub-dominant (Arthur et al. 2004, Krumholz & Matzner 2009, Mathews 1969, Sales et al. 2014, Spitzer 1978). It might be sufficient to drive turbulence at a low level (Gritschneder et al. 2009) and even disrupt small clouds on short time-scales (Krumholz, Matzner & McKee 2006; Walch et al. 2012), however, over-dense regions of the surrounding ISM will also be compressed into clumps and pillars (Dale, Bonnell & Whitworth 2007; Gritschneder et al. 2010; Walch et al. 2012) making further coupling more difficult.

A full radiation transfer treatment of ionizing radiation from massive stars in galaxy scale simulations is technically challenging (see e.g. Wise et al. 2012 for single scattering). It has been approximated in a Strömgren approach, i.e. the ISM around massive stars corresponding to a Strömgren sphere (Strömgren 1939) is ionized and heated to $\sim 10^4 \text{ K}$ (e.g. Hopkins, Quataert & Murray 2012a; Renaud et al. 2013) or in the optically thin regime (assuming escape fractions from 'clouds') with radiation field attenuation to follow the impact on gas cooling (e.g. Kannan et al. 2014). Kannan et al. (2014) claim a significant impact of the local UV radiation resulting in a suppression of star formation for Milky Way like galaxies ($\sim 40\%$) by increasing the cooling time and the equilibrium temperature.

It has been argued that the radiation pressure on dust of re-emitted and scattered infrared

radiation can result in a significant momentum input into the ISM,

$$\dot{P}_{rad} \sim (1 + \tau_{IR})L/c. \quad (11)$$

The efficiency of this process depends on the optical depth to the re-radiated long-wavelength emission of the dust, τ_{IR} , i.e. on the details of multiple scatterings in optically thick regions surrounding the young stars. Based on small scale simulations, Krumholz & Thompson (2013) argue that the momentum input does not exceed L/c due to the structure, and therefore inefficient trapping, developing in the ISM (Krumholz & Thompson 2012). However, using a different radiation transport method, Davis et al. (2014) find a slightly stronger coupling of the radiation. In an attempt to approximately include this effect in high resolution galaxy scale simulations Hopkins, Quataert & Murray (2011, 2012a,b) add momentum to the surrounding gas either in a stochastic or continuous way and indicate that they can use this process to drive galaxy scale winds. Hopkins, Quataert & Murray (2011) give the gas particles initial kicks of the order the escape velocity from local 'gas clumps' or 'star clusters' (between 60kms^{-1} and $\sim 350\text{kms}^{-1}$ for 'clusters' with masses $\sim 10^5 - 10^9 M_{\odot}$) guaranteeing that dense regions become unbound before additional radiation pressure and supernovae can act. Locally they approximately compute τ_{IR} from the local gas properties assuming a high dust opacity of $\sim 5\text{cm}^2\text{g}^{-1}$ (see also Roškar et al. 2014) and use a model for attenuated radiation to compute the momentum input from all stars at large distances (Hopkins, Quataert & Murray 2011). This empirical implementation of radiation pressure may result in large scale galactic winds by a non-linear interaction of the different feedback mechanisms with the wind mass-loading changing as a function of galaxy properties (Hopkins, Quataert & Murray 2012a).

Other groups have followed similar paths to account for the full energy input of stellar populations and approximate the effect of radiation pressure. Agertz et al. (2013) have implemented the local momentum input as in Eq. 11 with photon trapping acting at early ($t \lesssim 3\text{Myr}$) embedded stages. Aumer et al. (2013) assume a large, fixed, value for the optical depth ($\tau_{IR} \sim 25$) and scale the momentum input with the local gas velocity dispersion and metallicity. In a cosmological context it has been demonstrated, using different codes, that such efficient momentum input and the resulting winds can promote the formation of disk galaxies with appropriately low conversion efficiencies (Ageret & Kravtsov 2015, Hopkins et al. 2014, see Fig. 2). However, Roškar et al. (2014) implemented an approximate radiation transfer for ultraviolet and infrared radiation, where the dust opacity becomes an important factor to regulate the feedback efficiency. They argue that the momentum input required to drive strong outflows at the same time disturbs the gas and the resulting stellar disk so much that it becomes impossible to retain the flat disk morphology. In summary, while many promising calculations have been made (see e.g. Rosdahl et al. 2015 for a first application of radiative transfer processes in galaxy-scale simulations), it is not yet clear how much radiation from young stars can really contribute to the driving of strong galactic outflows. For a complete understanding of this process more accurate models for dust evolution in galaxy formation simulations have to be considered. Good steps forward have been recently made also in this direction (e.g. Bekki 2015; McKinnon, Torrey & Vogelsberger 2016; Zhukovska et al. 2016)

3.4 Magnetic fields and cosmic rays

Magnetic fields and cosmic rays (CRs), relativistic high-energy particles, mostly protons and electrons, are an integral, non-thermal component of the interstellar medium. In the

solar neighborhood the energy density in CRs, magnetic fields and the kinetic energy density are comparable and significantly higher than the thermal pressure (Boulares & Cox 1990, Ferrière 2001). CR spectra have been measured over many orders of magnitude from $E_{\text{CR}} \sim 10^7 \text{ eV}$ up to the energies of $E_{\text{CR}} \sim 10^{20} \text{ eV}$. As the galactic CR energy spectrum is rather steep with $P \propto E^{-2.7}$ the majority of the energy is deposited at lower energies with a peak at around a few GeV , which is the expected range of significant dynamical impact of CRs on the ISM within a star forming galaxy. The main acceleration mechanism for galactic CRs, in particular those below the 'knee' in the CR spectrum is considered to be *diffusive shock acceleration* (DSA, see e.g. Bell 1978, Blandford & Ostriker 1978) and *non-linear DSA* (Malkov & O'C Drury 2001) in shocks of supernova remnants (SNR) (see Hillas 2005, for a review, and recent observations by Ackermann et al. 2013). Although both electrons and protons are accelerated in strong shocks, the protons carry most of the energy stored as cosmic rays.

The fraction of energy generated in supernova shocks is highly uncertain and this process can, of course, not be simulated in galaxy scale simulations. The estimates mostly range between 5 and 30 % of the total supernova explosion energy (Ellison et al. 2010, Kang & Jones 2006) with increasingly fundamental, ab initio calculations now being made (e.g. Caprioli, Pop & Spitkovsky 2015). If a significant fraction is 'stored' in cosmic rays - which cool much slower than thermal gas by hadronic interactions and Coulomb and ionization losses - they can be carried over large distances and significantly impact the ISM, provided the coupling between CRs and the thermal gas is strong enough (e.g. Breitschwerdt, McKenzie & Voelk 1991; Zweibel & Heiles 1997). CRs diffuse from the shocks and, later on, stream through the ISM. The bulk of CRs may be trapped at first by scattering at self-excited Alfvén waves, which causes a slowed down outward diffusion and additional momentum transfer to the gas (Caprioli, Pop & Spitkovsky 2015). Once the cosmic rays are able to escape the supernova remnant, a streaming instability will be excited if the necessary conditions for the dynamical coupling between the CRs and the gas are met (i.e. a large-scale CR gradient towards the galactic halo is required, Kuhsrud & Pearce 1969), effectively transferring CR energy and momentum to the thermal gas. In addition the CRs exert a pressure on the thermal gas by scattering off Alfvén waves. It is therefore expected that CRs have a significant impact on the thermal and dynamical properties of the ISM. The propagation of cosmic rays through the ISM is complex and often approximated by diffusion with coefficients of the order $\kappa_{\text{CR}} \propto 10^{28} - 10^{29} \text{ cm}^2 \text{ s}^{-1}$ (e.g. Strong & Moskalenko 1998, Tabatabaei et al. 2013, Trotta et al. 2011). Locally the diffusion might be anisotropic with significantly smaller coefficients perpendicular to the magnetic field lines. On global galactic scales of the Milky Way, however, the diffusion can be considered isotropic (Strong, Moskalenko & Ptuskin 2007). The lifetime of the several GeV cosmic ray fluid is known from radioactive dating to be roughly 10 million years.

In addition to thermal and radiation pressure caused by stellar feedback, CRs turn out to be an important agent on galactic scales and, once accelerated in regions of local feedback from star formation, they might be efficient in supporting or even driving galactic outflows. Already in the beginning of the 90's it has been proposed that the combined effect of thermal pressure, MHD waves, and an effective (non-thermal) CR pressure (McKenzie & Voelk 1982) is able to drive a galactic wind (Breitschwerdt, McKenzie & Voelk 1991, 1993), even if the star formation rate is moderate. Recent observations of the starburst galaxy M82 (VERITAS Collaboration et al. 2009) reveal CR densities which are 500 times higher than in the Milky Way and thus clearly link the CR density with regions of highly efficient star formation. Other groups have argued that the galactic wind in M82 is purely driven by

strong stellar feedback (Chevalier & Clegg 1985; Völk, Aharonian & Breitschwerdt 1996). However, in normal spirals like the Milky Way, stellar feedback is probably not strong enough to drive a large-scale galactic wind. Nevertheless, recent ROSAT observations of the Milky Way show extended, soft X-ray emission, which is best explained with a kpc-scale wind for which the cosmic ray pressure may be essential (Everett et al. 2008).

In galaxy scale hydrodynamics simulations with SPH and AMR codes, cosmic rays have recently been included as a separate fluid, as their mean free path is shorter than the typical length scales resolved (Skilling 1975). The fluid is treated as a relativistic gas with $\gamma_{\text{cr}} = 4/3$ and is advected with the gas. The resulting total pressure is $p_{\text{tot}} = p_{\text{th}} + p_{\text{cr}}$ with $p_{\text{cr}} = (\gamma_{\text{cr}} - 1)E_{\text{cr}}$. In addition the cosmic rays are allowed to diffuse through the ISM. This is treated approximately either by streaming (Uhlig et al. 2012) or by isotropic diffusion with a typical diffusion coefficient (Booth et al. 2013, Enßlin et al. 2007, Jubelgas et al. 2008, Salem & Bryan 2014). In simulations following magnetic fields the diffusion is treated anisotropically with one or two orders of magnitude lower diffusion coefficients along the magnetic field lines (Hanasz et al. 2013, Pakmor et al. 2016, Yang et al. 2012).

All simulations including cosmic rays on galactic scales indicate that they can significantly support the driving of bipolar galactic winds with velocities exceeding the local escape speed and with mass loading greater than unity. The winds are driven by the additional pressure gradient due to cosmic rays in low density regions (Booth et al. 2013; Hanasz et al. 2013; Pakmor et al. 2016; Salem & Bryan 2014; Salem, Bryan & Corlies 2016; Uhlig et al. 2012). This process is only efficient if cosmic rays can diffuse out of the high density regions, where they are dynamically unimportant, to build-up a galaxy wide vertical gradient (see e.g. Booth et al. 2013, Uhlig et al. 2012). The mass loading of cosmic ray driven winds is higher for lower mass galaxies (Booth et al. 2013, Uhlig et al. 2012, Wadepuhl & Springel 2011) but also for gas rich massive galaxies the effect is significant (Hanasz et al. 2013). Cosmic ray driven outflows can also support stable configurations of open magnetic field lines originating from regions of high star formation rates (Hanasz et al. 2013). These simulations might also be able to explain the detection of strong magnetic fields at large radii ($\sim 50\text{kpc}$) around star forming galaxies at intermediate and high redshift (Bernet, Miniati & Lilly 2013).

Recently, simulations of the impact of cosmic rays on the interstellar medium on smaller scales have confirmed the ideas brought forward by larger scale galaxy formation simulations and analytic estimates. It was shown by Girichidis et al. (2016a), using magneto-hydrodynamic simulations with anisotropic diffusion that cosmic rays indeed support the launching of outflows from galactic disks and the basic results seems to be insensitive of the magneto-hydrodynamical method used, details of the star formation algorithm and the presence of self-gravity (Simpson et al. 2016). It remains to be seen whether the supporting role of cosmic rays (i.e. the pressure gradient) for the driving of outflows is significant or whether the computations still suffer from inaccuracies in capturing the accurate effect of supernova explosions on the formation of a hot, wind driving, gas phase.

The simulations presented above can only be the starting point for more detailed investigations of the potential importance of cosmic rays for the driving of galactic outflows. In galaxy scale simulations, the galactic ISM is in general unresolved, with a significantly simplified treatment of energy injection by SNe as well as cosmic ray transport. Also the global and local evolution of the galactic magnetic field has to be considered and significant progress has been made recently (Dolag, Bykov & Diaferio 2008; Dolag et al. 2005; Dolag & Stasyszyn 2009; Dubois & Teyssier 2010; Kotarba et al. 2010, 2009; Pakmor, Marinacci & Springel 2014; Pakmor et al. 2016; Pakmor & Springel 2013; Rieder & Teyssier 2016). If it

turns out that CRs and magnetic fields are indeed as important as suggested they have the potential to become a 'global player', regulating the evolution of the ISM and the efficiency of galaxy formation across cosmic times.

3.5 Mechanical and radiative AGN feedback

While the significant work done by many groups using 'thermal AGN feedback' (see Section 2.3) has solid motivation and has produced many quite useful results, the somewhat arbitrary physical implementation has troubling aspects that several groups have attempted to remedy. First, there is no physical means specified for communicating the energy from the black holes to the surrounding gas in these treatments (see discussion in Ostriker et al. 2010). In actual AGN systems, there are high velocity winds and radiation output for both of which there is a momentum associated with the energy transfer and there is a spatial direction for the momentum outflow (Churazov et al. 2005, Fabian 2012, Merloni & Heinz 2008). But in a purely thermal feedback approach these physical factors are missing and, more importantly, the mass to which the thermal feedback energy is distributed is not specified or defined by a heating threshold (Section 2.3). Adding this energy to a very small mass would produce very high temperatures and radiative energy losses, adding it to a very large mass would produce small additional velocities compared to the virial velocities in the galaxy, so adding to the 'just right' amount of mass seems to be required. But if the added feedback energy is deposited with the appropriate accompanying momentum, as observed in BAL winds, the energy redistribution is achieved by physical means.

There exists a characteristic electromagnetic spectrum for AGN with peaks in the infrared, ultraviolet and X-ray (e.g. Sazonov, Ostriker & Sunyaev 2004) that can be taken as the emitted output with the ratio of electromagnetic output to mass accretion given by the Soltan argument (Soltan 1982). In addition to relativistic jets there are also broad-line winds observed to be commonly emitted by AGN (Yuan & Narayan 2014) and these too have been calibrated to the accretion rate empirically (Arav et al. (2013), see also Krolik 1999). Thus one can specify the output in mass, energy, momentum and radiation in various bands per mass accreted on the basis of approximate matches to observed AGN, and then the thermal, mechanical and radiative coupling of these components to the surrounding medium should be handled automatically by the hydro codes being utilized. When taking this approach (and including the Eddington force rather than putting in a limit) the accretion rate self-adjusts, so no arbitrary multiplicative 'boost' factors may be needed in implementing the Bondi-Lyttleton accretion. First attempts to approximately include the effects of UV and X-ray emission from accreting black holes have been made (e.g. Bieri et al. 2016, Choi et al. 2015, Hambrick et al. 2011, Roos et al. 2015, Vogelsberger et al. 2013). Both mechanical (BAL) and radiative effects are included in Choi et al. (2016) for cosmological simulations and in Hopkins et al. (2016) for high-resolution simulations of galactic centers. However, in the end, the results of this more complex approach are in fact similar to those of the thermal feedback approach with regard to regulating the overall mass growth of the central black hole, but other aspects are very different. For example, the fluctuation level of the kinetic feedback is far more extreme with 'on' periods rarely exceeding several million years and a small overall duty cycle being expected. And, as noted earlier, correct prediction of the thermal X-ray emission from massive galaxies provides a strong test of the feedback mechanism which indicates that including a kinetic wind component is essential (Choi et al. 2015, Weinberger et al. 2016).

Jets from AGN are frequently observed and feedback from this mechanism is sometimes

called 'radio mode' (Fabian 2012, Heckman & Best 2014). Some cosmological galaxy evolution treatments have included this process (e.g. Dubois et al. 2014), the reality of which is not in doubt. But narrow relativistic jets effectively drill through the ISM within galaxies, leaving a dramatic imprint on the surrounding cluster gas but probably not communicating significant amounts of energy or momentum to the ISM of the parent galaxy (Vernaleo & Reynolds 2006). However, potential coupling mechanisms e.g. turbulent mixing and dissipation exist and are studied in detail with higher resolution simulations (Babul, Sharma & Reynolds 2013; Gaspari, Brighenti & Temi 2012; Li & Bryan 2014; Omma et al. 2004; Scannapieco & Brüggén 2008). Jets being extremely important in regulating cooling flows within clusters are probably less important than other, more prosaic processes in determining the internal evolution of galaxies.

4 Conclusion & Outlook

Since the advent of self-consistent cosmological numerical simulations about 35 years ago significant progress in understanding galaxy formation has been made. Modern supercomputers and numerical algorithms have become powerful enough to allow the simulation of individual galaxies at relatively high resolution as well as the evolution of galaxy populations in representative cosmological volumes. With different numerical techniques (smoothed particle hydrodynamics, meshless particle hydrodynamics, adaptive mesh refinement and moving mesh hydrodynamics, see review by Somerville & Davé 2015)) it is now possible to simulate galaxy populations (at spatial resolutions of 0.5 - 3 kpc) with a realistic cosmological evolution of sizes, abundances, star formation rates, dark matter fractions, gas fractions as well as stellar and black hole masses, from well defined initial conditions, for a direct comparison to observational galaxy surveys (e.g. Davé et al. 2013, Hirschmann et al. 2014, Khandai et al. 2015, Schaye et al. 2015, Sijacki et al. 2015).

Zoom simulations of individual galaxies (at resolutions $< 500pc$) allow a detailed investigation of the formation processes and the consequences for the internal galaxy structure for direct comparison to high resolution observations (e.g. Aumer, White & Naab 2014; Dubois et al. 2013b; Genel et al. 2014; Guedes et al. 2011; Hopkins et al. 2014; Marinacci, Pakmor & Springel 2014; Naab et al. 2014; Stinson et al. 2013; Wetzel et al. 2016). Simulations of this kind (see also Forbes et al. 2016; Hu et al. 2016; Renaud, Bournaud & Duc 2015; Richings & Schaye 2016; Rosdahl et al. 2015) with high enough spatial resolution to represent the multi-phase interstellar medium structure and stellar feedback more accurately accounting for major effects like stellar winds, radiation and supernovae have the potential to shed more light into the detailed physical processes governing galaxy formation.

The rapid recent progress can be considered a success in our quest for a better understanding of galaxy formation. It was mainly triggered by the realization that thermal energy input from supernovae is most likely insufficient to trigger outflows and 'galactic winds' with other mechanisms being explored as the relevant drivers. These outflows, however, play a major - if not the dominant - role for regulating the formation of galaxies at low and high masses. They are most likely driven by energy injection from newly formed stellar populations (cosmic rays, radiation and winds, in addition to supernovae) and accreting black holes. As the outflows are launched on parsec and sub-parsec scales, well below the resolution and physical complexity limit of any cosmological simulation this has triggered a wealth of sub-resolution models for stellar and AGN feedback (see Section 2.2.1 and 2.3). The fact that many models - even if conceptually very different - driving a 'reasonable galactic wind' can 'successfully' reproduce galaxy abundances and disk galaxy morphology

gies (see e.g. Figs. 4 and 2) indicates that the essential characteristics of the problem has been disclosed. However, the empirical nature of the subresolution models limit the predictive power of the simulations and the literature becomes enriched by parameter studies of particular implementations despite obvious shortcomings of the respective models which are compensated by adjusted parameters. 'Delayed cooling', 'stochastic thermal', and 'non-thermal' feedback models may significantly overestimate the energy and momentum input into the ISM and the 'delay' time-scales are uncertain. 'Decoupled wind' models might not capture (i.e. underestimate) the energy coupling to the local ISM and result in unrealistic wind structures. Empirical 'momentum driving' models rely on uncertain coupling efficiencies for infrared radiation. Similarly, almost all AGN feedback models - on cosmological scales - are of empirical nature with accretion and energy conversion efficiencies adjusted, in a plausible fashion, to match observed scaling relations.

It will be a major theoretical challenge in theoretical galaxy formation to understand stellar and AGN feedback in detail and identify physically correct sub-resolution models taking into account all relevant physical processes. First promising steps in this direction have been made from high resolution galaxy scale simulations as well as simulations on smaller scales. A full accounting for the energy input from stellar populations (e.g. Agertz et al. 2013; Hopkins, Quataert & Murray 2012b), the long range effect of low and high energy radiation from stars and AGN (e.g. Bieri et al. 2016, Choi et al. 2012, Kannan et al. 2014, Roos et al. 2015, Rosdahl et al. 2015, Vogelsberger et al. 2013) and the consideration of other significant non-thermal components of the ISM, namely magnetic fields and cosmic rays (e.g. Booth et al. 2013, Hanaasz et al. 2013, Pakmor et al. 2016, Salem & Bryan 2014, Uhlig et al. 2012) are probably the most promising areas of galaxy formation research in the future. These research directions mainly refer to number (2) of our physics problem (Section 1.1): the knowledge of the physical processes primarily responsible for understanding each phase of galactic evolution. Starting with well defined initial conditions we can now roughly reproduce the scales and internal structures of common galaxy types and laboring with increasing physical precision to correctly model the detailed processes involved in feedback from stars and super-massive black holes.

Acknowledgements

The authors acknowledge valuable input on the manuscript from O. Agertz, R. Dave, A. Dekel, Y. Dubois, P. Girichidis, M. Hanaasz, M. Hirschmann, P. Hopkins, N. Khandai, B. Moster, T. Peters, E. Puchwein, M. Rafieferantsoa, V. Springel, G. Stinson, R. Teyssier, H. Übler, M. Vogelsberger, and S. Zhukovska. The authors are particularly grateful for the many detailed and valuable comments from J. Kormendy, D. Nelson and J. Schaye.

LITERATURE CITED

1. Abadi MG, Navarro JF, Steinmetz M, Eke VR. 2003a. *Ap. J.* 591:499–514
2. Abadi MG, Navarro JF, Steinmetz M, Eke VR. 2003b. *Ap. J.* 597:21–34
3. Ackermann M, Ajello M, Allafort A, Baldini L, Ballet J, et al. 2013. *Science* 339:807–811
4. Agertz O, Kravtsov AV. 2015. *Ap. J.* 804:18
5. Agertz O, Kravtsov AV, Leitner SN, Gnedin NY. 2013. *Ap. J.* 770:25
6. Agertz O, Moore B, Stadel J, Potter D, Miniati F, et al. 2007. *MNRAS* 380:963–978
7. Agertz O, Teyssier R, Moore B. 2011. *MNRAS* 410:1391–1408
8. Anderson ME, Gaspari M, White SDM, Wang W, Dai X. 2015. *MNRAS* 449:3806–3826
9. Anglés-Alcázar D, Davé R, Faucher-Giguère CA, Özel F, Hopkins PF. 2016. *ArXiv e-prints*

10. Anglés-Alcázar D, Davé R, Özel F, Oppenheimer BD. 2014. *Ap. J.* 782:84
11. Anglés-Alcázar D, Özel F, Davé R. 2013. *Ap. J.* 770:5
12. Angulo RE, Springel V, White SDM, Jenkins A, Baugh CM, Frenk CS. 2012. *MNRAS* 426:2046–2062
13. Arav N, Borguet B, Chamberlain C, Edmonds D, Danforth C. 2013. *MNRAS* 436:3286–3305
14. Arthur SJ, Kurtz SE, Franco J, Albarrán MY. 2004. *Ap. J.* 608:282–296
15. Aumer M, White SDM, Naab T. 2014. *MNRAS* 441:3679–3695
16. Aumer M, White SDM, Naab T, Scannapieco C. 2013. *MNRAS* 434:3142–3164
17. Babul A, Sharma P, Reynolds CS. 2013. *Ap. J.* 768:11
18. Bahé YM, Crain RA, Kauffmann G, Bower RG, Schaye J, et al. 2016. *MNRAS* 456:1115–1136
19. Balogh ML, Pearce FR, Bower RG, Kay ST. 2001. *MNRAS* 326:1228–1234
20. Barai P, Viel M, Borgani S, Tescari E, Tornatore L, et al. 2013. *MNRAS* 430:3213–3234
21. Barai P, Viel M, Murante G, Gaspari M, Borgani S. 2014. *MNRAS* 437:1456–1475
22. Barnes JE. 1988. *Ap. J.* 331:699–717
23. Barnes JE. 1992. *Ap. J.* 393:484–507
24. Barnes JE. 1998. *Dynamics of Galaxy Interactions*. In *Saas-Fee Advanced Course 26: Galaxies: Interactions and Induced Star Formation*
25. Barnes JE. 2002. *MNRAS* 333:481–494
26. Barnes JE, Hernquist L. 1992. *Annu. Rev. Astron. Astrophys.* 30:705–742
27. Barnes JE, Hernquist L. 1996. *Ap. J.* 471:115
28. Bédorf J, Portegies Zwart S. 2013. *MNRAS* 431:767–780
29. Behroozi PS, Conroy C, Wechsler RH. 2010. *Ap. J.* 717:379–403
30. Behroozi PS, Wechsler RH, Conroy C. 2013. *Ap. J.* 770:57
31. Bekki K. 1998. *Ap. J. Let.* 502:L133
32. Bekki K. 2015. *MNRAS* 449:1625–1649
33. Bekki K, Shioya Y. 1997. *Ap. J. Let.* 478:L17
34. Bell AR. 1978. *MNRAS* 182:147–156
35. Bendo GJ, Barnes JE. 2000. *MNRAS* 316:315–325
36. Berlind AA, Weinberg DH. 2002. *Ap. J.* 575:587–616
37. Bernardi M, Meert A, Sheth RK, Vikram V, Huertas-Company M, et al. 2013. *MNRAS* 436:697–704
38. Bernet ML, Miniati F, Lilly SJ. 2013. *Ap. J. Let.* 772:L28
39. Bezanson R, van Dokkum PG, Tal T, Marchesini D, Kriek M, et al. 2009. *Ap. J.* 697:1290–1298
40. Bieri R, Dubois Y, Rosdahl J, Wagner AY, Silk J, Mamon GA. 2016. *ArXiv e-prints*
41. Bigiel F, Leroy A, Walter F, Brinks E, de Blok WJG, et al. 2008. *Astron. J.* 136:2846–2871
42. Binney J. 1977. *Ap. J.* 215:483–491
43. Binney J, Tabor G. 1995. *MNRAS* 276:663
44. Binney J, Tremaine S. 2008. *Galactic Dynamics: Second Edition*. Princeton University Press
45. Birnboim Y, Dekel A. 2003. *MNRAS* 345:349–364
46. Blaauw A. 1961. *BAIN* 15:265
47. Bland-Hawthorn J, Gerhard O. 2016. *Annu. Rev. Astron. Astrophys.* 54:529–596
48. Blandford RD, Ostriker JP. 1978. *Ap. J. Let.* 221:L29–L32
49. Blanton MR, Moustakas J. 2009. *Annu. Rev. Astron. Astrophys.* 47:159–210
50. Blondin JM, Wright EB, Borkowski KJ, Reynolds SP. 1998. *Ap. J.* 500:342–354
51. Bluck AFL, Conselice CJ, Bouwens RJ, Daddi E, Dickinson M, et al. 2009. *MNRAS* 394:L51–L55
52. Bogdán Á, Forman WR, Vogelsberger M, Bourdin H, Sijacki D, et al. 2013. *Ap. J.* 772:97
53. Bois M, Bournaud F, Emsellem E, Alatalo K, Blitz L, et al. 2010. *MNRAS* 406:2405–2420
54. Bois Mea. 2011. *MNRAS* 416:1654–1679
55. Bondi H. 1952. *MNRAS* 112:195
56. Bondi H, Hoyle F. 1944. *MNRAS* 104:273
57. Booth CM, Agertz O, Kravtsov AV, Gnedin NY. 2013. *Ap. J. Let.* 777:L16
58. Booth CM, Schaye J. 2009. *MNRAS* 398:53–74
59. Boulares A, Cox DP. 1990. *Ap. J.* 365:544–558

60. Bournaud F, Chapon D, Teyssier R, Powell LC, Elmegreen BG, et al. 2011a. *Ap. J.* 730:4
61. Bournaud F, Combes F, Jog CJ. 2004. *Astron. Astrophys.* 418:L27–L30
62. Bournaud F, Dekel A, Teyssier R, Cacciato M, Daddi E, et al. 2011b. *Ap. J. Let.* 741:L33
63. Bournaud F, Jog CJ, Combes F. 2005. *Astron. Astrophys.* 437:69–85
64. Bournaud F, Jog CJ, Combes F. 2007. *Astron. Astrophys.* 476:1179–1190
65. Bouwens RJ, Illingworth GD, Oesch PA, Franx M, Labbé I, et al. 2012. *Ap. J.* 754:83
66. Bovy J, Allende Prieto C, Beers TC, Bizyaev D, da Costa LN, et al. 2012. *Ap. J.* 759:131
67. Bower RG, Benson AJ, Malbon R, Helly JC, Frenk CS, et al. 2006. *MNRAS* 370:645–655
68. Boylan-Kolchin M, Bullock JS, Kaplinghat M. 2011. *MNRAS* 415:L40–L44
69. Boylan-Kolchin M, Ma CP, Quataert E. 2005. *MNRAS* 362:184–196
70. Breitschwerdt D, McKenzie JF, Voelk HJ. 1991. *Astron. Astrophys.* 245:79–98
71. Breitschwerdt D, McKenzie JF, Voelk HJ. 1993. *Astron. Astrophys.* 269:54–66
72. Brighenti F, Mathews WG. 2006. *Ap. J.* 643:120–127
73. Brook CB, Governato F, Roškar R, Stinson G, Brooks AM, et al. 2011. *MNRAS* 415:1051–1060
74. Brook CB, Stinson G, Gibson BK, Roškar R, Wadsley J, Quinn T. 2012. *MNRAS* 419:771–779
75. Brook CB, Stinson G, Gibson BK, Shen S, Macciò AV, et al. 2014. *MNRAS* 443:3809–3818
76. Bryan GL, Norman ML, O’Shea BW, Abel T, Wise JH, et al. 2014. *Ap. J. Suppl.* 211:19
77. Bryan SE, Mao S, Kay ST, Schaye J, Dalla Vecchia C, Booth CM. 2012. *MNRAS* 422:1863–1879
78. Bullock JS, Wechsler RH, Somerville RS. 2002. *MNRAS* 329:246–256
79. Bundy K, Bershady MA, Law DR, Yan R, Drory N, et al. 2015. *Ap. J.* 798:7
80. Cappellari ea. 2011. *MNRAS* 416:1680–1696
81. Cappellari M, Emsellem E, Krajnović D, McDermid RM, Scott N, et al. 2011. *MNRAS* 413:813–836
82. Caprioli D, Pop AR, Spitkovsky A. 2015. *Ap. J. Let.* 798:L28
83. Castor JI, Abbott DC, Klein RI. 1975. *Ap. J.* 195:157–174
84. Catinella B, Schiminovich D, Kauffmann G, Fabello S, Wang J, et al. 2010. *MNRAS* 403:683–708
85. Cen R, Ostriker J. 1992a. *Ap. J.* 393:22–41
86. Cen R, Ostriker JP. 1992b. *Ap. J. Let.* 399:L113–L116
87. Cenarro AJ, Trujillo I. 2009. *Ap. J. Let.* 696:L43–L47
88. Ceverino D, Klypin A. 2009. *Ap. J.* 695:292–309
89. Chevalier RA. 1982. *Ap. J.* 258:790–797
90. Chevalier RA, Clegg AW. 1985. *Nature* 317:44
91. Choi E, Naab T, Ostriker JP, Johansson PH, Moster BP. 2014. *MNRAS* 442:440–453
92. Choi E, Ostriker JP, Naab T, Johansson PH. 2012. *Ap. J.* 754:125
93. Choi E, Ostriker JP, Naab T, Oser L, Moster BP. 2015. *MNRAS* 449:4105–4116
94. Choi E, Ostriker JP, Naab T, Somerville RS, Hirschmann M, et al. 2016. *ArXiv e-prints*
95. Christensen C, Quinn T, Governato F, Stilp A, Shen S, Wadsley J. 2012. *MNRAS* 425:3058–3076
96. Christensen CR, Davé R, Governato F, Pontzen A, Brooks A, et al. 2016. *Ap. J.* 824:57
97. Churazov E, Sazonov S, Sunyaev R, Forman W, Jones C, Böhringer H. 2005. *MNRAS* 363:L91–L95
98. Cimatti A, Nipoti C, Cassata P. 2012. *MNRAS* 422:L62
99. Cioffi DF, McKee CF, Bertschinger E. 1988. *Ap. J.* 334:252–265
100. Ciotti L, D’Ercole A, Pellegrini S, Renzini A. 1991. *Ap. J.* 376:380–403
101. Ciotti L, Ostriker JP. 1997. *Ap. J. Let.* 487:L105–L108
102. Ciotti L, Ostriker JP. 2001. *Ap. J.* 551:131–152
103. Cisternas M, Jahnke K, Inskip KJ, Kartaltepe J, Koekemoer AM, et al. 2011. *Ap. J.* 726:57
104. Cole S, Lacey CG, Baugh CM, Frenk CS. 2000. *MNRAS* 319:168–204
105. Conroy C, Wechsler RH. 2009. *Ap. J.* 696:620–635
106. Conroy C, Wechsler RH, Kravtsov AV. 2006. *Ap. J.* 647:201–214
107. Courteau S, Cappellari M, de Jong RS, Dutton AA, Emsellem E, et al. 2014. *Reviews of Modern Physics* 86:47–119
108. Cox TJ, Dutta SN, Di Matteo T, Hernquist L, Hopkins PF, et al. 2006a. *Ap. J.* 650:791–811
109. Cox TJ, Jonsson P, Primack JR, Somerville RS. 2006b. *MNRAS* 373:1013–1038
110. Crain RA, McCarthy IG, Frenk CS, Theuns T, Schaye J. 2010. *MNRAS* 407:1403–1422

111. Crain RA, Schaye J, Bower RG, Furlong M, Schaller M, et al. 2015. *MNRAS* 450:1937–1961
112. Cretton N, Naab T, Rix HW, Burkert A. 2001. *Ap. J.* 554:291–297
113. Croton DJ, Springel V, White SDM, De Lucia G, Frenk CS, et al. 2006. *MNRAS* 365:11–28
114. Daddi E, Bournaud F, Walter F, Dannerbauer H, Carilli CL, et al. 2010. *Ap. J.* 713:686–707
115. Daddi E, Dickinson M, Morrison G, Chary R, Cimatti A, et al. 2007. *Ap. J.* 670:156–172
116. Daddi E, Renzini A, Pirzkal N, Cimatti A, Malhotra S, et al. 2005. *Ap. J.* 626:680–697
117. Dai X, Bregman JN, Kochanek CS, Rasia E. 2010. *Ap. J.* 719:119–125
118. Dalcanton JJ, Spergel DN, Summers FJ. 1997. *Ap. J.* 482:659–676
119. Dale JE, Bonnell IA. 2008. *MNRAS* 391:2–13
120. Dale JE, Bonnell IA, Whitworth AP. 2007. *MNRAS* 375:1291–1298
121. Dale JE, Ngoumou J, Ercolano B, Bonnell IA. 2013. *MNRAS* 436:3430–3445
122. Dale JE, Ngoumou J, Ercolano B, Bonnell IA. 2014. *MNRAS* 442:694–712
123. Dalla Vecchia C, Schaye J. 2008. *MNRAS* 387:1431–1444
124. Dalla Vecchia C, Schaye J. 2012. *MNRAS* 426:140–158
125. Damjanov I, Abraham RG, Glazebrook K, McCarthy PJ, Caris E, et al. 2011. *Ap. J. Let.* 739:L44
126. Davé R, Finlator K, Oppenheimer BD. 2011. *MNRAS* 416:1354–1376
127. Davé R, Katz N, Oppenheimer BD, Kollmeier JA, Weinberg DH. 2013. *MNRAS* 434:2645–2663
128. Davé R, Thompson RJ, Hopkins PF. 2016. *ArXiv e-prints*
129. Davis SW, Jiang YF, Stone JM, Murray N. 2014. *ArXiv e-prints*
130. de Avillez MA. 2000. *MNRAS* 315:479–497
131. de Avillez MA, Breitschwerdt D. 2004. *Astron. Astrophys.* 425:899–911
132. de Avillez MA, Breitschwerdt D. 2005. *Astron. Astrophys.* 436:585–600
133. De Lucia G, Blaizot J. 2007. *MNRAS* 375:2–14
134. de Vaucouleurs G. 1948. *Annales d’Astrophysique* 11:247
135. de Zeeuw PT, Bureau M, Emsellem E, Bacon R, Carollo CM, et al. 2002. *MNRAS* 329:513–530
136. Debuhr J, Quataert E, Ma CP. 2011. *MNRAS* 412:1341–1360
137. Debuhr J, Quataert E, Ma CP, Hopkins P. 2010. *MNRAS* 406:L55–L59
138. Dekel A, Birnboim Y, Engel G, Freundlich J, Goerdt T, et al. 2009. *Nature* 457:451–454
139. Dekel A, Cox TJ. 2006. *MNRAS* 370:1445–1453
140. Dekel A, Silk J. 1986. *Ap. J.* 303:39–55
141. Di Matteo P, Jog CJ, Lehnert MD, Combes F, Semelin B. 2009a. *Astron. Astrophys.* 501:L9–L13
142. Di Matteo P, Pipino A, and Lehnert MD, Combes F, Semelin B. 2009b. *Astron. Astrophys.* 499:427–437
143. Di Matteo T, Khandai N, DeGraf C, Feng Y, Croft RAC, et al. 2012. *Ap. J. Let.* 745:L29
144. Di Matteo T, Springel V, Hernquist L. 2005. *Nature* 433:604–607
145. Diemand J, Kuhlen M, Madau P. 2007. *Ap. J.* 667:859–877
146. Dolag K, Bykov AM, Diaferio A. 2008. *Space Science Rev.* 134:311–335
147. Dolag K, Grasso D, Springel V, Tkachev I. 2005. *J. of Cosmo. and Astrop. Phys.* 1:9
148. Dolag K, Stasyszyn F. 2009. *MNRAS* 398:1678–1697
149. D’Onghia E, Burkert A. 2004. *Ap. J. Let.* 612:L13–L16
150. Draine BT. 2011. *Physics of the Interstellar and Intergalactic Medium*
151. Dressler A. 1980. *Ap. J.* 236:351–365
152. Dubois Y, Devriendt J, Slyz A, Teyssier R. 2012. *MNRAS* 420:2662–2683
153. Dubois Y, Gavazzi R, Peirani S, Silk J. 2013a. *ArXiv e-prints*
154. Dubois Y, Gavazzi R, Peirani S, Silk J. 2013b. *MNRAS* 433:3297–3313
155. Dubois Y, Pichon C, Welker C, Le Borgne D, Devriendt J, et al. 2014. *MNRAS* 444:1453–1468
156. Dubois Y, Teyssier R. 2010. *Astron. Astrophys.* 523:A72
157. Duncan K, Conselice CJ, Mortlock A, Hartley WG, Guo Y, et al. 2014. *MNRAS* 444:2960–2984
158. Efstathiou G, Eastwood JW. 1981. *MNRAS* 194:503–525
159. Eggen OJ, Lynden-Bell D, Sandage AR. 1962. *Ap. J.* 136:748
160. Ellison DC, Patnaude DJ, Slane P, Raymond J. 2010. *Ap. J.* 712:287–293
161. Elmegreen BG, Scalo J. 2004. *Annu. Rev. Astron. Astrophys.* 42:211–273

162. Enßlin TA, Pfrommer C, Springel V, Jubelgas M. 2007. *Astron. Astrophys.* 473:41–57
163. Everett JE, Zweibel EG, Benjamin RA, McCammon D, Rocks L, Gallagher III JS. 2008. *Ap. J.* 674:258–270
164. Evrard AE. 1988. *MNRAS* 235:911–934
165. Fabian AC. 2012. *Annu. Rev. Astron. Astrophys.* 50:455–489
166. Fabian AC, Sanders JS, Taylor GB, Allen SW, Crawford CS, et al. 2006. *MNRAS* 366:417–428
167. Fabjan D, Borgani S, Tornatore L, Saro A, Murante G, Dolag K. 2010. *MNRAS* 401:1670–1690
168. Fagioli M, Carollo CM, Renzini A, Lilly SJ, Onodera M, Tacchella S. 2016. *ArXiv e-prints*
169. Fall SM. 1979. *Nature* 281:200–202
170. Fall SM, Efstathiou G. 1980. *MNRAS* 193:189–206
171. Farouki RT, Shapiro SL. 1982. *Ap. J.* 259:103–115
172. Faucher-Giguère CA, Lidz A, Zaldarriaga M, Hernquist L. 2009. *Ap. J.* 703:1416–1443
173. Feldmann R, Carollo CM, Mayer L. 2011. *Ap. J.* 736:88
174. Feldmann R, Carollo CM, Mayer L, Renzini A, Lake G, et al. 2010. *Ap. J.* 709:218–240
175. Feldmann R, Gnedin NY, Kravtsov AV. 2012. *Ap. J.* 747:124
176. Feldmann R, Mayer L. 2014. *ArXiv e-prints*
177. Ferrière KM. 2001. *Reviews of Modern Physics* 73:1031–1066
178. Finlator K, Davé R. 2008. *MNRAS* 385:2181–2204
179. Fogarty LMR, Scott N, Owers MS, Brough S, Croom SM, et al. 2014. *MNRAS* 443:485–503
180. Forbes JC, Krumholz MR, Goldbaum NJ, Dekel A. 2016. *Nature* 535:523–525
181. Förster Schreiber NM, Genzel R, Bouché N, Cresci G, Davies R, et al. 2009. *Ap. J.* 706:1364–1428
182. Frenk CS, White SDM. 2012. *Annalen der Physik* 524:507–534
183. Frenk CS, White SDM, Bode P, Bond JR, Bryan GL, et al. 1999. *Ap. J.* 525:554–582
184. Fryxell B, Olson K, Ricker P, Timmes FX, Zingale M, et al. 2000. *Ap. J. Suppl.* 131:273–334
185. Furlong M, Bower RG, Theuns T, Schaye J, Crain RA, et al. 2015. *MNRAS* 450:4486–4504
186. Gabor JM, Bournaud F. 2013. *MNRAS* 434:606–620
187. Gabor JM, Davé R. 2012. *MNRAS* 427:1816–1829
188. Gaburov E, Nitadori K. 2011. *MNRAS* 414:129–154
189. Gao L, Navarro JF, Frenk CS, Jenkins A, Springel V, White SDM. 2012. *MNRAS* 425:2169–2186
190. Gaspari M, Brighenti F, Temi P. 2012. *MNRAS* 424:190–209
191. Gatto A, Walch S, Low MMM, Naab T, Girichidis P, et al. 2015. *MNRAS* 449:1057–1075
192. Gatto A, Walch S, Naab T, Girichidis P, Wünsch R, et al. 2016. *ArXiv e-prints*
193. Geen S, Rosdahl J, Blaizot J, Devriendt J, Slyz A. 2015. *MNRAS* 448:3248–3264
194. Genel S, Fall SM, Hernquist L, Vogelsberger M, Snyder GF, et al. 2015. *Ap. J. Let.* 804:L40
195. Genel S, Naab T, Genzel R, Förster Schreiber NM, Sternberg A, et al. 2012. *Ap. J.* 745:11
196. Genel S, Vogelsberger M, Nelson D, Sijacki D, Springel V, Hernquist L. 2013. *MNRAS* 435:1426–1442
197. Genel S, Vogelsberger M, Springel V, Sijacki D, Nelson D, et al. 2014. *MNRAS* 445:175–200
198. Genzel R, Eckart A, Ott T, Eisenhauer F. 1997. *MNRAS* 291:219–234
199. Genzel R, Förster Schreiber NM, Rosario D, Lang P, Lutz D, et al. 2014. *Ap. J.* 796:7
200. Genzel R, Tacconi LJ, Eisenhauer F, Förster Schreiber NM, Cimatti A, et al. 2006. *Nature* 442:786–789
201. Georgakakis A, Coil AL, Laird ES, Griffith RL, Nandra K, et al. 2009. *MNRAS* 397:623–633
202. Gerritsen JPE. 1997. *Star formation and the interstellar medium in galaxy simulations*. Ph.D. thesis, Groningen University, the Netherlands, (1997)
203. Gies DR, Bolton CT. 1986. *Ap. J. Suppl.* 61:419–454
204. Gingold RA, Monaghan JJ. 1977. *MNRAS* 181:375–389
205. Giodini S, Pierini D, Finoguenov A, Pratt GW, Boehringer H, et al. 2009. *Ap. J.* 703:982–993
206. Girichidis P, Naab T, Walch S, Hanasz M, Mac Low MM, et al. 2016a. *Ap. J. Let.* 816:L19
207. Girichidis P, Walch S, Naab T, Gatto A, Wünsch R, et al. 2016b. *MNRAS* 456:3432–3455
208. Glover SCO, Clark PC. 2012. *MNRAS* 421:9–19
209. Glover SCO, Mac Low MM. 2007. *Ap. J.* 659:1317–1337

210. Gnat O, Sternberg A. 2007. *Ap. J. Suppl.* 168:213–230
211. Gnedin NY, Tassis K, Kravtsov AV. 2009. *Ap. J.* 697:55–67
212. González-García AC, Balcells M. 2005. *MNRAS* 357:753–772
213. Gonzalez AH, Sivanandam S, Zabludoff AI, Zaritsky D. 2013. *Ap. J.* 778:14
214. Governato F, Brook C, Mayer L, Brooks A, Rhee G, et al. 2010. *Nature* 463:203–206
215. Governato F, Mayer L, Wadsley J, Gardner JP, Willman B, et al. 2004. *Ap. J.* 607:688–696
216. Governato F, Willman B, Mayer L, Brooks A, Stinson G, et al. 2007. *MNRAS* 374:1479–1494
217. Grand RJJ, Springel V, Gómez FA, Marinacci F, Pakmor R, et al. 2016. *MNRAS* 459:199–219
218. Gritschneider M, Burkert A, Naab T, Walch S. 2010. *Ap. J.* 723:971–984
219. Gritschneider M, Naab T, Walch S, Burkert A, Heitsch F. 2009. *Ap. J. Let.* 694:L26–L30
220. Guedes J, Callegari S, Madau P, Mayer L. 2011. *Ap. J.* 742:76
221. Guo Q, White S. 2014. *MNRAS* 437:3228–3235
222. Guo Q, White S, Boylan-Kolchin M, De Lucia G, Kauffmann G, et al. 2011. *MNRAS* 413:101–131
223. Guo Q, White S, Li C, Boylan-Kolchin M. 2010. *MNRAS* 404:1111–1120
224. Guo Q, White SDM. 2008. *MNRAS* 384:2–10
225. Haardt F, Madau P. 2012. *Ap. J.* 746:125
226. Haid S, Walch S, Naab T, Seifried D, Mackey J, Gatto g. 2016. *MNRAS* 460:2962–2978
227. Hambrick DC, Ostriker JP, Naab T, Johansson PH. 2011. *Ap. J.* 738:16
228. Hanasz M, Lesch H, Naab T, Gawryszczak A, Kowalik K, Wóltański D. 2013. *Ap. J. Let.* 777:L38
229. Hayward CC, Torrey P, Springel V, Hernquist L, Vogelsberger M. 2014. *MNRAS* 442:1992–2016
230. Hearin AP, Watson DF. 2013. *MNRAS* 435:1313–1324
231. Heavens A, Panter B, Jimenez R, Dunlop J. 2004. *Nature* 428:625–627
232. Heckman TM. 2003. *Starburst-Driven Galactic Winds*. In *Revista Mexicana de Astronomía y Astrofísica Conference Series*, eds. V Avila-Reese, C Firmani, CS Frenk, C Allen, vol. 17 of *Revista Mexicana de Astronomía y Astrofísica*, vol. 27
233. Heckman TM, Armus L, Miley GK. 1990. *Ap. J. Suppl.* 74:833–868
234. Heckman TM, Best PN. 2014. *Annu. Rev. Astron. Astrophys.* 52:589–660
235. Heckman TM, Lehnert MD, Strickland DK, Armus L. 2000. *Ap. J. Suppl.* 129:493–516
236. Heitsch F, Naab T, Walch S. 2011. *MNRAS* 415:271–278
237. Hennebelle P, Iffrig O. 2014. *Astron. Astrophys.* 570:A81
238. Henriques BMB, White SDM, Thomas PA, Angulo R, Guo Q, et al. 2015. *MNRAS* 451:2663–2680
239. Hernquist L. 1989. *Nature* 340:687–691
240. Hernquist L. 1992. *Ap. J.* 400:460–475
241. Hernquist L. 1993a. *Ap. J. Suppl.* 86:389–400
242. Hernquist L. 1993b. *Ap. J.* 409:548–562
243. Hernquist L, Katz N. 1989. *Ap. J. Suppl.* 70:419–446
244. Hewitt JW, Yusef-Zadeh F, Wardle M. 2009. *Ap. J. Let.* 706:L270–L274
245. Heyl JS, Hernquist L, Spergel DN. 1994. *Ap. J.* 427:165–173
246. Hill AS, Joung MR, Mac Low MM, Benjamin RA, Haffner LM, et al. 2012. *Ap. J.* 750:104
247. Hillas AM. 2005. *Journal of Physics G Nuclear Physics* 31:95
248. Hilz M, Naab T, Ostriker JP. 2013. *MNRAS* 429:2924–2933
249. Hilz M, Naab T, Ostriker JP, Thomas J, Burkert A, Jesseit R. 2012. *MNRAS* 425:3119–3136
250. Hirschmann M, Dolag K, Saro A, Bachmann L, Borgani S, Burkert A. 2014. *MNRAS* 442:2304–2324
251. Hirschmann M, Naab T, Davé R, Oppenheimer BD, Ostriker JP, et al. 2013. *MNRAS* 436:2929–2949
252. Hirschmann M, Naab T, Somerville RS, Burkert A, Oser L. 2012. *MNRAS* 419:3200–3222
253. Hoffman L, Cox TJ, Dutta S, Hernquist L. 2009. *Ap. J.* 705:920–925
254. Hoffman L, Cox TJ, Dutta S, Hernquist L. 2010. *Ap. J.* 723:818–844
255. Hopkins PF. 2015. *MNRAS* 450:53–110
256. Hopkins PF, Cox TJ, Dutta SN, Hernquist L, Kormendy J, Lauer TR. 2009a. *Ap. J. Suppl.* 181:135–182
257. Hopkins PF, Hayward CC, Narayanan D, Hernquist L. 2012. *MNRAS* 420:320–339
258. Hopkins PF, Hernquist L, Cox TJ, Di Matteo T, Martini P, et al. 2005. *Ap. J.* 630:705–715

259. Hopkins PF, Hernquist L, Cox TJ, Di Matteo T, Robertson B, Springel V. 2006. *Ap. J. Suppl.* 163:1–49
260. Hopkins PF, Hernquist L, Cox TJ, Keres D, Wuyts S. 2009b. *Ap. J.* 691:1424–1458
261. Hopkins PF, Kereš D, Murray N, Hernquist L, Narayanan D, Hayward CC. 2013. *MNRAS* 433:78–97
262. Hopkins PF, Kereš D, Oñorbe J, Faucher-Giguère CA, Quataert E, et al. 2014. *MNRAS* 445:581–603
263. Hopkins PF, Lauer TR, Cox TJ, Hernquist L, Kormendy J. 2009c. *Ap. J. Suppl.* 181:486–532
264. Hopkins PF, Narayanan D, Murray N. 2013. *MNRAS* 432:2647–2653
265. Hopkins PF, Quataert E. 2011. *MNRAS* 415:1027–1050
266. Hopkins PF, Quataert E, Murray N. 2011. *MNRAS* 417:950–973
267. Hopkins PF, Quataert E, Murray N. 2012a. *MNRAS* 421:3522–3537
268. Hopkins PF, Quataert E, Murray N. 2012b. *MNRAS* 421:3488–3521
269. Hopkins PF, Torrey P, Faucher-Giguère CA, Quataert E, Murray N. 2016. *MNRAS* 458:816–831
270. Hoyle F, Lyttleton RA. 1939. *Proceedings of the Cambridge Philosophical Society* 35:405
271. Hu CY, Naab T, Walch S, Glover SCO, Clark PC. 2016. *MNRAS* 458:3528–3553
272. Hu CY, Naab T, Walch S, Moster BP, Oser L. 2014. *MNRAS* 443:1173–1191
273. Hubber DA, Falle SAEG, Goodwin SP. 2013. *MNRAS* 432:711–727
274. Iffrig O, Hennebelle P. 2015. *Astron. Astrophys.* 576:A95
275. Janka HT. 2012. *Annual Review of Nuclear and Particle Science* 62:407–451
276. Jesseit R, Cappellari M, Naab T, Emsellem E, Burkert A. 2009. *MNRAS* 397:1202–1214
277. Jesseit R, Naab T, Peletier RF, Burkert A. 2007. *MNRAS* 376:997–1020
278. Johansson PH, Naab T, Burkert A. 2009. *Ap. J.* 690:802–821
279. Johansson PH, Naab T, Ostriker JP. 2009. *Ap. J. Let.* 697:L38–L43
280. Johansson PH, Naab T, Ostriker JP. 2012. *Ap. J.* 754:115
281. Joseph RD, Wright GS. 1985. *MNRAS* 214:87–95
282. Joung MKR, Mac Low MM. 2006. *Ap. J.* 653:1266–1279
283. Jubelgas M, Springel V, Enßlin T, Pfrommer C. 2008. *Astron. Astrophys.* 481:33–63
284. Kalberla PMW, Kerp J. 2009. *Annu. Rev. Astron. Astrophys.* 47:27–61
285. Kang H, Jones TW. 2006. *Astroparticle Physics* 25:246–258
286. Kannan R, Stinson GS, Macciò AV, Hennawi JF, Woods R, et al. 2014. *MNRAS* 437:2882–2893
287. Katz N. 1992. *Ap. J.* 391:502–517
288. Katz N, Gunn JE. 1991. *Ap. J.* 377:365–381
289. Katz N, Weinberg DH, Hernquist L. 1996. *Ap. J. Suppl.* 105:19
290. Kauffmann G, Heckman TM, White SDM, Charlot S, Tremonti C, et al. 2003. *MNRAS* 341:33–53
291. Kauffmann G, White SDM, Guiderdoni B. 1993. *MNRAS* 264:201
292. Keller BW, Wadsley J, Couchman HMP. 2015. *MNRAS* 453:3499–3509
293. Keller BW, Wadsley J, Couchman HMP. 2016. *MNRAS*
294. Kennicutt RC. 1998. *Ap. J.* 498:541
295. Kennicutt RC, Evans NJ. 2012. *Annu. Rev. Astron. Astrophys.* 50:531–608
296. Kennicutt Jr. RC, Calzetti D, Walter F, Helou G, Hollenbach DJ, et al. 2007. *Ap. J.* 671:333–348
297. Kereš D, Katz N, Weinberg DH, Davé R. 2005. *MNRAS* 363:2–28
298. Khandai N, Di Matteo T, Croft R, Wilkins S, Feng Y, et al. 2015. *MNRAS* 450:1349–1374
299. Khochfar S, Burkert A. 2006. *Astron. Astrophys.* 445:403–412
300. Khochfar S, Ostriker JP. 2008. *Ap. J.* 680:54–69
301. Khochfar S, Silk J. 2006. *MNRAS* 370:902–910
302. Kim CG, Kim WT, Ostriker EC. 2011. *Ap. J.* 743:25
303. Kim CG, Ostriker EC. 2015a. *Ap. J.* 802:99
304. Kim CG, Ostriker EC. 2015b. *Ap. J.* 815:67
305. Kim CG, Ostriker EC, Kim WT. 2013. *Ap. J.* 776:1
306. Kim Jh, Abel T, Agertz O, Bryan GL, Ceverino D, et al. 2014. *Ap. J. Suppl.* 210:14
307. Klypin AA, Trujillo-Gomez S, Primack J. 2011. *Ap. J.* 740:102
308. Kobayashi C. 2004. *MNRAS* 347:740–758

309. Kobayashi C. 2005. *MNRAS* 361:1216–1226
310. Kocevski DD, Faber SM, Mozena M, Koekemoer AM, Nandra K, et al. 2012. *Ap. J.* 744:148
311. Koopmans LVE, Bolton A, Treu T, Czoske O, Auger MW, et al. 2009. *Ap. J. Let.* 703:L51–L54
312. Kormendy J. 1999. *The Central Structure of Elliptical Galaxies and the Stellar-Dynamical Search for Supermassive Black Holes*. In *Galaxy Dynamics - A Rutgers Symposium*, eds. DR Merritt, M Valluri, JA Sellwood, vol. 182 of *Astronomical Society of the Pacific Conference Series*
313. Kormendy J, Drory N, Bender R, Cornell ME. 2010. *Ap. J.* 723:54–80
314. Kormendy J, Fisher DB, Cornell ME, Bender R. 2009. *Ap. J. Suppl.* 182:216–309
315. Kormendy J, Freeman KC. 2016. *Ap. J.* 817:84
316. Kormendy J, Ho LC. 2013. *Annu. Rev. Astron. Astrophys.* 51:511–653
317. Korpi MJ, Brandenburg A, Shukurov A, Tuominen I, Nordlund Å. 1999. *Ap. J. Let.* 514:L99–L102
318. Kotarba H, Karl SJ, Naab T, Johansson PH, Dolag K, et al. 2010. *Ap. J.* 716:1438–1452
319. Kotarba H, Lesch H, Dolag K, Naab T, Johansson PH, Stasyszyn FA. 2009. *MNRAS* 397:733–747
320. Kravtsov A, Vikhlinin A, Meshcheryakov A. 2014. *ArXiv e-prints*
321. Kravtsov AV. 2003. *Ap. J. Let.* 590:L1–L4
322. Kravtsov AV, Berlind AA, Wechsler RH, Klypin AA, Gottlöber S, et al. 2004. *Ap. J.* 609:35–49
323. Kravtsov AV, Borgani S. 2012. *Annu. Rev. Astron. Astrophys.* 50:353–409
324. Kravtsov AV, Klypin AA, Bullock JS, Primack JR. 1998. *Ap. J.* 502:48–58
325. Kravtsov AV, Klypin AA, Khokhlov AM. 1997. *Ap. J. Suppl.* 111:73–94
326. Krolik JH. 1999. *Active galactic nuclei : from the central black hole to the galactic environment*
327. Krumholz MR. 2013. *MNRAS* 436:2747–2762
328. Krumholz MR, Matzner CD. 2009. *Ap. J.* 703:1352–1362
329. Krumholz MR, Matzner CD, McKee CF. 2006. *Ap. J.* 653:361–382
330. Krumholz MR, Thompson TA. 2012. *Ap. J.* 760:155
331. Krumholz MR, Thompson TA. 2013. *MNRAS* 434:2329–2346
332. Kudritzki RP, Puls J. 2000. *Annu. Rev. Astron. Astrophys.* 38:613–666
333. Kuhlen M, Krumholz MR, Madau P, Smith BD, Wise J. 2012. *Ap. J.* 749:36
334. Kulsrud R, Pearce WP. 1969. *Ap. J.* 156:445
335. Lackner CN, Cen R, Ostriker JP, Joung MR. 2012. *MNRAS* 425:641–656
336. Laporte CFP, White SDM, Naab T, Gao L. 2013. *MNRAS* 435:901–909
337. Larson RB. 1974. *MNRAS* 169:229–246
338. Le Brun AMC, McCarthy IG, Melin JB. 2015. *MNRAS* 451:3868–3881
339. Le Brun AMC, McCarthy IG, Schaye J, Ponman TJ. 2014. *MNRAS* 441:1270–1290
340. Leitherer C, Schaerer D, Goldader JD, Delgado RMG, Robert C, et al. 1999. *Ap. J. Suppl.* 123:3–40
341. Leroy AK, Walter F, Brinks E, Bigiel F, de Blok WJG, et al. 2008. *Astron. J.* 136:2782–2845
342. Li C, White SDM. 2009. *MNRAS* 398:2177–2187
343. Li M, Bryan GL, Ostriker JP. 2016. *ArXiv e-prints*
344. Li M, Ostriker JP, Cen R, Bryan GL, Naab T. 2015. *Ap. J.* 814:4
345. Li Y, Bryan GL. 2014. *Ap. J.* 789:54
346. Li Y, Mac Low MM, Klessen RS. 2005. *Ap. J. Let.* 620:L19–L22
347. Li YS, White SDM. 2008. *MNRAS* 384:1459–1468
348. Lu Z, Mo HJ, Lu Y, Katz N, Weinberg MD, et al. 2015. *MNRAS* 450:1604–1617
349. Lucy LB. 1977. *Astron. J.* 82:1013–1024
350. Mac Low MM, McCray R. 1988. *Ap. J.* 324:776–785
351. Malkov MA, O’C Drury L. 2001. *Reports on Progress in Physics* 64:429–481
352. Man AWS, Toft S, Zirm AW, Wuyts S, van der Wel A. 2012. *Ap. J.* 744:85
353. Mandelbaum R, Seljak U, Kauffmann G, Hirata CM, Brinkmann J. 2006. *MNRAS* 368:715–731
354. Marinacci F, Fraternali F, Nipoti C, Binney J, Ciotti L, Londrillo P. 2011. *MNRAS* 415:1534–1542
355. Marinacci F, Pakmor R, Springel V. 2014. *MNRAS* 437:1750–1775
356. Marinacci F, Pakmor R, Springel V, Simpson CM. 2014. *MNRAS* 442:3745–3760
357. Marri S, White SDM. 2003. *MNRAS* 345:561–574
358. Martin CL. 1999. *Ap. J.* 513:156–160

359. Martin CL. 2005. *Ap. J.* 621:227–245
360. Martin CL, Shapley AE, Coil AL, Kornei KA, Murray N, Pancoast A. 2013. *Ap. J.* 770:41
361. Martizzi D, Faucher-Giguère CA, Quataert E. 2015. *MNRAS* 450:504–522
362. Martizzi D, Fielding D, Faucher-Giguère CA, Quataert E. 2016. *MNRAS* 459:2311–2326
363. Martizzi D, Jimmy, Teyssier R, Moore B. 2014. *MNRAS* 443:1500–1508
364. Martizzi D, Teyssier R, Moore B. 2012. *MNRAS* 420:2859–2873
365. Martizzi D, Teyssier R, Moore B, Wentz T. 2012. *MNRAS* 422:3081–3091
366. Mathews WG. 1969. *Ap. J.* 157:583
367. McCarthy IG, Schaye J, Bower RG, Ponman TJ, Booth CM, et al. 2011. *MNRAS* 412:1965–1984
368. McCarthy IG, Schaye J, Ponman TJ, Bower RG, Booth CM, et al. 2010. *MNRAS* 406:822–839
369. McKee CF, Ostriker JP. 1977. *Ap. J.* 218:148–169
370. McKenzie JF, Voelk HJ. 1982. *Astron. Astrophys.* 116:191–200
371. McKinnon R, Torrey P, Vogelsberger M. 2016. *MNRAS* 457:3775–3800
372. Merloni A, Heinz S. 2008. *MNRAS* 388:1011–1030
373. Meza A, Navarro JF, Steinmetz M, Eke VR. 2003. *Ap. J.* 590:619–635
374. Mihos JC, Hernquist L. 1994a. *Ap. J. Let.* 437:L47–L50
375. Mihos JC, Hernquist L. 1994b. *Ap. J.* 437:611–624
376. Mihos JC, Hernquist L. 1994c. *Ap. J. Let.* 431:L9–L12
377. Mihos JC, Hernquist L. 1996. *Ap. J.* 464:641
378. Mo H, van den Bosch FC, White S. 2010. *Galaxy Formation and Evolution*
379. Mo HJ, Mao S, White SDM. 1998. *MNRAS* 295:319–336
380. Monaco P, Murante G, Borgani S, Dolag K. 2012. *MNRAS* 421:2485–2497
381. Moster BP, Macciò AV, Somerville RS, Naab T, Cox TJ. 2011. *MNRAS* 415:3750–3770
382. Moster BP, Naab T, White SDM. 2013. *MNRAS* 428:3121–3138
383. Moster BP, Somerville RS, Maulbetsch C, van den Bosch FC, Macciò AV, et al. 2010. *Ap. J.* 710:903–923
384. Moustakas J, Coil AL, Aird J, Blanton MR, Cool RJ, et al. 2013. *Ap. J.* 767:50
385. Mulchaey JS. 2000. *Annu. Rev. Astron. Astrophys.* 38:289–335
386. Muratov AL, Kereš D, Faucher-Giguère CA, Hopkins PF, Quataert E, Murray N. 2015. *MNRAS* 454:2691–2713
387. Murray N, Ménard B, Thompson TA. 2011. *Ap. J.* 735:66
388. Murray N, Quataert E, Thompson TA. 2005. *Ap. J.* 618:569–585
389. Murray N, Quataert E, Thompson TA. 2010. *Ap. J.* 709:191–209
390. Muzzin A, Marchesini D, Stefanon M, Franx M, McCracken HJ, et al. 2013. *Ap. J.* 777:18
391. Naab T, Burkert A. 2003. *Ap. J.* 597:893–906
392. Naab T, Burkert A, Hernquist L. 1999. *Ap. J. Let.* 523:L133–L136
393. Naab T, Jesseit R, Burkert A. 2006. *MNRAS* 372:839–852
394. Naab T, Johansson PH, Ostriker JP. 2009. *Ap. J. Let.* 699:L178–L182
395. Naab T, Johansson PH, Ostriker JP, Efstathiou G. 2007. *Ap. J.* 658:710–720
396. Naab T, Khochfar S, Burkert A. 2006. *Ap. J. Let.* 636:L81–L84
397. Naab T, Oser L, Emsellem E, Cappellari M, Krajnović D, et al. 2014. *MNRAS* 444:3357–3387
398. Naab T, Ostriker JP. 2009. *Ap. J.* 690:1452–1462
399. Navarro JF, Benz W. 1991. *Ap. J.* 380:320–329
400. Navarro JF, Frenk CS, White SDM. 1995. *MNRAS* 275:56–66
401. Navarro JF, Steinmetz M. 1997. *Ap. J.* 478:13–28
402. Navarro JF, White SDM. 1993. *MNRAS* 265:271
403. Navarro JF, White SDM. 1994. *MNRAS* 267:401–412
404. Navarro-González J, Ricciardelli E, Quilis V, Vazdekis A. 2013. *MNRAS* 436:3507–3524
405. Negroponte J, White SDM. 1983. *MNRAS* 205:1009–1029
406. Nelson D, Genel S, Pillepich A, Vogelsberger M, Springel V, Hernquist L. 2016. *MNRAS* 460:2881–2904
407. Nelson D, Genel S, Vogelsberger M, Springel V, Sijacki D, et al. 2015. *MNRAS* 448:59–74

408. Nelson D, Vogelsberger M, Genel S, Sijacki D, Kereš D, et al. 2013. *MNRAS* 429:3353–3370
409. Newman AB, Ellis RS, Bundy K, Treu T. 2012a. *Ap. J.* 746:162
410. Newman SF, Genzel R, Förster-Schreiber NM, Shapiro Griffin K, Mancini C, et al. 2012b. *Ap. J.* 761:43
411. Nipoti C, Londrillo P, Ciotti L. 2003. *MNRAS* 342:501–512
412. Nipoti C, Treu T, Auger MW, Bolton AS. 2009. *Ap. J. Let.* 706:L86–L90
413. Noeske KG, Weiner BJ, Faber SM, Papovich C, Koo DC, et al. 2007. *Ap. J. Let.* 660:L43–L46
414. Norman CA, Ikeuchi S. 1989. *Ap. J.* 345:372–383
415. Novak GS, Ostriker JP, Ciotti L. 2011. *Ap. J.* 737:26
416. Okamoto T, Eke VR, Frenk CS, Jenkins A. 2005. *MNRAS* 363:1299–1314
417. Okamoto T, Frenk CS, Jenkins A, Theuns T. 2010. *MNRAS* 406:208–222
418. Omma H, Binney J, Bryan G, Slyz A. 2004. *MNRAS* 348:1105–1119
419. Oogi T, Habe A. 2013. *MNRAS* 428:641–657
420. Oppenheimer BD, Crain RA, Schaye J, Rahmati A, Richings AJ, et al. 2016. *MNRAS* 460:2157–2179
421. Oppenheimer BD, Davé R. 2006. *MNRAS* 373:1265–1292
422. Oppenheimer BD, Davé R. 2008. *MNRAS* 387:577–600
423. Oppenheimer BD, Davé R, Kereš D, Fardal M, Katz N, et al. 2010. *MNRAS* 406:2325–2338
424. Oppenheimer BD, Schaye J. 2013a. *MNRAS* 434:1063–1078
425. Oppenheimer BD, Schaye J. 2013b. *MNRAS* 434:1043–1062
426. Oser L, Naab T, Ostriker JP, Johansson PH. 2012. *Ap. J.* 744:63
427. Oser L, Ostriker JP, Naab T, Johansson PH, Burkert A. 2010. *Ap. J.*
428. Ostriker EC, Shetty R. 2011. *Ap. J.* 731:41
429. Ostriker JP. 1980. *Comments on Astrophysics* 8:177
430. Ostriker JP, Choi E, Ciotti L, Novak GS, Proga D. 2010. *Ap. J.* 722:642–652
431. Ostriker JP, Hausman MA. 1977. *Ap. J. Let.* 217:L125–L129
432. Ostriker JP, McKee CF. 1988. *Reviews of Modern Physics* 60:1–68
433. Ostriker JP, Peebles PJE. 1973. *Ap. J.* 186:467–480
434. Ostriker JP, Thuan TX. 1975. *Ap. J.* 202:353–364
435. Pakmor R, Marinacci F, Springel V. 2014. *Ap. J. Let.* 783:L20
436. Pakmor R, Pfrommer C, Simpson CM, Springel V. 2016. *Ap. J. Let.* 824:L30
437. Pakmor R, Springel V. 2013. *MNRAS* 432:176–193
438. Patel SG, Fumagalli M, Franx M, van Dokkum PG, van der Wel A, et al. 2013a. *Ap. J.* 778:115
439. Patel SG, van Dokkum PG, Franx M, Quadri RF, Muzzin A, et al. 2013b. *Ap. J.* 766:15
440. Peebles PJE. 1969. *Ap. J.* 155:393
441. Pelupessy FI, Di Matteo T, Ciardi B. 2007. *Ap. J.* 665:107–119
442. Pelupessy FI, Papadopoulos PP, van der Werf P. 2006. *Ap. J.* 645:1024–1042
443. Pérez-González PG, Rieke GH, Villar V, Barro G, Blaylock M, et al. 2008. *Ap. J.* 675:234–261
444. Pettini M, Shapley AE, Steidel CC, Cuby JG, Dickinson M, et al. 2001. *Ap. J.* 554:981–1000
445. Pilkington K, Few CG, Gibson BK, Calura F, Michel-Dansac L, et al. 2012. *Astron. Astrophys.* 540:A56
446. Piontek F, Steinmetz M. 2011. *MNRAS* 410:2625–2642
447. Planck Collaboration, Ade PAR, Aghanim N, Armitage-Caplan C, Arnaud M, et al. 2014. *Astron. Astrophys.* 571:A16
448. Pontzen A, Governato F. 2012. *MNRAS* 421
449. Poveda A, Ruiz J, Allen C. 1967. *Boletín de los Observatorios Tonantzintla y Tacubaya* 4:86–90
450. Price DJ, Federrath C. 2010. *MNRAS* 406:1659–1674
451. Puchwein E, Springel V. 2013. *MNRAS* 428:2966–2979
452. Puls J, Kudritzki RP, Herrero A, Pauldrach AWA, Haser SM, et al. 1996. *Astron. Astrophys.* 305:171
453. Qu Y, Di Matteo P, Lehnert M, van Driel W, Jog CJ. 2010. *Astron. Astrophys.* 515:A11
454. Qu Y, Helly JC, Bower RG, Theuns T, Crain RA, et al. 2017. *MNRAS* 464:1659–1675
455. Quinn PJ, Hernquist L, Fullagar DP. 1993. *Ap. J.* 403:74–93

456. Rahmati A, Schaye J, Bower RG, Crain RA, Furlong M, et al. 2015. *MNRAS* 452:2034–2056
457. Read JI, Hayfield T. 2012. *MNRAS* 422:3037–3055
458. Rees MJ, Ostriker JP. 1977. *MNRAS* 179:541–559
459. Renaud F, Bournaud F, Duc PA. 2015. *MNRAS* 446:2038–2054
460. Renaud F, Bournaud F, Emsellem E, Elmegreen B, Teyssier R, et al. 2013. *MNRAS* 436:1836–1851
461. Renzini A. 2006. *Annu. Rev. Astron. Astrophys.* 44:141–192
462. Renzini A, Andreon S. 2014. *MNRAS* 444:3581–3591
463. Renzini A, Peng Yj. 2015. *Ap. J. Let.* 801:L29
464. Richings AJ, Schaye J. 2016. *MNRAS* 458:270–292
465. Richings AJ, Schaye J, Oppenheimer BD. 2014. *MNRAS* 442:2780–2796
466. Rieder M, Teyssier R. 2016. *MNRAS* 457:1722–1738
467. Rix HW, Bovy J. 2013. *Astron. and Astrophys. Rev.* 21:61
468. Robertson B, Bullock JS, Cox TJ, Di Matteo T, Hernquist L, et al. 2006a. *Ap. J.* 645:986–1000
469. Robertson B, Cox TJ, Hernquist L, Franx M, Hopkins PF, et al. 2006b. *Ap. J.* 641:21–40
470. Robertson B, Hernquist L, Cox TJ, Di Matteo T, Hopkins PF, et al. 2006c. *Ap. J.* 641:90–102
471. Robertson B, Yoshida N, Springel V, Hernquist L. 2004. *Ap. J.* 606:32–45
472. Robertson BE, Kravtsov AV. 2008. *Ap. J.* 680:1083–1111
473. Rodriguez-Gomez V, Pillepich A, Sales LV, Genel S, Vogelsberger M, et al. 2016. *MNRAS* 458:2371–2390
474. Roos O, Juneau S, Bournaud F, Gabor JM. 2015. *Ap. J.* 800:19
475. Rosas-Guevara YM, Bower RG, Schaye J, Furlong M, Frenk CS, et al. 2015. *MNRAS* 454:1038–1057
476. Rosdahl J, Schaye J, Dubois Y, Kimm T, Teyssier R. 2016. *ArXiv e-prints*
477. Rosdahl J, Schaye J, Teyssier R, Agertz O. 2015. *MNRAS* 451:34–58
478. Rothberg B, Joseph RD. 2004. *Astron. J.* 128:2098–2143
479. Röttgers B, Naab T, Oser L. 2014. *MNRAS* 445:1065–1083
480. Roškar R, Teyssier R, Agertz O, Wetzstein M, Moore B. 2014. *MNRAS* 444:2837–2853
481. Rubin KHR, Prochaska JX, Koo DC, Phillips AC, Martin CL, Winstrom LO. 2014. *Ap. J.* 794:156
482. Saintonge A, Kauffmann G, Kramer C, Tacconi LJ, Buchbender C, et al. 2011. *MNRAS* 415:32–60
483. Salem M, Bryan GL. 2014. *MNRAS* 437:3312–3330
484. Salem M, Bryan GL, Corlies L. 2016. *MNRAS* 456:582–601
485. Sales LV, Marinacci F, Springel V, Petkova M. 2014. *MNRAS* 439:2990–3006
486. Sales LV, Navarro JF, Schaye J, Dalla Vecchia C, Springel V, Booth CM. 2010. *MNRAS* 409:1541–1556
487. Sánchez SF, Kennicutt RC, Gil de Paz A, van de Ven G, Vílchez JM, et al. 2012. *Astron. Astrophys.* 538:A8
488. Sanders DB, Soifer BT, Elias JH, Madore BF, Matthews K, et al. 1988. *Ap. J.* 325:74–91
489. Sazonov SY, Ostriker JP, Ciotti L, Sunyaev RA. 2005. *MNRAS* 358:168–180
490. Sazonov SY, Ostriker JP, Sunyaev RA. 2004. *MNRAS* 347:144–156
491. Scalo J, Elmegreen BG. 2004. *Annu. Rev. Astron. Astrophys.* 42:275–316
492. Scannapieco C, Tissera PB, White SDM, Springel V. 2005. *MNRAS* 364:552–564
493. Scannapieco C, Tissera PB, White SDM, Springel V. 2006. *MNRAS* 371:1125–1139
494. Scannapieco C, Wadepuhl M, Parry OH, Navarro JF, Jenkins A, et al. 2012. *MNRAS* 423:1726–1749
495. Scannapieco C, White SDM, Springel V, Tissera PB. 2009. *MNRAS* 396:696–708
496. Scannapieco E, Brügger M. 2008. *Ap. J.* 686:927–947
497. Scannapieco E, Brügger M. 2015. *Ap. J.* 805:158
498. Schaller M, Dalla Vecchia C, Schaye J, Bower RG, Theuns T, et al. 2015. *MNRAS* 454:2277–2291
499. Schawinski K, Treister E, Urry CM, Cardamone CN, Simmons B, Yi SK. 2011. *Ap. J. Let.* 727:L31
500. Schaye J, Crain RA, Bower RG, Furlong M, Schaller M, et al. 2015. *MNRAS* 446:521–554
501. Schaye J, Dalla Vecchia C. 2008. *MNRAS* 383:1210–1222
502. Schaye J, Dalla Vecchia C, Booth CM, Wiersma RPC, Theuns T, et al. 2010. *MNRAS* 402:1536–1560
503. Schmidt M. 1959. *Ap. J.* 129:243

504. Sedov LI. 1959. *Similarity and Dimensional Methods in Mechanics*
505. Serra P, Oosterloo T, Morganti R, Alatalo K, Blitz L, et al. 2012. *MNRAS* 422:1835–1862
506. Serra P, Oser L, Krajinović D, Naab T, Oosterloo T, et al. 2014. *MNRAS* 444:3388–3407
507. Shakura NI, Sunyaev RA. 1973. *Astron. Astrophys.* 24:337–355
508. Shankar F, Lapi A, Salucci P, De Zotti G, Danese L. 2006. *Ap. J.* 643:14–25
509. Shapley AE. 2011. *Annu. Rev. Astron. Astrophys.* 49:525–580
510. Sharma P, Roy A, Nath BB, Shchekinov Y. 2014. *MNRAS* 443:3463–3476
511. Shen S, Mo HJ, White SDM, Blanton MR, Kauffmann G, et al. 2003. *MNRAS* 343:978–994
512. Shlosman I, Frank J, Begelman MC. 1989. *Nature* 338:45–47
513. Sijacki D, Springel V, Di Matteo T, Hernquist L. 2007. *MNRAS* 380:877–900
514. Sijacki D, Vogelsberger M, Genel S, Springel V, Torrey P, et al. 2015. *MNRAS* 452:575–596
515. Sijacki D, Vogelsberger M, Kereš D, Springel V, Hernquist L. 2012. *MNRAS* 424:2999–3027
516. Silk J. 1977. *Ap. J.* 211:638–648
517. Silk J, Rees MJ. 1998. *Astron. Astrophys.* 331:L1–L4
518. Silva MDV, Napiwotzki R. 2011. *MNRAS* 411:2596–2614
519. Simpson CM, Pakmor R, Marinacci F, Pfrommer C, Springel V, et al. 2016. *Ap. J. Let.* 827:L29
520. Skilling J. 1975. *MNRAS* 172:557–566
521. Slyz AD, Devriendt JEG, Bryan G, Silk J. 2005. *MNRAS* 356:737–752
522. Sofue Y, Rubin V. 2001. *Annu. Rev. Astron. Astrophys.* 39:137–174
523. Soltan A. 1982. *MNRAS* 200:115–122
524. Somerville RS, Davé R. 2015. *Annu. Rev. Astron. Astrophys.* 53:51–113
525. Somerville RS, Primack JR. 1999. *MNRAS* 310:1087–1110
526. Sommer-Larsen J, Gelato S, Vedel H. 1999. *Ap. J.* 519:501–512
527. Sommer-Larsen J, Toft S. 2010. *Ap. J.* 721:1755–1764
528. Song M, Finkelstein SL, Ashby MLN, Grazian A, Lu Y, et al. 2016. *Ap. J.* 825:5
529. Spergel DN, Bean R, Doré O, Nolta MR, Bennett CL, et al. 2007. *Ap. J. Suppl.* 170:377–408
530. Spitzer L. 1978. *Physical processes in the interstellar medium*
531. Springel V. 2000. *MNRAS* 312:859–879
532. Springel V. 2005. *MNRAS* 364:1105–1134
533. Springel V. 2010a. *MNRAS* 401:791–851
534. Springel V. 2010b. *Annu. Rev. Astron. Astrophys.* 48:391–430
535. Springel V, Di Matteo T, Hernquist L. 2005a. *Ap. J. Let.* 620:L79–L82
536. Springel V, Di Matteo T, Hernquist L. 2005b. *MNRAS* 361:776–794
537. Springel V, Hernquist L. 2003. *MNRAS* 339:289–311
538. Springel V, Hernquist L. 2005. *Ap. J. Let.* 622:L9–L12
539. Springel V, Wang J, Vogelsberger M, Ludlow A, Jenkins A, et al. 2008. *MNRAS* 391:1685–1711
540. Springel V, White SDM, Jenkins A, Frenk CS, Yoshida N, et al. 2005. *Nature* 435:629–636
541. Stadel J, Potter D, Moore B, Diemand J, Madau P, et al. 2009. *MNRAS* 398:L21–L25
542. Steidel CC, Erb DK, Shapley AE, Pettini M, Reddy N, et al. 2010. *Ap. J.* 717:289–322
543. Stinson G, Seth A, Katz N, Wadsley J, Governato F, Quinn T. 2006. *MNRAS* 373:1074–1090
544. Stinson GS, Bailin J, Couchman H, Wadsley J, Shen S, et al. 2010. *MNRAS* 408:812–826
545. Stinson GS, Brook C, Macciò AV, Wadsley J, Quinn TR, Couchman HMP. 2013. *MNRAS* 428:129–140
546. Stone JM, Gardiner TA, Teuben P, Hawley JF, Simon JB. 2008. *Ap. J. Suppl.* 178:137–177
547. Strickland DK, Stevens IR. 2000. *MNRAS* 314:511–545
548. Strömberg B. 1939. *Ap. J.* 89:526
549. Strong AW, Moskalenko IV. 1998. *Ap. J.* 509:212–228
550. Strong AW, Moskalenko IV, Ptuskin VS. 2007. *Annual Review of Nuclear and Particle Science* 57:285–327
551. Sun M, Voit GM, Donahue M, Jones C, Forman W, Vikhlinin A. 2009. *Ap. J.* 693:1142–1172
552. Tabatabaei FS, Schinnerer E, Murphy EJ, Beck R, Groves B, et al. 2013. *Astron. Astrophys.* 552:A19
553. Tacconi LJ, Genzel R, Neri R, Cox P, Cooper MC, et al. 2010. *Nature* 463:781–784

554. Tacconi LJ, Neri R, Genzel R, Combes F, Bolatto A, et al. 2013. *Ap. J.* 768:74
555. Tammann GA, Loeffler W, Schroeder A. 1994. *Ap. J. Suppl.* 92:487–493
556. Taylor G. 1950. *Royal Society of London Proceedings Series A* 201:159–174
557. Teyssier R. 2002. *Astron. Astrophys.* 385:337–364
558. Teyssier R, Chapon D, Bournaud F. 2010. *Ap. J. Let.* 720:L149–L154
559. Teyssier R, Moore B, Martizzi D, Dubois Y, Mayer L. 2011. *MNRAS* 414:195–208
560. Teyssier R, Pontzen A, Dubois Y, Read JI. 2013. *MNRAS* 429:3068–3078
561. Thacker RJ, Couchman HMP. 2000. *Ap. J.* 545:728–752
562. Thomas D, Maraston C, Bender R, Mendes de Oliveira C. 2005. *Ap. J.* 621:673–694
563. Toomre A, Toomre J. 1972. *Ap. J.* 178:623–666
564. Tornatore L, Borgani S, Dolag K, Matteucci F. 2007. *MNRAS* 382:1050–1072
565. Treu T. 2010. *Annu. Rev. Astron. Astrophys.* 48:87–125
566. Trotta R, Jóhannesson G, Moskalenko IV, Porter TA, Ruiz de Austri R, Strong AW. 2011. *Ap. J.* 729:106
567. Truelove JK, McKee CF. 1999. *Ap. J. Suppl.* 120:299–326
568. Trujillo I, Conselice CJ, Bundy K, Cooper MC, Eisenhardt P, Ellis RS. 2007. *MNRAS* 382:109–120
569. Übler H, Naab T, Oser L, Aumer M, Sales LV, White SDM. 2014. *MNRAS* 443:2092–2111
570. Uhlig M, Pfrommer C, Sharma M, Nath BB, Enßlin TA, Springel V. 2012. *MNRAS* 423:2374–2396
571. Vale A, Ostriker JP. 2004. *MNRAS* 353:189–200
572. Vale A, Ostriker JP. 2006. *MNRAS* 371:1173–1187
573. van den Bosch FC, Abel T, Croft RAC, Hernquist L, White SDM. 2002. *Ap. J.* 576:21–35
574. van der Kruit PC, Freeman KC. 2011. *Annu. Rev. Astron. Astrophys.* 49:301–371
575. van der Wel A, Franx M, van Dokkum PG, Skelton RE, Momcheva IG, et al. 2014. *Ap. J.* 788:28
576. van Dokkum PG, Abraham R, Merritt A, Zhang J, Geha M, Conroy C. 2015. *Ap. J. Let.* 798:L45
577. van Dokkum PG, Franx M, Kriek M, Holden B, Illingworth GD, et al. 2008. *Ap. J. Let.* 677:L5–L8
578. van Dokkum PG, Whitaker KE, Brammer G, Franx M, Kriek M, et al. 2010. *Ap. J.* 709:1018–1041
579. Veilleux S, Cecil G, Bland-Hawthorn J. 2005. *Annu. Rev. Astron. Astrophys.* 43:769–826
580. Velazquez H, White SDM. 1999. *MNRAS* 304:254–270
581. VERITAS Collaboration, Acciari VA, Aliu E, Arlen T, Aune T, et al. 2009. *Nature* 462:770–772
582. Vernaleo JC, Reynolds CS. 2006. *Ap. J.* 645:83–94
583. Vikhlinin A, Kravtsov A, Forman W, Jones C, Markevitch M, et al. 2006. *Ap. J.* 640:691–709
584. Villumsen JV. 1983. *MNRAS* 204:219–236
585. Vogelsberger M, Genel S, Sijacki D, Torrey P, Springel V, Hernquist L. 2013. *MNRAS* 436:3031–3067
586. Vogelsberger M, Genel S, Springel V, Torrey P, Sijacki D, et al. 2014. *MNRAS* 444:1518–1547
587. Völk HJ, Aharonian FA, Breitschwerdt D. 1996. *Space Science Rev.* 75:279–297
588. Wadepuhl M, Springel V. 2011. *MNRAS* 410:1975–1992
589. Wadsley JW, Stadel J, Quinn T. 2004. *New Astronomy* 9:137–158
590. Wadsley JW, Veeravalli G, Couchman HMP. 2008. *MNRAS* 387:427–438
591. Walch S, Girichidis P, Naab T, Gatto A, Glover SCO, et al. 2015. *MNRAS* 454:238–268
592. Walch S, Naab T. 2015. *MNRAS* 451:2757–2771
593. Walch SK, Whitworth AP, Bisbas T, Wünsch R, Hubber D. 2012. *MNRAS* 427:625–636
594. Wang L, Dutton AA, Stinson GS, Macciò AV, Penzo C, et al. 2015. *MNRAS* 454:83–94
595. Watkins LL, Evans NW, An JH. 2010. *MNRAS* 406:264–278
596. Weil ML, Eke VR, Efstathiou G. 1998. *MNRAS* 300:773–789
597. Weinberger R, Springel V, Hernquist L, Pillepich A, Marinacci F, et al. 2016. *ArXiv e-prints*
598. Wellons S, Torrey P, Ma CP, Rodriguez-Gomez V, Pillepich A, et al. 2016. *MNRAS* 456:1030–1048
599. Werk JK, Prochaska JX, Tumlinson J, Peebles MS, Tripp TM, et al. 2014. *Ap. J.* 792:8
600. Wetzell AR, Hopkins PF, Kim Jh, Faucher-Giguère CA, Kereš D, Quataert E. 2016. *Ap. J. Let.* 827:L23
601. Whitaker KE, van Dokkum PG, Brammer G, Franx M. 2012. *Ap. J. Let.* 754:L29
602. White SDM. 1978. *MNRAS* 184:185–203

603. White SDM. 1979a. *Ap. J. Let.* 229:L9–L13
604. White SDM. 1979b. *MNRAS* 189:831–852
605. White SDM, Rees MJ. 1978. *MNRAS* 183:341–358
606. Wiersma RPC, Schaye J, Smith BD. 2009. *MNRAS* 393:99–107
607. Williams RJ, Quadri RF, Franx M. 2011. *Ap. J. Let.* 738:L25
608. Wise JH, Abel T, Turk MJ, Norman ML, Smith BD. 2012. *MNRAS* 427:311–326
609. Wong T, Blitz L. 2002. *Ap. J.* 569:157–183
610. Woods RM, Wadsley J, Couchman HMP, Stinson G, Shen S. 2014. *MNRAS* 442:732–740
611. Wu X, Gerhard O, Naab T, Oser L, Martinez-Valpuesta I, et al. 2014. *MNRAS* 438:2701–2715
612. Wuyts S, Cox TJ, Hayward CC, Franx M, Hernquist L, et al. 2010. *Ap. J.* 722:1666–1684
613. Wuyts S, Förster Schreiber NM, van der Wel A, Magnelli B, Guo Y, et al. 2011. *Ap. J.* 742:96
614. Xue XX, Rix HW, Zhao G, Re Fiorentin P, Naab T, et al. 2008. *Ap. J.* 684:1143–1158
615. Yang HYK, Ruzkowski M, Ricker PM, Zweibel E, Lee D. 2012. *Ap. J.* 761:185
616. Yang X, Mo HJ, van den Bosch FC. 2003. *MNRAS* 339:1057–1080
617. Yang X, Mo HJ, van den Bosch FC, Bonaca A, Li S, et al. 2013. *Ap. J.* 770:115
618. Young LM, Bureau M, Davis TA, Combes F, McDermid RM, et al. 2011. *MNRAS* 414:940–967
619. Yuan F, Narayan R. 2014. *Annu. Rev. Astron. Astrophys.* 52:529–588
620. Zavala J, Frenk CS, Bower R, Schaye J, Theuns T, et al. 2016. *MNRAS* 460:4466–4482
621. Zhukovska S, Dobbs C, Jenkins EB, Klessen RS. 2016. *Ap. J.* 831:147
622. Zweibel EG, Heiles C. 1997. *Nature* 385:131–136
623. Zwicky F. 1957. *Morphological astronomy*